

Improving the sustainability and effectiveness of oxidative processes for water and wastewater purification

*Original*

Improving the sustainability and effectiveness of oxidative processes for water and wastewater purification / Farinelli, Giulio. - (2021 May 06), pp. 1-148.

*Availability:*

This version is available at: 11583/2903514 since: 2021-05-31T16:52:54Z

*Publisher:*

Politecnico di Torino

*Published*

DOI:

*Terms of use:*

Altro tipo di accesso

This article is made available under terms and conditions as specified in the corresponding bibliographic description in the repository

*Publisher copyright*

(Article begins on next page)



# ScuDo

Scuola di Dottorato ~ Doctoral School  
WHAT YOU ARE, TAKES YOU FAR



Doctoral Dissertation  
Doctoral Program in Environmental Engineering (33<sup>th</sup> Cycle)

# Improving the sustainability and effectiveness of oxidative processes for water and wastewater purification

**Giulio Farinelli**

\* \* \* \* \*

## Supervisors

Prof. Alberto Tiraferri

## Doctoral Examination Committee:

Prof. Renato Baciocchi, Referee, Università degli studi di Roma "Tor Vergata"

Prof. Gilles Mailhot, Referee, Institut de Chimie de Clermont-Ferrand

Prof. Manuela Antonelli, Committee, Politecnico di Milano

Prof. Tiziana Tosco, Committee, Politecnico di Torino

Prof. Davide Vione, Committee, Università degli studi di Torino

Politecnico di Torino  
February 27, 2021



This thesis is licensed under a Creative Commons License, Attribution - Noncommercial - NoDerivative Works 4.0 International: see <http://www.creativecommons.org>. The text may be reproduced for non-commercial purposes, provided that credit is given to the original author.

I hereby declare that the contents and organisation of this dissertation constitute my own original work and does not compromise in any way the rights of third parties, including those relating to the security of personal data.

A handwritten signature in black ink, reading "Giulio Farinelli", positioned above a horizontal dotted line.

Giulio Farinelli  
Turin, February 26, 2021



# Summary

The growth of the population has occurred alongside the increase of industrial, agricultural and, correspondingly, waste production. It is no longer possible to evade the evidence of a tight nexus among human activities and the influence on the environment humans are part of. Indeed, the intensification of industrial activities turns into an unrelenting development of new classes of chemicals that are potentially harmful. If not properly managed, these substances may reach water resources through aqueous effluents, thus representing a risk for both the environment and human health. Moreover, the increasing demand of drinkable water worldwide follows the population growth. Access to safe water is not available everywhere and often untreated water sources are biologically contaminated. With this respect, oxidation processes are a promising tool against both chemical and biological contaminations of water effluents. This thesis investigation aims to increase the sustainability and the effectiveness of the classic Fenton oxidation process designing new and improved processes. A systematic approach is also presented to promote improved approaches for wastewater disinfection.

The first section of the investigation focuses on new strategies to thwart the diffusion of emerging chemical contaminants in water effluents. The identification of a clean, safe, versatile, efficient, cheap, and easy-to-handle approach is of crucial importance in water purification. The classic Fenton process is selected as a starting point for new developments in this direction. The use of effective iron ligands is the general strategy proposed to overcome some of the limitations of the Fenton process, namely, its inadequate selectivity, need to work under acidic pH conditions, undesirable by-products formation, sludge production, and high consumption of harmful compounds. A chitosan-iron system is proposed and efficiently applied as a polymeric organo-metallic catalyst in the degradation of chemical contaminants in water at circumneutral pH. A new and easy-to-use

analytical method is discussed to discriminate among a metal-based and a free-radical oxidation mechanism, giving rise, respectively, to potentially selective and unselective processes. Selectivity is intended as both the ability to discriminate among different contaminants and the ability to favour oxidation of certain chemical positions in a contaminant. This work strongly suggests that an iron-ligand complex promotes a metal-based mechanism at circumneutral pH. Moreover, metabisulfite is proposed as an efficient and safer substitute of hydrogen peroxide as reactant in metal-based catalysed oxidation processes.

The second section of the investigation focuses on the impact of oxidative and non-oxidative biocides in water disinfection. The general objective of this section is to evaluate the real risk of the tested disinfectants to generate disinfection by-products, hence to define a strategy to limit disinfection by-products generation and promote a safer management of disinfectants. In this dissertation, disinfection by-products are generally intended as halogenated by-products. Study of the disinfection mechanism is the approach undertaken not only to understand the process, but to identify safer disinfection routes. Potential oxidants and non-oxidant disinfectants are investigated and applied in the disinfection of a real wastewater. Three safe biocides are identified, namely, thiazolinones, hydrogen peroxide, and metabisulfite. They are evaluated in terms cost-benefit analysis, efficiency toward biological contaminants, and environmental impacts. Moreover, an investigation of the mechanism of disinfection by-products generation in the use of peracetic acid is discussed. The study shows that peracetic acid, an increasingly adopted oxidant for wastewater disinfection, can act as organic substrate in the generation of bromoform if bromide is present in the aqueous matrix.

Overall, the results of this dissertation aim at promoting more sustainable processes for the removal of chemical and biological contamination from water. The study follows a general approach whereby investigation of the reaction mechanisms is performed to gain insight of the oxidation phenomena. This insight is in turn the basis of the exploration of systems with direct implications for engineering applications.





# Acknowledgments

This work was supported financially through the Ph.D. scholarship from MIUR. The studies presented in chapter 2 and 3 occurred through the financial support by Università di Torino, Politecnico di Torino, Compagnia di San Paolo, and the Spanish Ministry of Science, Innovation and Universities (MICIU).

# Contents

<b>1</b>	<b>Introduction.....</b>	<b>1</b>
<b>1.1</b>	<b>Targets contaminants: chemical and biological perspectives .....</b>	<b>2</b>
1.1.1	Contaminants of Emerging Concern .....	2
1.1.2	Biological contaminants and disinfection by-products .....	4
<b>1.2</b>	<b>From oxidations to Advanced Oxidation Processes: an overview .....</b>	<b>5</b>
<b>1.3</b>	<b>AOPs in biochemical and biomimetic processes .....</b>	<b>8</b>
<b>1.4</b>	<b>Thesis hypotheses and objectives.....</b>	<b>10</b>
<b>2</b>	<b>AOPs from living systems to water treatment: a sustainable approach..</b>	<b>12</b>
<b>2.1</b>	<b>Metabisulfite as Unconventional Reagent for Green Oxidation of Emerging Contaminants Using an Iron-based Catalyst .....</b>	<b>14</b>
2.1.1	Introduction .....	14
2.1.2	Materials and Methods .....	16
2.1.2.1	<i>Chemicals .....</i>	<i>16</i>
2.1.2.2	<i>Preparation of the Fe-TAML stock solution .....</i>	<i>16</i>
2.1.2.3	<i>Protocol of the oxidation experiments .....</i>	<i>16</i>
2.1.2.4	<i>Analytical methods .....</i>	<i>17</i>
2.1.2.5	<i>Electrochemical measurements .....</i>	<i>18</i>
2.1.3	Results and Discussion.....	18
2.1.3.1	<i>Performance of different reagents towards the degradation of phenol .....</i>	<i>18</i>
2.1.3.2	<i>Comparison of metabisulfite (<math>S_2O_5^{2-}</math>) and hydrogen peroxide in the degradation of CECs.....</i>	<i>22</i>
2.1.3.3	<i>Discussion on the nature of the active species and the reaction mechanism.....</i>	<i>24</i>
2.1.4	Conclusions .....	30
<b>2.2</b>	<b>Fe-Chitosan Complexes for Oxidative Degradation of Emerging Contaminants in Water: Structure, Activity, and Reaction Mechanism.....</b>	<b>31</b>
2.2.1	Introduction .....	31
2.2.2	Materials and Methods .....	32
2.2.2.1	<i>Chemicals .....</i>	<i>32</i>
2.2.2.2	<i>Preparation of the chitosan solid films .....</i>	<i>32</i>
2.2.2.3	<i>Oxidation experiments: Homogeneous conditions .....</i>	<i>33</i>
2.2.2.4	<i>Oxidation experiments: Heterogeneous conditions .....</i>	<i>34</i>
2.2.2.5	<i>Analytical methods .....</i>	<i>34</i>
2.2.2.6	<i>Modeling of the chitosan dimer conformations .....</i>	<i>34</i>
2.2.2.7	<i>Modeling of the chitosan-Fe complex.....</i>	<i>35</i>
2.2.2.8	<i>Kinetic model of reaction .....</i>	<i>35</i>

2.2.3	Results and Discussion.....	36
2.2.3.1	<i>Chitosan-metal interaction and catalytic efficiency of the complex.....</i>	36
2.2.3.2	<i>Homogeneous degradation of contaminants by CS-Fe complexes.....</i>	38
2.2.3.3	<i>Insights into the reaction mechanism and the nature of the active species .....</i>	39
2.2.3.4	<i>CS-Fe(III) as heterogeneous catalytic material .....</i>	43
2.2.4	Conclusions .....	45
<b>2.3</b>	<b>Natural Iron Ligands Promote a Metal-Based Oxidation Mechanism for the Fenton Reaction in Water Environments.....</b>	<b>46</b>
2.3.1	Introduction .....	46
2.3.2	Materials and Methods .....	49
2.3.2.1	<i>Chemicals .....</i>	49
2.3.2.2	<i>Reaction conditions .....</i>	49
2.3.2.3	<i>Analytical conditions .....</i>	49
2.3.3	Results and Discussion.....	50
2.3.3.1	<i>Iron ligands promote the preferential formation of cyclohexanol.....</i>	50
2.3.3.2	<i>Switching the mechanism from free radical to metal-based catalysis .....</i>	54
2.3.3.3	<i>Evidence of the effect of pH on the traditional Fenton process.....</i>	56
2.3.4	Conclusions .....	57
<b>2.4</b>	<b>Summary .....</b>	<b>58</b>
<b>3</b>	<b>Impact of oxidative and non-oxidative processes in disinfection .....</b>	<b>60</b>
<b>3.1</b>	<b>Evaluation of the Effectiveness, Safety, and Feasibility of 9 Potential Biocides to Disinfect Acidic Landfill Leachate from Algae and Bacteria.....</b>	<b>61</b>
3.1.1	Introduction .....	61
3.1.2	Materials and Methods .....	63
3.1.2.1	<i>Chemicals, reagents, and water matrices used in the study .....</i>	63
3.1.2.2	<i>Microalgae sampling and counting .....</i>	65
3.1.2.3	<i>Bacterial methods: LB, saline solution, and bacterial suspension preparation .....</i>	65
3.1.2.4	<i>Determination of the minimum inhibitory concentration (MIC) of E. coli, and determination of bacterial disinfection kinetics by biocides.....</i>	65
3.1.2.5	<i>Methodology of life cycle analysis (LCA).....</i>	66
3.1.3	Results and Discussion.....	67
3.1.3.1	<i>Disinfection targets and principal characteristics of the studied biocides .....</i>	67
3.1.3.2	<i>Disinfection efficacy .....</i>	71
3.1.3.3	<i>Generation of disinfection by-products .....</i>	75
3.1.3.4	<i>Metabisulfite, H<sub>2</sub>O<sub>2</sub>, and MIT: logistics of implementation.....</i>	77
3.1.3.5	<i>Environmental impacts, economic analysis, and overall review of biocides.....</i>	78
3.1.4	Conclusion.....	80
<b>3.2</b>	<b>Formation of Halogenated By-products upon Water Treatment with Peracetic Acid.....</b>	<b>81</b>

3.2.1	Introduction .....	81
3.2.2	Materials and Methods .....	83
3.2.2.1	<i>Chemicals and real wastewater</i> .....	83
3.2.2.2	<i>Analytical Methods</i> .....	83
3.2.2.3	<i>PAA solution characterization</i> .....	84
3.2.3	Results and Discussion .....	85
3.2.3.1	<i>Stability of the peracetic acid mixture in the presence of halides</i> .....	85
3.2.3.2	<i>Formation of trihalomethanes</i> .....	87
3.2.3.3	<i>Reaction mechanism and prevailing species</i> .....	89
3.2.3.4	<i>Implications for PAAM use in real waters</i> .....	93
3.3	Summary .....	94
4	Final conclusion and perspectives .....	96
5	References .....	101

# List of Tables

Table 2.1.1 Onset potential for the oxidation of the studied contaminants of emerging concern. The onset potential is reported for both the first and the successive scans of the CVs.....	28
Table 2.3.1 A/K ratio for the oxidation of cyclohexane at different pH values with citric, malic and quinic acid as iron ligands. The pH was fixed with phosphate buffer except for pH 3 (HClO <sub>4</sub> ). The reaction time was 30 min. ....	54
Table 3.1.1 Main characteristics of the contaminated groundwater from analysis of the samples and historical data obtained from the treatment plant management. ....	64
Table 3.1.2 Molecular structure, mode of action (MOA), and mechanism of DBPs generation for each biocide investigated in this study. In the fourth column, “oxidizing” (O), “electrophilic” (E), and “reductant” (R) refer to the main MOA of each biocide. The last column presents the redox potential for each oxidant biocide.....	68
Table 3.1.3 Concentration of total THMs and other halogenated compounds upon disinfection of the contaminated groundwater through addition of the various biocides at different dosage.....	75
Table 3.2.1 Formation of CHBr <sub>3</sub> in solutions consisting of: AA (2.8 mM) and HBrO at different concentrations (2; 10 mM); AA (2.8 mM), H <sub>2</sub> O <sub>2</sub> (1.5 mM), and KBr (10 mM). ....	90
Table 3.2.2 Formation of CHBr <sub>3</sub> in solutions with HBrO 2 mM and different organic substrates (AcOH; Propionic acid; Butyric acid) at 2 mM. ....	92

# List of Figures

Figure 2.1.1 Degradation of phenol with different reagents. Reagents were (a) sulfite, (b) metabisulfite, (c) persulfate, and (d)  $\text{H}_2\text{O}_2$ . The reactions were carried out in phosphate buffer (10 mM) by adding 0.1 mM of reagent every 10 minutes (*i.e.*, at  $t = 0, 10$ , and  $20$  min), with the exception of  $\text{H}_2\text{O}_2$  that was added only once at the beginning ( $t = 0$ ). Initial conditions were  $[\text{Fe-TAML}] = 0.01$  mM;  $[\text{PhOH}] = 0.1$  mM. ....20

Figure 2.1.2 Degradation of phenol with metabisulfite as reagent. The reactions were carried out in phosphate buffer (10 mM), with initial concentrations  $[\text{Fe-TAML}] = 0.01$  mM;  $[\text{PhOH}] = 0.1$  mM, and adding one aliquot of metabisulfite with initial concentrations of (a) 0.3 mM and (b) 0.1 mM. ....22

Figure 2.1.3 Degradation percentage of the studied contaminants of emerging concern. Metabisulfite or  $\text{H}_2\text{O}_2$  were used as reagents at different pH values. The reactions were carried out for 60 min in phosphate buffer (10 mM), by adding 0.1 mM of reagent every 10 minutes for a total of three additions (at 0, 10, and 20 min). Initial conditions were  $[\text{Fe-TAML}] = 0.01$  mM, and  $[\text{Contaminant}] = 0.1$  mM. ....24

Figure 2.1.4 Effects of different quenchers on the degradation reaction. Quenchers were  $t\text{-BuOH}$  (40 mM) or  $2\text{-PrOH}$  (133 mM), tested in the degradation of (a, b) phenol or (c-f) BP3. The reagents were (a-d) metabisulfite or (e, f)  $\text{H}_2\text{O}_2$ , and the pH was 7 (left column) or 11 (right column). Reactions were carried out in phosphate buffer (10 mM), adding 0.1 mM metabisulfite (or  $\text{H}_2\text{O}_2$ ) every 10 min, for a total of three additions (at 0, 10, and 20 min). Initial conditions were:  $[\text{Fe-TAML}] = 0.01$  mM;  $[\text{PhOH}] = [\text{BP3}] = 0.1$  mM. ....27

Figure 2.1.5 Reaction pathways in the activation of reagents by Fe-TAML. (a) Established pathway for the activation of hydrogen peroxide as discussed by Ghosh et al., and (b) proposed pathway for the activation of metabisulfite. ....28

Figure 2.2.1 Stoichiometry of the metal-chitosan complexes. (a) Metal concentration of saturation (equivalence point) in the CS-metal complexes at a chitosan concentration of 433 mg/L, from UV titration. (b) Phenol ( $\text{PhOH}$ ) degradation resulting from the use of different CS-metal complexes as homogeneous catalysts after one addition of  $\text{H}_2\text{O}_2$ . The reaction was performed with metal: $\text{PhOH}$ : $\text{H}_2\text{O}_2 = 1:1:1$  mass concentration ratio, and metal concentration as in (a). ....37

Figure 2.2.2 Chitosan-Fe complexes in the degradation of organic contaminants. (a) Influence of metal concentration in the CS-Fe(III, II) complexes (CS concentration 433 mg/L) used as homogeneous catalysts for phenol ( $\text{PhOH}$ )

degradation. (b) Degradation of three contaminants of emerging concern with the use of the CS-Fe(III) complex as homogeneous catalyst. (c, d) Degradation of PhOH and formation of byproducts (they were recognized as the mono-hydroxylated byproducts) monitored with LC-MS using (c) the CS-FeCl<sub>3</sub> complex or (d) the CS-FeSO<sub>4</sub> complex as homogeneous catalyst. The reactions were performed with metal:contaminant:H<sub>2</sub>O<sub>2</sub> = 1:1:3 mass concentration ratio, and metal concentration as in Figure 1a. The same conditions were applied to conduct the reactions using the CS-FeCl<sub>3</sub> complex related to (a-c). The reaction conditions with the CS-FeSO<sub>4</sub> complex were adjusted (metal:phenol:H<sub>2</sub>O<sub>2</sub> = 1:1:30 mass concentration ratio) to obtain the same kinetics of degradation observed in the CS-FeCl<sub>3</sub> complex. The lines connecting the data points are intended only as a guide for the eye. ....39

Figure 2.2.3 Phenol degradation resulting from the use of CS-Fe(III, II) complexes applied as homogeneous catalysts obtained with different iron salts (FeCl<sub>3</sub>, Fe(NO<sub>3</sub>)<sub>3</sub>, FeSO<sub>4</sub>, FeCl<sub>2</sub>). The reactions were performed with metal:PhOH:H<sub>2</sub>O<sub>2</sub> = 1:1:3 mass concentration ratio, and metal concentration as in Figure 2.2.1a. ....40

Figure 2.2.4 Modeling of the chitosan-Fe complexes as catalysts. (a) Free-energy surface of the CS dimer along the  $\phi$  and  $\psi$  torsional angles (see Methods). Three minimum free-energy structures ( $\alpha$ ,  $\beta$ ,  $\gamma$ ) identified are indicated on the right. The  $\alpha$  and  $\beta$  CS-structures were further used to study the structure of the catalytic species. (b) Molecular structure of a ferryl species optimized at the DFT level (TPSSH/def2-TZVP) in the  $\alpha$  and  $\beta$  conformations. The spin density distribution (at the TPSSH/def2-TZVP level) is shown as in surface representation at +0.05 (-0.05) isovalue for  $\alpha$  ( $\beta$ ) spin density. Kinetic models for (c) Fe<sup>2+</sup> and (d) Fe<sup>3+</sup>. In c and d, the substrate, ferryl, and the free radical lines are related to the trend of Orange II, metal-based product, and free-radical product, respectively, obtained in the simulation. The lines connecting the data points are intended only as a guide for the eye. ....41

Figure 2.2.5 Chitosan-Fe complexes as heterogeneous catalysts. (a) Phenol degradation resulting from the use of CS-Fe(III, II) films applied as heterogeneous catalysts obtained with different iron salts, *i.e.*, FeCl<sub>3</sub>, Fe(NO<sub>3</sub>)<sub>3</sub>, FeSO<sub>4</sub>, or FeCl<sub>2</sub>. CS-FeCl<sub>3</sub> and CS-FeSO<sub>4</sub> films were tested in two cycles in order to evaluate their cycling efficiency. The films were obtained from an initial solution containing 2% chitosan in the presence of FeCl<sub>3</sub>=13.8 mM, Fe(NO<sub>3</sub>)<sub>3</sub>=13.8 mM, FeSO<sub>4</sub>=9.2 mM, or FeCl<sub>2</sub>=9.2 mM. The reactions were performed with metal:PhOH:H<sub>2</sub>O<sub>2</sub> = 1:0.5:0.5 mass concentration ratio, and metal concentration as in Figure 1a. The oxidant was added in one aliquot. (b) Evaluation of leaching of Fe(III) from the surface of the CS-Fe(III) film. The blue and the green line represent the reference

spectra of Fe(III) 0.1 mM and CS. (c) XRD and (d) EDX analyses of the surface of a pure chitosan film and of a CS-Fe(III) film.....	44
Figure 2.3.1 Proposed mechanism for cyclohexane oxidation. A: free radical path with Russel termination type. B: a metal-based path.....	48
Figure 2.3.2 A/K ratio observed in the oxidation of cyclohexane with different iron ligands at pH 7 (phosphate buffer) and with the classic Fenton process at pH 3 (perchloric acid) after 30 min of reaction. ....	51
Figure 2.3.3 Fraction of degraded cyclohexane with respect to the total degraded amount (circles, right axis) and trend of selectivity, <i>i.e.</i> , A/K ratio (squares, left axis), as a function of time in a system containing hydrogen peroxide as reactant and a) citric acid, b) malic acid, or c) quinic acid as iron ligands. The pH of the aqueous system was buffered at 7 (phosphate buffer). The solid lines connecting the circles are only intended as a guide for the eye. ....	53
Figure 2.3.4 A/K ratio observed after 30 min of reaction in the oxidation of cyclohexane with EDTA and EDDS as iron ligands, added at different concentrations. The runs were carried out at pH 3. The condition of no added Ligand ( $[\text{Ligand}]/[\text{Fe(II)}] = 0$ ) corresponds to the classic Fenton process. The solid lines are only intended as a guide for the eye. The dashed line depicts the expected A/K ratio for a pure free radicals-based catalysis.....	56
Figure 2.3.5 A/K ratio observed in the classic Fenton process performed at different pH values.....	57
Figure 3.1.1 Mode of action of the biocides investigated in this study. Please note that chloroplasts are present only in algae. ....	68
Figure 3.1.2 Minimum inhibitory concentration (MIC) of the biocides toward <i>E. coli</i> inactivation. (a, b) Results of light absorbance of the <i>E. coli</i> suspension as a function of biocide concentration. The lines are only intended as guides for the eye. The control values of the stationary phase resulted in the OD <sub>600</sub> range 3.5-5.5, from which solution spiking to OD <sub>600</sub> $1 \pm 0.1$ was carried out. The standard deviation is 20% for each result. (c) Summary of MIC values. No MIC values could be determined for sulfite and persulfate up to 10 mM biocide concentration. ....	72
Figure 3.1.3 Disinfection of microalgae and <i>E. coli</i> in the real contaminated groundwater matrix. (a) Removal rates of microalgae at varying biocide concentration. (b, c) Bacteria disinfection kinetics. In (b), metabisulfite and hydrogen peroxide were added at their MIC. Blank 1 shows the matrix effect on <i>E. coli</i> viability; blank 2 shows the matrix effect on <i>E. coli</i> viability by buffering the suspension at pH 7 before plating; blank 3 shows the matrix effect on <i>E. coli</i> viability by buffering the suspension at pH 7 before biocide addition. In (c), <i>E. coli</i> disinfection results obtained with a biocide concentration of 0.03 mM are shown. The lines are only intended as guides for the eye.....	74



Figure 3.1.4 (a) Trend of tribromomethane concentration in water as a function of DBNPA and MIT concentrations. The lines are only intended as guides for the eye. (b) Proposed scheme of DBNPA disinfection mechanism and tribromomethane generation. ....77

Figure 3.1.5 Evaluation of the biocides in terms of performance, environmental impacts, and cost of use. (a) Summary of safety and disinfection efficacy expressed as (x axis) DBP generation, (y axis) MIC, and (z axis) microalgae removal (at dosage of 1.5 mM). (b) Cost of deployment to treat one m<sup>3</sup> of wastewater, based on the optimal dosage found in this study. (c) Endpoint results of ReCiPe methodology in LCA; light shade, white, and dark shade colors refer to the categories “resources”, “human health”, and “ecosystem quality”, respectively. (d) Results of ReCiPe analysis and indication of the energy costs from CED analysis. In (b-d), only the three most promising biocides are presented, namely, MIT, hydrogen peroxide, and metabisulfite. ....79

Figure 3.2.1 Consumption of total oxidants in the presence of halides. (a) Consumption in a solution of PAA (1.5 mM) with KBr present at different concentrations. (b) Consumption in a solution of PAA (1.5 mM) with NaCl present at different concentrations. Lines connecting the data points are only intended as guides for the eye. (c) Consumption in a solution of PAA (1.5 mM) and KBr (10 mM). (d) Consumption in a solution of H<sub>2</sub>O<sub>2</sub> (1.5 mM) and KBr (10 mM). In (c, d), a solution of catalase (6.7 ppm) allowed for discrimination between PAA and H<sub>2</sub>O<sub>2</sub>. The results imply that H<sub>2</sub>O<sub>2</sub> is not consumed by KBr, while PAA is. ....86

Figure 3.2.2 Formation of CHBr<sub>3</sub> in the presence of PAA and halides. (a) CHBr<sub>3</sub> measured in solution as a function of KBr (10; 100; 1000 mM) and PAA (1.5; 15 mM). (b) CHBr<sub>3</sub> measured in solution in the presence of PAA, at different initial concentrations of PAA (15; 50; 150 mM) in a solution consisting of KBr (0.1 M) and NaCl (5 M). Only CHBr<sub>3</sub> was detected among the possible trihalomethanes. The star symbol (\*) over the bars indicates experiments at equivalent concentrations of PAA and KBr, (a) without and (b) with NaCl. ....88

Figure 3.2.3 Formation of CHBr<sub>3</sub> as a function of pH. CHBr<sub>3</sub> produced in solutions of varying pH, starting with: (blue) a solution containing PAA (1.5 mM) and KBr (10 mM); (orange) a solution containing AA (2.8 mM) and HBrO (2 mM). ....90

Figure 3.2.4 Rationalization of the possible reaction mechanism causing the formation of CHBr<sub>3</sub> in the presence of PAAM and Br<sup>-</sup>. The proposed mechanism is based on the Hell-Volhard-Zelinsky reaction. ....91

Figure 3.2.5 Final rationalization of the steps occurring to produce CHBr<sub>3</sub> in a solution containing PAA and bromide. ....92

Figure 3.2.6 Formation of organohalogens in a real contaminated groundwater containing chloride and bromide and in which PAAM is added as disinfectant...94



# Chapter 1

## 1 Introduction

The earliest definition of oxidation originally implied a reaction with oxygen to form an oxide. The reaction between dioxygen and a fuel, namely, a combustion, was virtually the first oxidative reaction discovered and handled by human beings, with dioxygen the first established oxidizing agent.

In history, fire, hence a product of oxidation, has been a symbol of purification from both a religious and a public health standpoint. Indeed, throughout the Great Plague of London (1665-1666), the authorities, thinking the outbreak could also be airborne, ordered giant street bonfires and house fires to be kept burning day and night, in the hope that the air would be cleansed.<sup>1</sup> Tragically and somewhat ironically, the Great Plague of London turned into the Great Fire of London (1666), which destroyed large portions of the city.<sup>1</sup> At the time, some people believed that fire had eradicated the plague, and this debate is still rather open in the community.<sup>1</sup> The Great Fire may have helped ending the plague outbreak, but it certainly devastated the City of London.

With the advancement of science and technology, the management and reliability of oxidation processes advanced greatly, and at the same time their definition has been refined. At present, oxidation is regarded as the “loss of electrons or an increase in the oxidation state of an atom, an ion, or of certain atoms in a molecule”.<sup>2</sup> To date, scientists have available a class of chemotherapeutics that might selectively inhibit cancer growth by increasing the activity of reactive oxygen species (ROS) over the cytotoxic threshold of the cancer cells.<sup>3,4</sup> While an oxidative process developing within the body may be able to inhibit cancer, it is also capable of harming a human being. Several studies have discussed the involvement of the Fenton reaction at the root of cancer itself.

<sup>5-8</sup> The Fenton process can occur in our organism due to an overaccumulation of iron and hydrogen peroxide ( $\text{H}_2\text{O}_2$ ) within our cells. <sup>9</sup> These species react and generate high levels of hydroxyl radical, a typical ROS and a strong oxidant ( $E^\circ=1.9\div2.8$  V vs. NHE)<sup>10</sup>, which can damage the DNA, hence initiate cancer. <sup>9</sup> In our organism, cytochromes<sup>11</sup> and other biological species (e.g., sulfur-iron clusters)<sup>12,13</sup> modulate oxidation reactions preventing the generation of free radical processes which can initiate cancer. Of distinct interest is the Cytochrome P450, which modulates the selective oxidation of exogenous and endogenous toxic compounds. <sup>14,15</sup> Correspondingly, oxidation reactions can be engineered as a beneficial tool to degrade contaminants in the water purification field. However, as much as in our organism unrestrained oxidations are dangerous, also the major drawback of uncontrolled oxidation processes in water treatment is represented by possible parasitic reactions that lead to the formation of harmful by-products. <sup>16</sup> The well-known disruptive power of oxidations is mighty and threatening, ergo of crucial importance is to elucidate the mechanisms involved in the oxidative processes and to improve control over their efficacy and safety.

This dissertation focuses on oxidation as a beneficial tool in water purification, for both contaminants removal and disinfection. The reaction mechanisms and the efficiency of different oxidation processes are discussed. Some specific studies to prevent harmful by-products in water disinfection are presented. The general objective of the thesis is to enhance the sustainability and effectiveness of (some) traditional oxidation processes while maintaining the ease of implementation in engineered applications.

## **1.1 Targets contaminants: chemical and biological perspectives**

### **1.1.1 Contaminants of Emerging Concern**

“Water is not a commercial product like any other but, rather, a heritage which must be protected, defended and treated as such”. This is the fundamental principle of the Water Framework Directive (WFD - 2000/60/EC) of the European parliament. Water is overall a fragile matrix: it plays an essential role to life but, at the same time water resources are highly susceptible to changes and pressures imposed on the systems that comprise them, be that from climate change or from overconsumption by human activities. Access to high-quality water is often local and intermittent, and constantly threatened by contamination and parochial interests.

Down-to-drain is a way to (supposedly) get rid of hundreds of chemical products derived from houses, agriculture, livestock, industry, and hospital activities which, if not treated, become a source of pollution. The WFD established a European common strategy to tackle the spread of water pollution in the communitarian territory. In 2001, a list was promulgated that includes 33 priority substances or group of substances to be controlled (Decision n.2455/2001/EC). Subsequently, Directive 2008/105/EC defined the Environmental Quality Standards (EQSs), namely, the maximum allowable concentrations of 41 compounds (33 identified in 2001, 8 already present in the regulation). Finally, Directive 2013/39/EU revised the list of priority substances, whose number was increased to 45, as well as their EQSs. One of the goals of the recent legislation has been to establish a mechanism of constant monitoring of emerging hazardous compounds in the aquatic environments, in order to evaluate the risks related to their presence in European water bodies. This mechanism is called Watch List (WL).<sup>17</sup> WL has the purpose to support the prioritisation exercises of emerging substances in line with Art. 16 of Directive 2000/60/EC and is based on the monitoring of emerging substances throughout the European territory, at least for a period of 4 years and on a limited number of significant stations.<sup>17</sup> The list of substances to be monitored shall be updated every two years and substances that are not found in the environment at significant concentrations shall be eliminated by the Commission. The first WL was adopted in 2015 (in Decision 2015/495/EU) and subsequently updated in 2018 (in Decision 2018/840/EU). In 2020, a selection of substances was proposed for the 3<sup>rd</sup> WL in a JRC Report.<sup>18</sup> The inclusion of a substance or a group of substances depends on its own risk factors, which is defined according to harmonized assessment methods.<sup>17</sup>

The contaminants added to the WLs are the so-called contaminants of emerging concern (CECs). A CEC is a compound detected in water bodies which may be detrimental to ecosystems or human health and still not regulated under local environmental laws. A CEC has to be monitored in order to verify its impacts, eventually include the compound in the priority list, and then in the local environmental regulation. Diclofenac, estrogens like EE2 (17-alfa-ethinilestradiol) and E2 (17-betaestradiolo), and antibiotics are emblematic examples of CECs. Diclofenac is a widely used anti-inflammatory drug and only 6-7%<sup>19,20</sup> of the intake amount is finally metabolized, the rest being secreted by urines and faeces. EE2 is the major principle of the contraceptive pill and it is used in various other hormonal therapies.<sup>21</sup> E2 is naturally biosynthesized in human body and daily secreted.<sup>22</sup> EE2, E2, and diclofenac are all endocrine disruptors. The chronic assumption of an endocrine disruptor is related to a plethora of potential effect on the health of humans and other organisms, such as learning disabilities, cognitive

and brain development problems, deformation of the body, breast cancer, prostate cancer, as well as sexual development issues, such as feminizing of males or masculinizing effects on females.<sup>23–26</sup> Moreover, antibiotics release into the environment may cause antibiotic resistance, which neutralizes their effect.<sup>27,28</sup> If the risk of a CEC is found to be significant, a decontamination strategy should be immediately ready to be implemented ideally at the contamination source. Therefore, the research work to define the best CECs treatment strategy should proceed alongside that to understand their potential risk.

While estrogens can be degraded by biological treatments,<sup>29</sup> antibiotics, diclofenac, and several other CECs are recalcitrant and require other type of treatments for their removal from water.<sup>30</sup> Membrane filtration is a promising strategy in the removal of micropollutants in both wastewater and drinking water.<sup>31</sup> However, filtration does not degrade contaminants, and creates a concentrated stream that must be managed carefully, or which require further treatment. On the other hand, oxidation processes can effectively degrade micropollutants, representing a valid alternative or complement to membrane treatment in the management of micropollutants in a water management system.<sup>32</sup>

### 1.1.2 Biological contaminants and disinfection by-products

CECs represent a critical source of water pollution; however, they are not as widespread as biological contaminants, which include bacteria, viruses, protozoan, and parasites.<sup>33</sup> These are responsible of waterborne diseases. Recent studies reported that two and a half billion people (more than a third of the world's population) have no access to sanitized water, and more than 1.5 million children die each year from diarrheal diseases.<sup>34,35</sup> All diarrheal diseases are caused by numerous viral, bacterial, or parasitic infections and are estimated as the waterborne diseases that cause the highest rates of morbidity and mortality. Specifically, it is estimated that 4 billion cases of such diseases and around 2 million associated deaths occur annually.<sup>36,37</sup> Unfortunately, in several countries and areas, disinfection strategies are generally too expensive for the local economies. Even where chemicals are effectively applied to control microbiological contamination, issues may arise concerning the formation of disinfection by-products (DBPs). Various investigations have found a numerical increased risk for cancer of the urinary bladder and colon, as well as some reproductive/developmental effects, among consumers of chlorinated water.<sup>38</sup> The underlying basis for these health effects appears to be precisely the presence of DBPs formed during a disinfection process. The typical DBPs associated with chlorination are trihalomethanes (THMs) and halogenated by-products, which are indeed associated with several carcinogenic and teratogenic effects. It is highly

important to identify biocides able to effectively disinfect water, by reducing the impact of DBPs on the environment and human health.<sup>39</sup>

Chlorine is an oxidant; thus, possible alternatives can be found in the same class of biocides. Ozone, chlorine dioxide, hydrogen peroxide ( $\text{H}_2\text{O}_2$ ), and peracetic acid (PAA) are all possible alternative oxidants. However, despite the fact that all of these alternative compounds drastically reduce the formation of THMs compared with chlorine, they are not a panacea. Ozone is highly expensive and generates bromate in the presence of bromide (bromate is a suspected carcinogenic compound).<sup>40,41</sup>  $\text{H}_2\text{O}_2$  is a less effective disinfectant and its deployment is associated with safety issues.<sup>42</sup> Chlorine dioxide and peracetic acid may be the most successful alternative oxidants for disinfection. However, recent studies have demonstrated that the former could generate chlorite and chlorate, both harmful DBPs, together with traces of tribromomethane, while the latter represents a potential source of THMs in the presence of bromide in water, as also proven in this thesis.<sup>43,44</sup> Other classes of biocides, such as lytic biocides (*i.e.*, quaternary ammonium salts), electrophilic biocides (*i.e.*, thiazolinones), and reductants (sulfites) may represent a valid alternative to chlorination.<sup>45–48</sup> However, also these compounds may generate THMs in specific conditions, as evaluated in this thesis. Therefore, there is no perfect and unique strategy to sanitize water; conversely, there are numerous strategies at hand that need to be adapted to the specific circumstances. To preserve ecosystems and prevent antibiotic resistance, not only natural biodiversity, but also the “biodiversity” of the disinfection strategies should be promoted and improved.

## **1.2 From oxidations to Advanced Oxidation Processes: an overview**

From the discovery of dioxygen as oxidizing agent and the expanded ability to employ this reagent in chemical reactions, many other oxidizing agents were discovered and developed. Also, the definition of “oxidation” has been adapted to the latest discoveries. Since also metals and chemical compounds that do not contain oxygen were identified as oxidant agents, the oxidation definition was improved from “a reaction with oxygen to form an oxide” to “a loss of electrons or an increase in the oxidation state of an atom, an ion, or of certain atoms in a molecule”.<sup>2</sup>

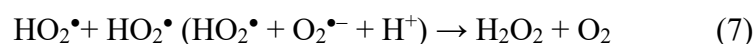
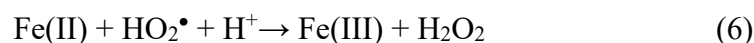
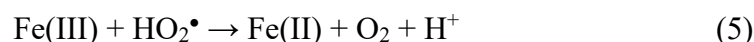
In 1894 H.J.H. Fenton postulated a reaction named after himself that paved the way for a new era in chemistry.<sup>49</sup> He fortuitously discovered that irons combined with oxidizing agents had higher oxidative capacity than that of its separate components. In the first implementation of the process hydrogen



peroxide, tartaric acid, a base, and iron(II) salt were mixed in the same bulk.<sup>49</sup> Thereafter, the components of “Fenton reaction” or “Fenton reagent” were generalized in what we refer today as Fenton chemistry:

- 1) the use of an oxidant,
- 2) a metal in its reduced form and
- 3) the involvement of higher oxidation states of the metal.

Initially Fenton reaction involved iron(II) and H<sub>2</sub>O<sub>2</sub>. Currently, it was discovered that many metals can be used to facilitate the reaction, involving Cu, Mn, V, Co;<sup>50</sup> persulfate and/or organic peroxides can also be activated, and the H<sub>2</sub>O<sub>2</sub> can be replaced by hypochlorous acid other oxides.<sup>51–54</sup> When considering the Fenton reaction, a substantial fraction of the community agrees with the mechanism initially proposed by Haber and Weiss,<sup>55,56</sup> which includes the formation of •OH. See the scheme below:



However, the Fenton reaction mechanism is still under debate. For instance, Bossmann and co-workers proposed the involvement of a ferryl species [Fe(IV)=O]<sup>2+</sup> and other studies supported this hypothesis.<sup>57–61</sup>

The Fenton chemistry represents the traditional example of an advanced oxidation process (AOP).<sup>62</sup> AOPs also include photolysis of H<sub>2</sub>O<sub>2</sub> or O<sub>3</sub>, photocatalysis (light based AOPs), electron-beam, plasma technologies, supercritical water oxidation, wet air oxidation, water sonolysis, and other processes.<sup>63</sup> AOPs are based on the *in-situ* generation of strong oxidants: the vast majority of available AOPs encompass the formation of the hydroxyl radical (•OH), but also processes based on other oxidizing species exist, exploiting sulfate or chlorine radicals.<sup>64</sup> AOPs have been extended to several applications during the course of history. Fenton himself continued his research using this reaction for the synthesis

of hydroxylated compounds.<sup>65</sup> In 1980s, AOPs were proposed in potable water treatments for the first time. By virtue of the high oxidative power of the  $\bullet\text{OH}$  ( $E^\circ=1.9\div2.7$  V vs. NHE)<sup>10</sup> and of its radical, hence wide-ranging (and unselective) behavior, AOPs represent a highly promising strategy toward the degradation of organic pollutants, micropollutants, and generally the transformation of oxidizable compounds.<sup>10,63,66</sup>

In particular, the removal of organic pollutants from water is currently carried out mainly by means of separation processes (e.g., sedimentation, flocculation, filtration, electrocoagulation, adsorption on active carbon)<sup>67</sup> or biological treatment.<sup>68</sup> However, separation processes concentrate contaminants in sludge or solids that must be managed or destroyed elsewhere, and biological treatment is not sufficiently effective in the removal of many biorecalcitrant pollutants (*vide supra*).<sup>30</sup> Numerous AOPs have been recently developed to destroy the organic pollutants into the water bulk, without the need of separation and post-treatment processes. AOPs have the advantage to destroy unselectively any organic pollutant directly in water with reactor volumes that are smaller than the typical biological ones. The employment of these new technologies would ideally provide the complete decomposition of biorecalcitrant compounds, thus preventing their persistence in the environment, but also allowing the recycling or reuse of water in the perspective of circular economy. However, the unselective behavior of  $\bullet\text{OH}$ , as well as of all the other radicals generated in AOPs, is also the major drawback of this strategy. If mineralization, namely, the transformation of TOC in  $\text{H}_2\text{O}$  and  $\text{CO}_2$ , is not reached during the application of AOPs, intermediate product generation is one of the most critical factors for the process viability. The concomitant presence of halogens and dissolved organic matter (DOM) while an AOP occurs, usually leads to the formation of potentially carcinogenic halogenated by-products.<sup>39,69</sup> Also, in the presence of bromide and chloride,  $\bullet\text{OH}$  may generate bromate and chlorate, other harmful by-products.<sup>64</sup> Beside the generation of harmful by-products, another critical aspect of AOPs is the ease of scavenging  $\bullet\text{OH}$  in the presence of typical species of real wastewater, such as inorganic ions and DOM itself.<sup>64</sup>

The Fenton process is generally still considered the most viable AOP in water treatment due to the ease and low costs of its implementation. However, beside the aforementioned limitations, typical of all AOPs, other practical limitations related to Fenton process must be considered. First, iron(III) involved in the Fenton reaction tends to precipitate as hydroxide under basic pH conditions. In order to limit the precipitation of iron(III) as hydroxide, the pH needs to be adjusted to acidic pH, generally  $\text{pH}\sim 3$ .<sup>70</sup> However, due to the unavoidable precipitation of iron hydroxide and organic matter during the process, a large

amount of sludge is generated, which then needs to be disposed of.<sup>70</sup> Also,  $\text{H}_2\text{O}_2$  stored in large volume and at high concentration is an explosive reactant.<sup>42</sup> Not everywhere are in place infrastructures or trained employees available to manage a high number of harmful compounds, such as acids, bases, and hydrogen peroxide, which may represent a major issue for the security and safety in the workplace. Therefore, new strategies to increase the viability and sustainability of AOPs are necessary.

### 1.3 AOPs in biochemical and biomimetic processes

Iron is the most abundant transition metal on Earth, and not casually it is employed in many redox-active metalloproteins in living organisms.<sup>71</sup> By virtue of its electronic properties and its accessible redox potential, iron modulates several redox processes in biological systems.<sup>72</sup> Metalloproteins might be heme (*i.e.*, Cytochrome P450, methane monooxygenase)<sup>72,73</sup> or non-heme type (*i.e.*, Rieske dioxygenase, Taurine dioxygenase)<sup>74,75</sup> and they are used to activate dioxygen or hydrogen peroxide to generate high-valent oxoiron reactive intermediates. The heme type peroxidases, oxygenases and catalases, are characterized by a mononuclear iron-protophyrin IX active site.<sup>76</sup> The non-heme types generally involve simpler structures, namely, mononuclear iron centres that are coordinated to two histidines and a carboxylate group.<sup>74,75</sup> Cytochrome P450 and Rieske dioxygenase are the most studied heme and non-heme systems, respectively. Both promote extremely selective oxidation processes toward exogenous and endogenous compounds, mediated by a high-valent oxoiron which works as a highly reactive oxidant.<sup>73–75,77</sup> A high-valent oxoiron species promotes a metal-based process, which is the key strategy to enhance a selective reaction. Indeed, a metal-based process allows the molecular structure of the catalyst to lead the reaction path by means of steric and chemical interactions. Selectivity is intended as the ability of a process to discriminate both among compounds and among the positions in the molecular structure of a specific target compound.

Ranging from organic synthesis, where regio- and stereospecific oxidations are crucial, to water treatments, where mild, selective and clean oxidations would limit the formation of toxic by-products and increase the efficiency of the process toward specific compounds, selectivity is a crucial topic in the field of catalysis and biological systems. Indeed, both heme and non-heme structures have been emulated to synthesize catalysts for the selective oxidation of organic compounds.<sup>71,78</sup> Also, in the water treatment field, the literature reports numerous attempts to employ the Cytochrome P450 to perform selective oxidations of toxic compounds.<sup>79–81</sup> In the 00s, a non-heme organo-iron complex (Fe-TAML) was first synthesized and efficiently employed as a hydrogen peroxide activator in

water treatment.<sup>82</sup> Fe-TAML demonstrates the ability to degrade several toxic organic compounds through a high-valent oxo-iron species, hence increasing the selectivity of a classic Fenton process.<sup>83–86</sup> Moreover, Fe-TAML works under basic conditions rather than at acidic pH.<sup>85</sup> Beside Fe-TAML, also other iron complexes have been employed in water treatment. Citric acid and other natural organic acids (e.g., tartaric, quinic, malic, ascorbic acid) are widely recognized as effective iron chelators.<sup>87</sup> Citrate binds Fe(II) at the active site of aconitase and has been proposed to be a constituent of the low molecular weight cytosolic iron pool.<sup>88</sup> Furthermore, the ability of citrate to solubilize ferric hydroxide has been exploited by both plants and microbes.<sup>88</sup> Other than natural carboxyl acids, also artificial ligands, such as EDTA, EDDS, and NTA are effective iron chelators.<sup>87</sup>

All the resulting iron complexes from the ligands mentioned above have been demonstrated to work as hydrogen peroxide activators in the degradation of toxic compounds in water at near-neutral pH. However, their reaction mechanism is still under debate. The community is split in the two parties supporting one the importance of free radicals and other the dominance of metal-based species. Interestingly, Rush and Koppenol proposed that a metal-oxo species is generated in neutral solutions, while  $\bullet\text{OH}$  species dominated the process in acidic solutions of non-chelated iron.<sup>89,90</sup> Also, in this thesis a dominant metal-based behavior was proven when an iron-ligand complex is employed as hydrogen peroxide activator. On the other hand, Sutton et al. reached a different conclusion, proposing that free iron generates a metal-oxo species as the primary oxidant, while  $\bullet\text{OH}$  is dominant when chelated iron is present.<sup>91</sup> A reasonable rationalization of this apparent discrepancy is that metal-oxo species and  $\bullet\text{OH}$  can both be generated concurrently in a Fenton or Modified-Fenton system. Indeed, studying a Fenton process, Minero and co-workers concluded that  $\bullet\text{OH}$  (60% yield) and other species (e.g.,  $\text{FeO}^{2+}$ ) (40% yield) are formed simultaneously. In the same way, in a modified-Fenton process<sup>60</sup>, Yamazaki and Piette suggested that more than one type of oxidizing intermediate is present, and that the stoichiometry  $\bullet\text{OH}:\text{Fe(II)}$  is also a function of the nature of the prevailing iron chelators. Subsequently, the same authors noted the formation of several adducts other than the sole 5,5-dimethyl-1-pyrroline *N*-oxide (DMPO)–OH, which is supposed to be the only one formed in the presence of  $\bullet\text{OH}$ , hence suggesting the concomitant presence of more than one oxidant transient species. Prousek corroborated this conclusions stating that both species,  $\bullet\text{OH}$  and  $[\text{Fe(IV)=O}]^{2+}$ , can be formed in a modified-Fenton process. The possible dominant metal-based behavior in iron-chelated systems is the key strategy for a higher selectivity in the oxidation path, in the same way of biological non-heme systems.

Taking inspiration by biological systems, hence employing an effective iron ligand, would potentially overcome two major limitations of AOPs and of the Fenton process, namely, their non-selectivity and the need of acidic pH. Moreover, the implementation of a cheap, environmentally friendly and easy to handle hydrogen peroxide activator represents a highly viable tool in water treatment plants. Natural organic acids and artificial chelator are promising options. Gaining insight into their behavior in the oxidation process is crucial, also to promote the identification and synthesis of other iron complexes to act as effective catalysts in water treatment.

### 1.4 Thesis hypotheses and objectives

Oxidative processes are a powerful tool to control chemical and biological contaminations of water streams. Specifically, AOPs provide promising results in the degradation of biorecalcitrant CECs, while the use of oxidants is highly effective in water disinfection. However, as discussed above AOPs and oxidants may lead to the formation of more toxic by-products and intermediates.<sup>64</sup> Moreover, AOPs are often not sustainable due to the employment of harmful compounds, such as acids, bases, or toxic nanoparticles and due to the formation of large amount of sludge in the case of Fenton systems.<sup>70</sup> This thesis investigates new strategies to overcome the aforementioned limitations, to increase the sustainability and the effectiveness of oxidation processes. The study of reaction and disinfection mechanisms is exploited as a tool to gain insight into target processes and promote possible new frontiers of development.

In the second chapter, new and potentially more sustainable modified-Fenton systems are proposed and discussed for the degradation of CECs. A systematic investigation in the reaction mechanism when classic iron chelators are employed as hydrogen peroxide activators is discussed, paying attention to the possible mechanistic dichotomy between a free radical and a metal-based pathway. Biological systems teach us that oxidation routes mitigated by iron-coordinated active sites, such as Cytochrome P450 or the Rieske dioxygenase, are safer and more effective than other unmediated processes. Adopting the same “screenplay” of biological systems, the work discussed in this thesis attempts to substitute free-radical mechanisms with metal-based ones through the use of an iron complex, aiming to increase the selectivity of the process and solving other practical limitations implementing a safe hydrogen peroxide activator at near-neutral pH.

In the third chapter, oxidations are discussed with the goal of water disinfection. The general objective of this section is to evaluate the real risk of the tested disinfectants to generate DBPs, hence to define a strategy to limit DBPs generation and promote a safer management of disinfectants. Study of the

disinfection mechanism is the approach undertaken not only to understand the process, but to identify safer disinfection routes. Potential oxidants and non-oxidant disinfectants are investigated and applied in the disinfection of a real wastewater. Alternative compounds are proposed as possible alternative to more traditional disinfectants and their application is discussed in light of minimizing the production of harmful DBPs.

## Chapter 2

# 2 AOPs from living systems to water treatment: a sustainable approach\*

A sustainable process is intended as a process able to be reproduced numerous times in a defined reference system. Sustainable development takes into account the environmental, economic, and social perspectives. The route toward a sustainable technology or process considers both the feasibility of the process and the consequent stability of an ecosystem. With this respect, despite the fact that advanced oxidation is a powerful strategy toward water decontamination, AOPs rarely can be considered sustainable processes. For instance, the unselective behavior of the Fenton reaction and of traditional AOPs in general allows an effective degradation of a wide spectrum of contaminants. However, it does not allow control over the reaction pathway, an issue which may lead to the formation of harmful by-products.<sup>64</sup> Moreover, the Fenton process is somewhat inaccurately regarded as a catalytic process. Instead, by virtue of the radical reaction mechanism, the process generates a plethora of parasitic reactions which occur simultaneously.<sup>55</sup>

The Fenton process is partly catalytic due to the regeneration of iron(II) from iron(III). However, the turn-over is very low, due to the numerous concomitant parasitic reactions. A low or absent turn-over number means a higher

---

\* part of the content reported in this chapter, with permissions, has been already published in 187,190,294

consumption of the starting reagents (namely, iron salts and hydrogen peroxide), hence a waste of natural and economic resources. Also, the process requires the addition of acids and bases to adjust the pH.<sup>49</sup> Furthermore, the Fenton reaction generates a high amount of sludge which needs careful management. Other AOP, may avoid sludge formation or increase the selectivity of the process.<sup>10</sup> However, they generally employ toxic nanoparticles, expensive technologies, and unsafe reagents.<sup>66,92</sup> Therefore, increasing the sustainability of AOPs is of crucial importance.

The main objective of the studies discussed in this section is to investigate and optimize well-known oxidative catalytic processes with high turn-over number and at the same time, developing new catalytic and selective AOPs. The achievement of a more selective process is also an objective of these studies. A selective process may promote a safer reaction pathway and a more efficient oxidation toward specific contaminants. A metal-based mechanism was selected as the target mechanism to achieve a higher selectivity of the oxidation, in place of oxidation solely based on the activity of free radicals. The Fenton process is currently the most feasible AOP due to its efficiency, ease of implementation, and low cost. Therefore, it is a strong basis for an advancement of the state-of-the-art.

In the first part of this section, metabisulfite is studied as a safer substitute of hydrogen peroxide in the oxidation catalysed by Fe-TAML. Fe-TAML is a biodegradable iron complex generally used as activator of hydrogen peroxide or other oxidants. Fe-TAML promotes a metal-based oxidation of a wide spectrum of organic contaminants. It presents the optimum efficiency under basic pH and is active also at neutral pH, hence avoiding sludge formation and the need of adding acids and bases to change the pH is usually circumneutral water effluents. However, hydrogen peroxide might be a limiting element due to its explosive feature. Metabisulfite is proposed as an unconventional, effective and safer alternative to hydrogen peroxide, which may promote the implementation of the promising Fe-TAML system.

In the second part, a new iron-ligand system is manufactured to be used as both homogeneous and heterogeneous catalyst in the oxidation of emerging contaminants. Chitosan was the selected iron ligand, since this polymer is widely available, cheap, biodegradable, and environmentally friendly. The most probable transient species involved in the process are identified (namely metal-based ferryl species) in order to frame the possible higher selectivity of the process compared to the classic Fenton.

In the last part, a new analytical method to discriminate metal-based and free radical mechanism is developed and discussed. Common natural and artificial iron complexes are studied, as potential catalysts for oxidation. By virtue of its



structural symmetry, cyclohexane was selected as mechanistic probe. The ratio among its two main by-products, namely, cyclohexanol and cyclohexanone, provide insight into the reaction pathway. Common iron ligands are here proven to direct the reaction pathway towards a selective metal-based catalysis. Such a system may be more easily engineered than a free radical-based one to safely remove hazardous contaminants from water and minimize the production of harmful intermediates.

## **2.1 Metabisulfite as Unconventional Reagent for Green Oxidation of Emerging Contaminants Using an Iron-based Catalyst**

### **2.1.1 Introduction**

Micropollutants, such as pesticides, pharmaceuticals, and personal care products are persistent and biologically active substances. They are ubiquitous in aquatic environments and can jeopardize the life of plants, animals, and humans.<sup>17</sup> The Fenton reaction is a promising advanced oxidation process to reduce micropollutants in water, and it has been proven effective for the degradation of a wide variety of recalcitrant and/or non-biodegradable pollutants in industrial wastewaters.<sup>93</sup> The main reactions involved in Fenton oxidation cause the formation of reactive species, such as - mainly - hydroxyl radicals and/or superoxidized iron species.<sup>55,93</sup> The Fenton process works best in the pH range 2.5-4, with the highest degradation rates usually observed around pH 3.<sup>94</sup>

Living organisms metabolize micropollutants and potentially toxic endogenous and exogenous compounds with Cytochrome P450, an iron-based family of enzymes.<sup>14</sup> On this basis, Collins and co-workers have developed an innovative catalyst for water decontamination, the Fe-TAML activator, which mimics the oxidative activity of Cytochrome P450 by forming a stable iron-oxo species in water when it reacts with peroxides.<sup>82</sup> Fe-TAML has a large spectrum of applications in the removal of recalcitrant micropollutants and pathogens from water.<sup>86,95-97</sup> Its reaction usually takes place at room temperature and it is most effective in the pH range 7.5-11, with the highest rates usually observed around pH 10-11.<sup>98</sup> An oxidation process that is efficient under basic conditions may be more promising and useful than a process operating under acidic conditions (e.g., the traditional Fenton process), for two main reasons: (i) it does not require pH adjustments when the water effluent is already alkaline, as in the case of some

industrial effluents; (ii) it allows the co-precipitation of inorganic cations (e.g., toxic metals) potentially present in the effluent, thus reducing the need of an *ad hoc* treatment step and preventing their possible interfering activity.<sup>99</sup> In this sense, oxidation by Fe-TAML or other similar catalysts as tools to improve the Fenton reaction, is potentially advantageous compared to a classic Fenton process.

Hydrogen peroxide is preferentially used as Fenton reagent, because of its relatively low cost, availability on the market, and fair environmental compatibility. Hydrogen peroxide is also the preferred reagent in the case of oxidations activated by Fe-TAML.<sup>82,83,86,95,96</sup> In addition to hydrogen peroxide, Fe-TAML can activate hypochlorite, organic peroxides, and oxone.<sup>83,100</sup> However, not all these alternative reagents are convenient in every circumstance. For instance, hypochlorite may lead to the formation of potentially carcinogenic chlorinated by-products.<sup>39,101–103</sup> Organic peroxides and oxone, besides being explosive and unsafe, have a high cost. Therefore, they may not be easily employed to treat large flow rates, which are commonly encountered in wastewater treatment plants.<sup>104,105</sup> While being the current best choice, hydrogen peroxide has also important limitations related to operational safety, particularly when it is used in large amounts and concentrations.  $\text{H}_2\text{O}_2$  is highly reactive, and it forms explosive mixtures upon contact with organic compounds.<sup>42</sup> Furthermore, it is corrosive and irritant for eyes, mucous membranes and skin, and its relatively high vapor pressure poses health risks by inhalation even following short exposure.<sup>42</sup>  $\text{H}_2\text{O}_2$  has also been classified as a known animal carcinogen, with unknown relevance on humans.<sup>106</sup> Finally, the thermodynamic instability of  $\text{H}_2\text{O}_2$  results in relatively short shelf life, especially when stored in concentrated solutions and exposed to ambient temperature. For all these reasons, research is needed to identify more benign reagents that combine all the positive features of hydrogen peroxide while minimizing safety hazards and operational burdens.

In preliminary tests, we found that benign species, such as sulfite and metabisulfite, can be effectively activated by Fe-TAML towards the degradation of micropollutants. Despite its activity as a reductant, sulfite can be activated towards the oxidative degradation of organic compounds.<sup>107–109</sup> On the other hand, to the best of our knowledge, no report is present in the literature regarding this peculiar reactivity of metabisulfite,  $\text{S}_2\text{O}_5^{2-}$ . It is a potentially low-cost, low-risk, and eco-friendly reagent, with limited health effects (e.g., it is used to preserve alcoholic beverages) and a demonstrated absence of carcinogenic activity.<sup>110</sup> Given its generally reducing nature, metabisulfite is sometimes used as a quencher of oxidative processes, such as Fenton or hypochlorite treatments.<sup>111,112</sup>

This part offers a comprehensive study of the activity of metabisulfite with Fe-TAML, towards the oxidative degradation of a selection of environmental micropollutants of increasing worldwide concern. A discussion on the reaction mechanism and the nature of the active species in the Fe-TAML/metabisulfite system (as it will be shown later on, iron-oxo rather than radical based) is also provided. Fe-TAML is a well-known green catalyst for the oxidative degradation of various organic contaminants and other compounds.<sup>82</sup> However, the discovery of cleaner and safer reagents different from those previously proposed (e.g., H<sub>2</sub>O<sub>2</sub>) is a breakthrough in the field of advanced oxidation processes, because it opens the route towards greener cleaning systems.

### 2.1.2 Materials and Methods

#### 2.1.2.1 Chemicals

Fe(III)-TAML was purchased from GreenOx Catalysts Inc. (Pittsburgh, PA, U.S.A.) Sodium phosphate tribasic was obtained from Carlo Erba (Italy). All the other reagents, buffer solutions, and solvents were purchased from Sigma-Aldrich. Water was of Milli-Q quality (TOC 2 ppb, resistivity  $\geq 18.2$  M $\Omega$  cm).

#### 2.1.2.2 Preparation of the Fe-TAML stock solution

A stock solution of Fe-TAML was prepared by dissolving 520 mg Fe-TAML in 200 mL of a sodium hydroxide solution (0.05 M). The supernatant of this solution was used for further experiments. UV-Vis analysis was carried out to determine the effective Fe-TAML concentration at pH 7, by measuring light absorbance at 360 nm. From the known Fe-TAML absorption coefficient (6600 M<sup>-1</sup>cm<sup>-1</sup>), a stock solution with concentration of 3.1 mM was prepared. The stability of the catalyst in solution was spectrophotometrically checked every month. The stock solution was stored refrigerated (4 °C) under N<sub>2</sub> atmosphere.

#### 2.1.2.3 Protocol of the oxidation experiments

Three different reagents (sodium sulfite, SO<sub>3</sub><sup>2-</sup>, potassium metabisulfite, S<sub>2</sub>O<sub>5</sub><sup>2-</sup>, and sodium persulfate, S<sub>2</sub>O<sub>8</sub><sup>2-</sup>) were preliminarily tested, and their reactivity was compared with that of hydrogen peroxide. The most reactive compound, namely, metabisulfite, was then chosen to carry out further degradation experiments on several contaminants. Finally, the reaction mechanism with metabisulfite was investigated. The degradation experiments were carried out at room temperature, under continuous stirring for a maximum of 60 min. Reactions were tested at different pH values (7, 9, and 11), in 10 mL of phosphate buffer (total concentration 0.01 M). Under such conditions, the

demetallation of Fe-TAML via the general acid mechanism can be considered negligible.<sup>113,114</sup> As shown in previous literature reports, the demetallation kinetics of Fe-TAML increases as the pH decreases, or as the concentration of the buffering agents increases at constant pH. For these reasons, the phosphate buffer concentration used in this study was as low as reported in previous works.<sup>98,113</sup> It is important to note that the mechanism of demetallation has not yet been fully understood.<sup>113</sup>

Unless otherwise stated, the default initial concentrations in the experiments were as follows: 0.01 mM of Fe-TAML, 0.1 mM of the target contaminant, and 0.1 mM of reagent ( $\text{H}_2\text{O}_2$ ,  $\text{SO}_3^{2-}$ ,  $\text{S}_2\text{O}_5^{2-}$ , or  $\text{S}_2\text{O}_8^{2-}$ ). During some tests, stepwise additions of reagent corresponding each to a 0.1 mM concentration in the reaction system were made every 10 min, for a total of three additions. In all of these latter cases, the overall molar ratio of Fe-TAML:contaminant:reagent was 1:10:30. All the reactions were quenched by decreasing the pH to a final value  $< 3$ . Under acidic conditions, demetallation is promoted and the catalytic reaction is stopped as a consequence.<sup>113</sup> In some experiments involving metabisulfite, control tests were performed by analysis of the solutions immediately following reaction and without acidification. No significant differences in the concentration of contaminants were observed with or without acidification of the solution.

#### 2.1.2.4 Analytical methods

UV-vis spectrophotometric measurements were performed using a Cary 100 Scan double-beam instrument (Varian). The concentrations of contaminants in solution were monitored by high-performance liquid chromatography coupled with diode array detection (HPLC-DAD). The adopted LaChrom Elite instrument (VWR-Hitachi) was equipped with a L-2200 Autosampler (injection volume 60  $\mu\text{L}$ ), a L-2130 quaternary pump for low-pressure gradients, a L-2300 column oven (set at 40  $^\circ\text{C}$ ), and a L-2455 DAD detector. The column was a RP-C18 LichroCART (VWR Int., length 125 mm, diameter 4 mm), packed with LiChrospher 100 RP-18 (5  $\mu\text{m}$  diameter).

The different test contaminants were always eluted in isocratic mode, with a mixture of A = 5.7 mmol  $\text{L}^{-1}$   $\text{H}_3\text{PO}_4$  in water and B = methanol, at a flow rate of 1  $\text{mL min}^{-1}$ . The following conditions were used ( $\lambda$  = detection wavelength,  $t_R$  = retention time): acesulfame K (ACE, 5% B,  $\lambda$  = 220 nm and  $t_R$  = 4 min); atrazine (ATZ, 60% B,  $\lambda$  = 221 nm and  $t_R$  = 4.5 min); diclofenac (DCF, 65% B,  $\lambda$  = 275 nm and  $t_R$  = 8 min); ibuprofen (IBU, 70% B,  $\lambda$  = 222 nm and  $t_R$  = 6 min); naproxen (NPX, 60% B,  $\lambda$  = 220 nm and  $t_R$  = 6 min); oxybenzone (*aka* benzophenone-3, BP3, 70% B,  $\lambda$  = 280 nm and  $t_R$  = 5 min); phenol (PhOH, 30%

B,  $\lambda = 271$  nm and  $t_R = 5.5$  min); triclosan (TCS, 70% B,  $\lambda = 280$  nm and  $t_R = 9.6$  min).

Note that the study of the degradation of the investigated substrates cannot be considered in terms of the evolution of the Total Organic Carbon (TOC) in solution, because *i*) the Fe-TAML catalyst is in homogeneous form and *ii*) the organic TAML ligand increases the overall TOC value, thereby interfering with the assessment of contaminant mineralization. Still, the studied systems are unlikely to achieve substrate mineralization, as suggested by the occurrence of several unknown HPLC peaks, presumably accounted for by transformation intermediates (more hydrophilic than the original substrates on the basis of their chromatographic retention times), even at long reaction times.

#### 2.1.2.5 Electrochemical measurements

The redox properties and stability of the investigated substrates were electrochemically investigated. The electrochemical experiments were carried out through a standard photoelectrochemical set-up and a computer-controlled potentiostat (PGSTAT12, Autolab). The electrochemical cell was a conventional three-electrode cell. The counter and reference electrodes were a glassy carbon rod (diameter 2mm, length 75mm) and an Ag/AgCl/KCl (3 M) electrode, respectively. The working electrode was a 5 mm diameter glassy carbon disk. The electrolytic solution was 0.1 M NaClO<sub>4</sub> in CH<sub>3</sub>CN, purged with nitrogen gas. Cyclic Voltammeteries (CVs) were recorded between  $-0.4$  V and  $2.0$  V, at a scan rate of  $100 \text{ mV s}^{-1}$ . To better detect the onset of the anodic current, CVs were recorded on 10 mM solutions of each studied compound, with the exceptions of atrazine and acesulfame K. In the latter cases, CVs were recorded on saturated CH<sub>3</sub>CN solutions. The CVs here reported are the average of at least 3 successive scans, unless otherwise stated.

### 2.1.3 Results and Discussion

#### 2.1.3.1 Performance of different reagents towards the degradation of phenol

The activity of hydrogen peroxide in the degradation of various classes of contaminants with Fe-TAML is widely reported in the literature.<sup>83,84,86,96,115</sup> Therefore, H<sub>2</sub>O<sub>2</sub> was here used as a comparative standard. Figure 1 shows the catalytic degradation of phenol in 3-step addition experiments, using Fe-TAML and sulfite (SO<sub>3</sub><sup>2-</sup>, Figure 2.1.1a), metabisulfite (S<sub>2</sub>O<sub>5</sub><sup>2-</sup>, Figure 2.1.1b), persulfate (S<sub>2</sub>O<sub>8</sub><sup>2-</sup>, Figure 2.1.1c), and hydrogen peroxide (Figure 2.1.1d, only one addition) as reagents. After each addition of metabisulfite (one every 10 min, *i.e.*, at 0, 10,

and 20 min reaction time) there was a significant phenol degradation, soon followed by stabilization of the phenol concentration, with an overall step-like trend that closely mirrored the step-wise  $\text{S}_2\text{O}_5^{2-}$  additions. This finding is similar to recent results, obtained in the framework of the traditional Fenton reaction.<sup>116</sup> Duplicates and triplicates of these tests showed high reproducibility and are presented in Figure A1 in Appendix A. The repetitions showed high robustness and reproducibility of the adopted experimental procedures. All the reactions were quenched by decreasing the pH to a final value  $< 3$ . Under acidic conditions, demetallation (decomplexation of the Fe-TAML complex) is promoted and the catalytic reaction is stopped as a consequence, also considering the limited reactivity of Fe(III) species with  $\text{H}_2\text{O}_2$  and similar reagents in very acidic conditions.<sup>113</sup> Metabisulfite was more effective than sulfite towards phenol degradation, and the highest degradation efficiency for the two reagents was achieved at pH 11. On the other hand, persulfate did not show any activity toward the degradation of phenol (further insights below). Table A1 of Appendix A reports the degradation percentages reached at the end of the degradation experiments, for all the investigated conditions.

Wherever a significant reactivity was observed (*i.e.*, with sulfite, metabisulfite, and mainly hydrogen peroxide), phenol degradation was very fast immediately after the addition of the reagent. It then followed a rapid stabilization of the substrate concentration. This behavior prevented the details of the degradation kinetics to be monitored with the used experimental set-up, which was based on sample aliquots withdrawal from the reaction beaker, quenching of the reaction, and successive HPLC quantification of the residual substrate concentration. As a consequence, we could not measure the initial reaction rate. However, we could easily measure the degradation percentage, which is the most relevant information in the framework of water treatment. Additionally, such an approach allowed us to obtain sufficient insight into the reaction mechanism (*vide infra*). The first step of the reaction might be investigated by using the rather outmoded (and, unfortunately, not easily found nowadays) stopped-flow technique, which has proven for instance suitable for the investigation of the dark traditional Fenton process.<sup>60</sup>

## 2.1 Metabisulfite as Unconventional Reagent for Green Oxidation of Emerging Contaminants Using an Iron-based Catalyst

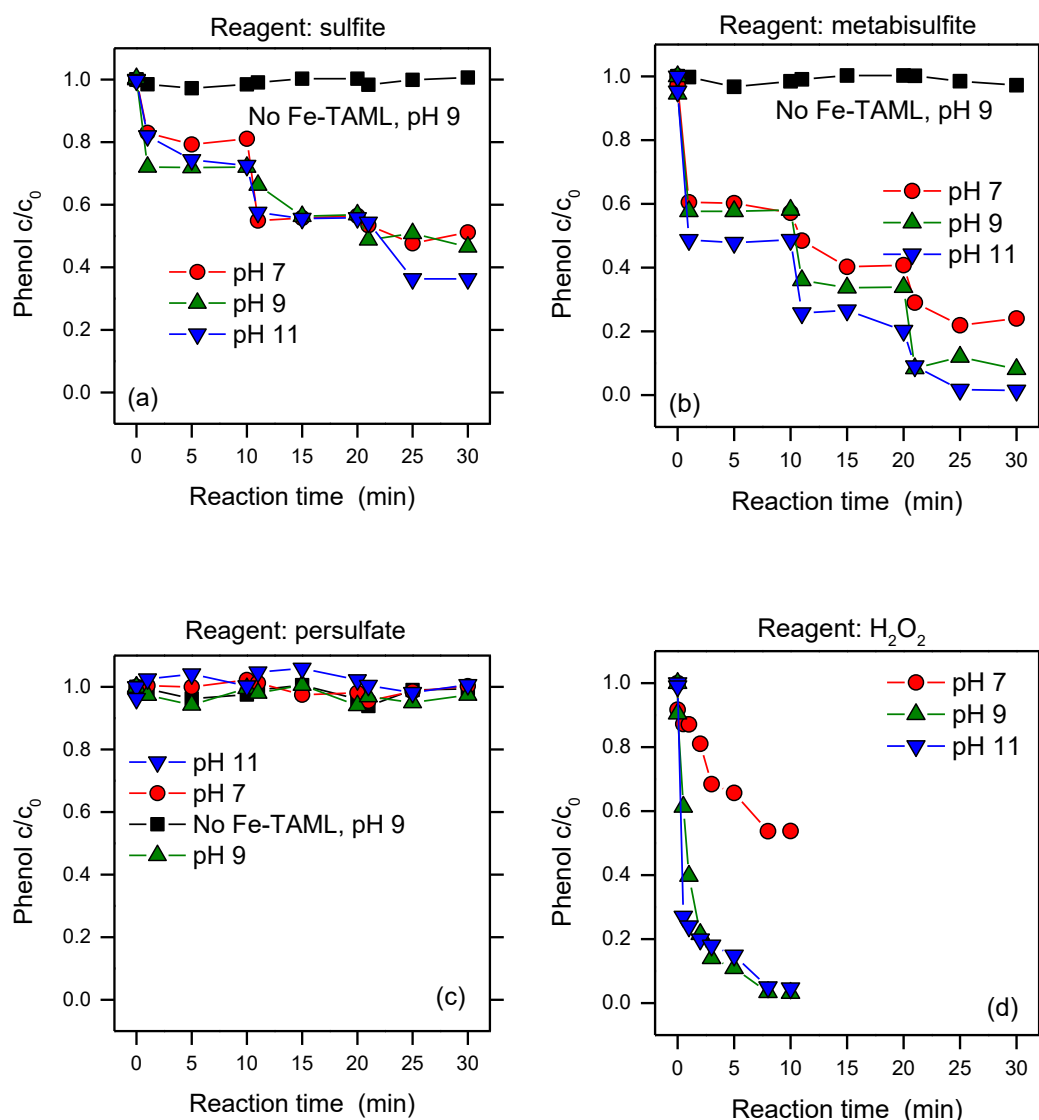


**Figure 2.1.1** Degradation of phenol with different reagents. Reagents were (a) sulfite, (b) metabisulfite, (c) persulfate, and (d)  $H_2O_2$ . The reactions were carried out in phosphate buffer (10 mM) by adding 0.1 mM of reagent every 10 minutes (*i.e.*, at  $t = 0, 10$ , and 20 min), with the exception of  $H_2O_2$  that was added only once at the beginning ( $t = 0$ ). Initial conditions were  $[Fe-TAML] = 0.01$  mM;  $[PhOH] = 0.1$  mM.

In general, the degradation efficiency was higher at basic pH values. Because phenol undergoes acid-base equilibrium ( $pK_a$  9.95),<sup>117</sup> at pH 9 the phenolate anion ( $PhO^-$ ) starts to be significantly present, while at pH 11 it prevails. Phenolate is more easily oxidized than neutral  $PhOH$ . In the case of  $H_2O_2$ , an almost complete degradation of phenol took place at both pH 9 and 11 with just

one hydrogen peroxide addition. In contrast, at pH 7 the  $\text{H}_2\text{O}_2$  treatment was less effective. The pH trend of the degradation efficiency was consistent with that reported by Collins et al. when using  $\text{H}_2\text{O}_2$ ; <sup>98</sup> please see further details in the Appendix A. Interestingly, the system containing Fe-TAML + persulfate was unable to induce significant degradation of phenol at any of the investigated pH values. It may be reasonable to assume that the inactivity of persulfate depends on poor complexation capability (steric hindrance) of the persulfate anion with the metal center of Fe-TAML (*vide infra*). <sup>118,119</sup>

The reported results suggest that metabisulfite is less effective than hydrogen peroxide in the degradation of phenol, but it is the most effective among the alternative reagents investigated here. Due to the lower cost and hazards of metabisulfite compared to  $\text{H}_2\text{O}_2$ , its reaction conditions were optimized, and its potential as a  $\text{H}_2\text{O}_2$  substitute was further investigated for the degradation of other contaminants of emerging concern (CECs). Some phenol degradation experiments were carried out to identify the experimental conditions able to maximize its transformation with metabisulfite. In particular, we wanted to assess whether the best degradation conditions could be reached with multi-step additions of metabisulfite at relatively low concentration, or with a single addition of the reagent at higher concentration. Figure 2.1.2 shows the results of the experiments carried out with Fe-TAML and metabisulfite at different pH values (7, 9, and 11), with only one addition of reagent at concentrations of 0.3 mM (Figure 2.1.2a) and 0.1 mM (Figure 2.1.2b; this latter experiment is similar to the first addition step reported in Figure 2.1.1b). While Figure 2.1.2b reported a slightly lower degradation percentage than Figure 2.1.1b at pH 7 (47% rather than 51% respectively), this difference is reasonably imputable to experimental errors during the measurement. Phenol concentration was monitored for up to 60 minutes. As expected, the reaction was very fast in the first 1-2 minutes after the addition of the reagent, and it followed a rapid stabilization of phenol concentration afterwards. The overall degradation performance was better when the concentration of metabisulfite was higher (*i.e.*, 0.3 mM), but the best results were definitely achieved when the same overall amount of metabisulfite was added in three separate steps (100% degradation, see Figure 2.1.1b), rather than in a single addition (80% degradation, Figure 2.1.2a). It is reasonable to assume that, in the case of a single large addition, the reagent itself partly scavenges the reactive species, as often observed in the classic Fenton process (note that metabisulfite has a reducing character). <sup>116</sup> In fact, within the same time interval, more reagent (higher concentration of metabisulfite) is available to react with the reactive species present in the system, compared with the addition of the same overall amount of reagent in separate steps. <sup>116</sup> Based on these results, the multiple addition approach appears to be the most rational way to use the  $\text{S}_2\text{O}_5^{2-}$  reagent,



## 2.1 Metabisulfite as Unconventional Reagent for Green Oxidation of Emerging Contaminants Using an Iron-based Catalyst

and it was chosen hereafter to perform the degradation of the contaminants under study.

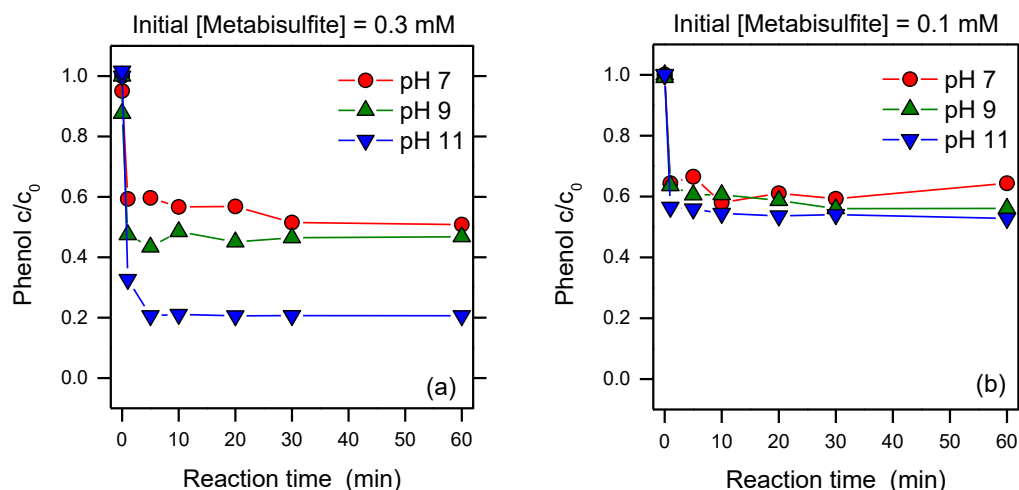


**Figure 2.1.2** Degradation of phenol with metabisulfite as reagent. The reactions were carried out in phosphate buffer (10 mM), with initial concentrations  $[\text{Fe-TAML}] = 0.01$  mM;  $[\text{PhOH}] = 0.1$  mM, and adding one aliquot of metabisulfite with initial concentrations of (a) 0.3 mM and (b) 0.1 mM.

### 2.1.3.2 Comparison of metabisulfite ( $\text{S}_2\text{O}_5^{2-}$ ) and hydrogen peroxide in the degradation of CECs

The ability of Fe-TAML to activate metabisulfite was tested against the degradation of additional micropollutants. Figure 2.1.3 shows the percentage of contaminant degradation after 1 h reaction time, when metabisulfite was used as reagent at different pH values (7, 9, and 11). The reaction was carried out by adding 0.1 mM of metabisulfite for a total of three times, once every ten minutes (*i.e.*, with a final concentration of 0.3 mM). After the last addition, the system was monitored for an additional forty minutes to observe possible further degradation of the tested contaminant (see Figures A2-A8 in the Appendix A for the whole-time trends). The same contaminants were also degraded following analogous protocol, but by using  $\text{H}_2\text{O}_2$  at pH 11 instead of  $\text{S}_2\text{O}_5^{2-}$ . This operational pH value was chosen because it is well known to maximize degradation efficiency with the couple Fe-TAML/ $\text{H}_2\text{O}_2$ .<sup>98</sup> The generally accepted reason for this pH behavior is twofold: (i) the Fe-TAML complex is involved in an acid-base equilibrium between the axial diaqua species  $[\text{FeL}(\text{OH}_2)_2]^-$  and the deprotonated form  $[\text{FeL}(\text{OH}_2)(\text{OH})]^{2-}$  ( $\text{L} = \text{TAML}$ ,  $\text{pK}_a > 11$ ); at the same time, (ii)  $\text{H}_2\text{O}_2$  behaves as well like a weak acid with  $\text{pK}_a \sim 11.2\text{--}11.6$ ;<sup>98,117</sup> see more details in Appendix A. Our experimental results suggest that metabisulfite and

hydrogen peroxide have similar activity toward the chosen contaminants. Specifically, Fe-TAML could activate efficiently both  $\text{S}_2\text{O}_5^{2-}$  and  $\text{H}_2\text{O}_2$  in the degradation of the phenolic compounds BP3, TCS, and PhOH. Moreover, both processes were also efficient in the degradation of DCF. On the other hand, although metabisulfite was marginally more active than hydrogen peroxide toward ACE, NPX, IBU, and ATZ, both reagents were largely ineffective towards these contaminants. Replicate tests suggested high reproducibility of these reaction processes, with final degradation yields from different tests always within 5% of the average value; see Figure A9 in Appendix A to see results from some test replicates.

Previous literature has reported that Fe-TAML forms an iron-oxo active species with peroxides.<sup>97,98,120</sup> The iron-oxo species is electrophilic, and it tends to react with electron-rich compounds that are easily oxidized. Coming back to our data, the complete degradation of PhOH and the inactivity of the process toward ACE (see Figure 2.1.3) are consistent with a peculiar role of oxidants with middle-high redox potential (such as iron-oxo species, *vide infra*) in both the Fe-TAML- $\text{H}_2\text{O}_2$  and the Fe-TAML- $\text{S}_2\text{O}_5^{2-}$  chemistry. Indeed, PhOH<sup>121</sup> is definitely electron-richer than ACE<sup>122</sup> (see also the electrochemical evidence reported below). The results, in terms of the Fe-TAML +  $\text{H}_2\text{O}_2$  reaction efficiency, may thus be rationalized with the different electronic structure of the contaminants, in agreement with Chen and White.<sup>123</sup> Then, because metabisulfite showed the same efficiency trend as  $\text{H}_2\text{O}_2$  towards the chosen contaminants, we can tentatively assume as a working hypothesis that there is a close analogy between the reactive species involved in the two cases.

Interestingly, when the Fe-TAML +  $\text{S}_2\text{O}_5^{2-}$  process led to quantitative or almost quantitative substrate transformation (*i.e.*, with PhOH, BP3, and TCS), the degradation efficiency was very similar at both pH 9 and 11, while the degradation at pH 7 was less effective. Conversely, when the degradation was inefficient (*i.e.*, with ACE, NPX, IBU, and ATZ), it was so at all the tested pH values. DCF is the only instance in which we observed a gradual increase of the degradation efficiency throughout the entire interval of increasing pH. Differently from DCF, the phenolic compounds PhOH, BP3 and TCS undergo acid-base equilibria in the pH interval 7-11, thereby yielding the corresponding easily oxidized phenolates at high pH.<sup>117</sup> For this reason, the case of DCF, which does not undergo acid-base equilibrium changes between pH 7 and 11, is likely to better reflect the genuine pH trend of the Fe-TAML +  $\text{S}_2\text{O}_5^{2-}$  reactivity. Note that a low Fe-TAML activity at pH 7 has already been reported in a previous paper describing the Fe-TAML activation of  $\text{H}_2\text{O}_2$ .<sup>98</sup>

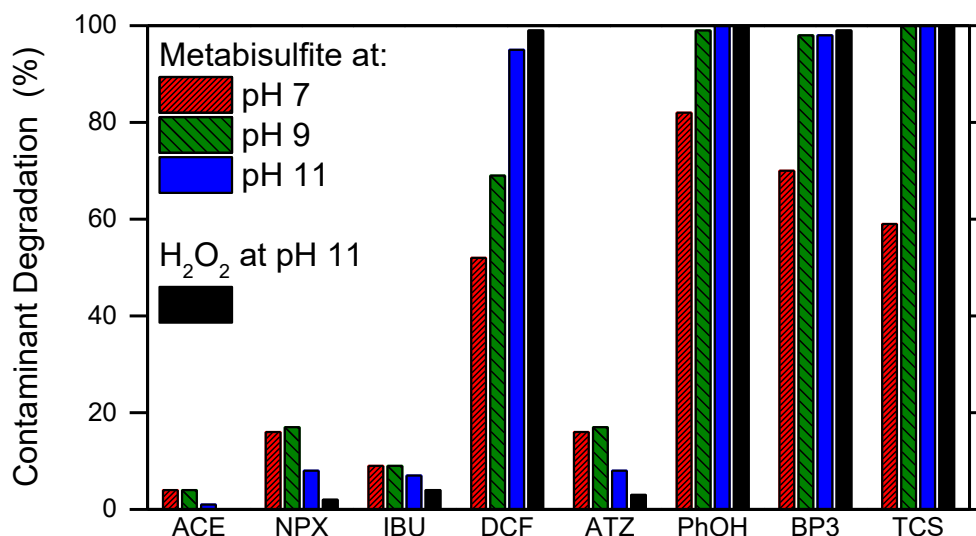


**Figure 2.1.3** Degradation percentage of the studied contaminants of emerging concern. Metabisulfite or H<sub>2</sub>O<sub>2</sub> were used as reagents at different pH values. The reactions were carried out for 60 min in phosphate buffer (10 mM), by adding 0.1 mM of reagent every 10 minutes for a total of three additions (at 0, 10, and 20 min). Initial conditions were [Fe-TAML] = 0.01 mM, and [Contaminant] = 0.1 mM.

Differently from the classic Fenton reaction at acidic pH, which is mainly driven by the production of hydroxyl radicals<sup>124</sup> and is usually poorly selective towards different pollutants, the Fe-TAML-activated process was more selective (see Figure 2.1.3). On the one hand, this means that a smaller number of contaminants can be targeted with Fe-TAML-Fenton compared to Fe<sup>2+</sup> + H<sub>2</sub>O<sub>2</sub>. However, higher selectivity (*i.e.*, the ability of the catalyst to discriminate amongst different compounds) might improve the degradation efficiency of target contaminants in a multi-polluted aqueous environment, especially in the presence of interfering agents such as the inherently harmless natural dissolved organic matter. Organic matter usually does not require a dedicated degradation step to detoxify a waste stream, but it is accidentally degraded by hydroxyl radicals and, by consuming them, it may considerably inhibit the traditional Fenton process.<sup>125</sup> In contrast, by virtue of higher selectivity, iron-oxo-based treatments may be less prone to interferences from organic matter.

### 2.1.3.3 Discussion on the nature of the active species and the reaction mechanism

While it is accepted that systems containing Fe-TAML + H<sub>2</sub>O<sub>2</sub> have an iron-oxo species as reactive transient,<sup>97,98,120</sup> there is no piece of information concerning the behavior of Fe-TAML + S<sub>2</sub>O<sub>5</sub><sup>2-</sup>, or the nature of the resulting active species. Indeed, this system is here described for the first time. As

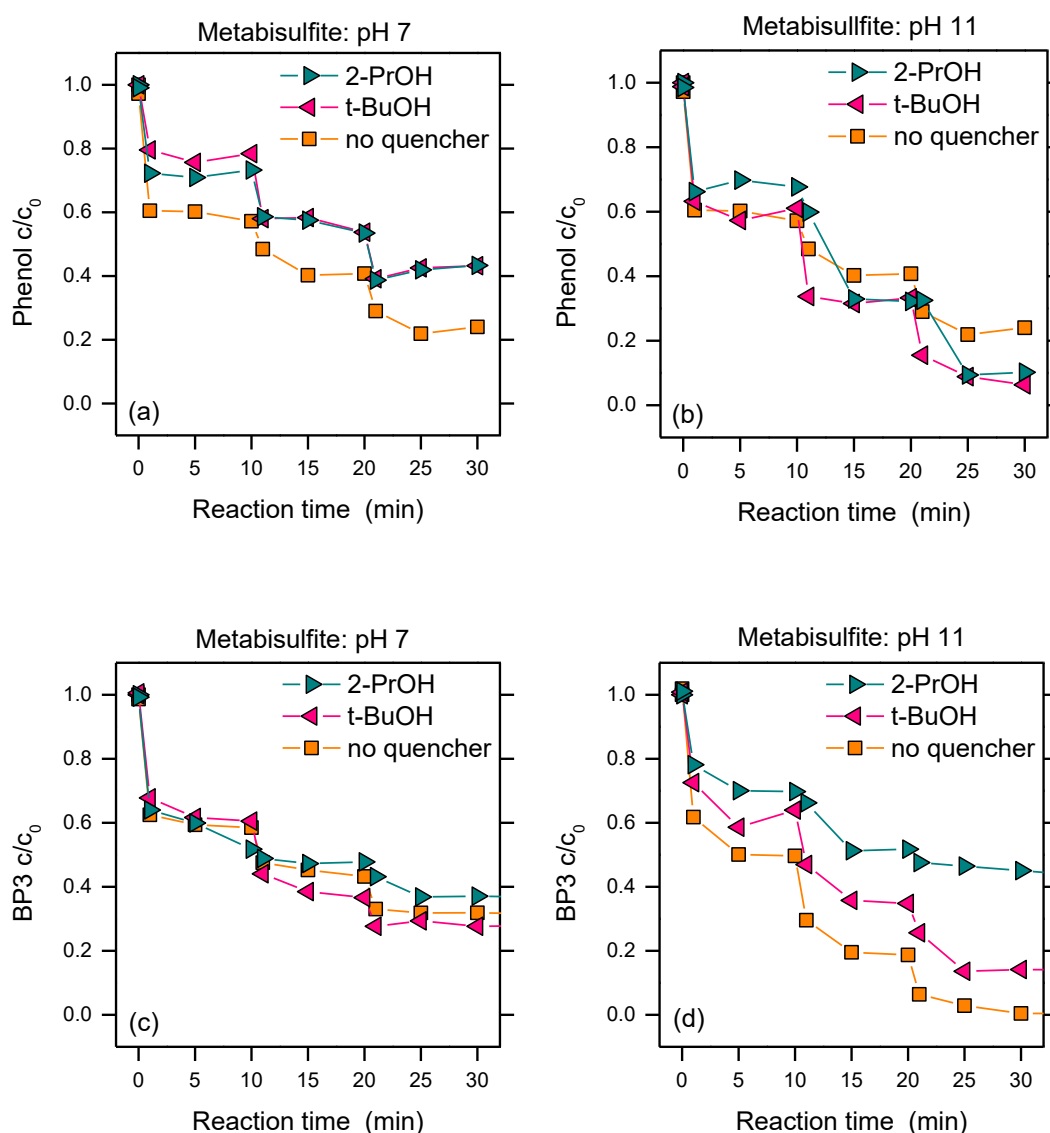
mentioned above, Fe-TAML + H<sub>2</sub>O<sub>2</sub> and Fe-TAML + S<sub>2</sub>O<sub>5</sub><sup>2-</sup> had analogous reactivity at pH 11 towards the studied substrates. Therefore, it is reasonable to hypothesize that the formed active species share some similarities. A series of tests were conducted to assess whether the main active species of Fe-TAML + S<sub>2</sub>O<sub>5</sub><sup>2-</sup> has radical or non-radical nature. Although we could not rely on any previous report concerning the S<sub>2</sub>O<sub>5</sub><sup>2-</sup>-based Fenton process, possible reactive radical species in, e.g., sulfite-based Fenton systems are hydroxyl (•OH) and sulfate (SO<sub>4</sub>•<sup>-</sup>).<sup>126</sup> In contrast, a Fe-based oxidant could trigger a non-radical pathway, in analogy with Fe-TAML + H<sub>2</sub>O<sub>2</sub>.

To get mechanistic insight into the studied process, *tert*-butanol (t-BuOH) and isopropyl alcohol (2-PrOH) were added into the solution as radical scavengers during the transformation of phenol. 2-PrOH is very reactive with hydroxyl radicals ( $k = 1.9 \times 10^9 \text{ M}^{-1} \text{ s}^{-1}$ ),<sup>127</sup> and significantly less so with sulfate radicals ( $k = 4 \times 10^7 \text{ M}^{-1} \text{ s}^{-1}$ ).<sup>128</sup> On the other hand, t-BuOH shows similar reactivity with both •OH ( $k = 4 \times 10^8 \text{ M}^{-1} \text{ s}^{-1}$ ) and SO<sub>4</sub>•<sup>-</sup> ( $k = 3.6 \times 10^8 \text{ M}^{-1} \text{ s}^{-1}$ ).<sup>127,128</sup> Different phenol degradation experiments were thus carried out with Fe-TAML and metabisulfite, in the presence of t-BuOH and 2-PrOH. Scavenger:phenol concentration ratios of 400:1 (t-BuOH) and 1330:1 (2-PrOH) were used. Considering the reaction rate constants of phenol/phenolate with •OH ( $k_{\text{PhOH}}$  and  $k_{\text{PhO}^-} \sim 10^{10} \text{ M}^{-1} \text{ s}^{-1}$ )<sup>127</sup> and SO<sub>4</sub>•<sup>-</sup> ( $k_{\text{PhOH}} = 2.2 \times 10^9 \text{ M}^{-1} \text{ s}^{-1}$ ,<sup>129</sup>  $k_{\text{PhO}^-}$  unknown but possibly similar, and  $< 10^{10} \text{ M}^{-1} \text{ s}^{-1}$ ),<sup>127</sup> it is expected that t-BuOH causes a ~95% inhibition of phenol degradation if •OH is the reactive species (*i.e.*, the degradation should be ~20 times lower with the alcohol). Moreover, almost total quenching by t-BuOH is expected in the case of SO<sub>4</sub>•<sup>-</sup>. Similarly, inhibition by PrOH should be quantitative with •OH, and in the order of ~90% with SO<sub>4</sub>•<sup>-</sup>.

The results shown in Figure 2.1.4a,b indicate that the alcohols caused limited inhibition of phenol degradation by Fe-TAML + S<sub>2</sub>O<sub>5</sub><sup>2-</sup> at pH 7, and practically no inhibition at pH 11. These results are not consistent with the occurrence of either •OH or SO<sub>4</sub>•<sup>-</sup> as the main reactive species, especially at the higher pH value (11), where we would expect inhibition to be much more evident in the case of a dominant role of the hydroxyl and sulfate radicals as reactive species of the process. From the data reported in Figure 2.1.4, it is not possible to provide a comprehensive explanation of the apparent slight inhibition of the process in the presence of 2-PrOH and t-BuOH. There are two possible reasonable explanations: (i) a minimal but not dominant portion of radical behavior exists in the process, (ii) a direct reaction between a non-radical active species and 2-PrOH and t-BuOH. Moreover, the two alcohols produced very similar and limited effects on the degradation of BP3, with both Fe-TAML + H<sub>2</sub>O<sub>2</sub> and Fe-TAML + S<sub>2</sub>O<sub>5</sub><sup>2-</sup>, at

## 2.1 Metabisulfite as Unconventional Reagent for Green Oxidation of Emerging Contaminants Using an Iron-based Catalyst

both pH 7 and 11 (see Figure 2.1.4c-f). This analogy in behavior further suggests that similar reactive species may be involved in Fe-TAML + H<sub>2</sub>O<sub>2</sub> and Fe-TAML + S<sub>2</sub>O<sub>5</sub><sup>2-</sup>. In the case of Fe-TAML + H<sub>2</sub>O<sub>2</sub>, the reactive species is well known to be of a non-radical nature.<sup>97,98,120</sup> By analogy, and given the overall results, it is reasonable to believe that an iron-oxo species may also occur in Fe-TAML+S<sub>2</sub>O<sub>5</sub><sup>2-</sup>. The limited, observed inhibition of the degradation process by alcohols would be due to the slight reactivity of the iron-oxo species (less oxidant with respect to •OH or SO<sub>4</sub>•<sup>-</sup>, *vide infra*) toward PrOH and t-BuOH, with no need to invoke radical-based reactions.



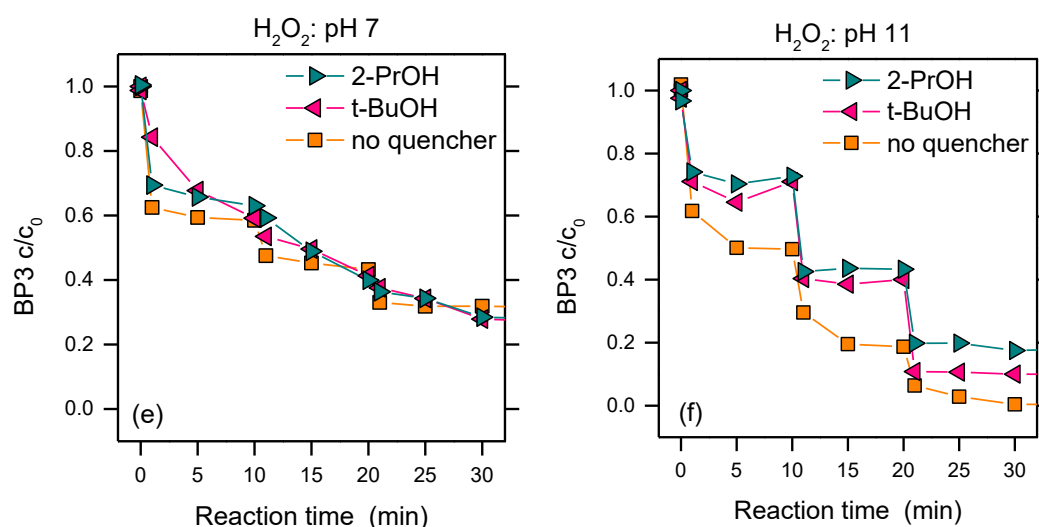


**Figure 2.1.4** Effects of different quenchers on the degradation reaction. Quenchers were t-BuOH (40 mM) or 2-PrOH (133 mM), tested in the degradation of (a, b) phenol or (c-f) BP3. The reagents were (a-d) metabisulfite or (e, f)  $H_2O_2$ , and the pH was 7 (left column) or 11 (right column). Reactions were carried out in phosphate buffer (10 mM), adding 0.1 mM metabisulfite (or  $H_2O_2$ ) every 10 min, for a total of three additions (at 0, 10, and 20 min). Initial conditions were:  $[Fe-TAML] = 0.01\text{ mM}$ ;  $[PhOH] = [BP3] = 0.1\text{ mM}$ .

A tentative outline of the mechanism of activation of  $H_2O_2$  by Fe-TAML has already been proposed (Figure 2.1.5a).<sup>98</sup> It has been reported that the activation of  $H_2O_2$  occurs via the heterolytic cleavage of its O-O bond, after coordination to the iron center. The cleavage of the O-O bond is reasonably helped by proton transfer, followed by water release and formation of an iron-oxo complex.<sup>98</sup> Taking inspiration from the hydrogen peroxide activation mechanism, in the case of the Fe-TAML/metabisulfite system, it is reasonable to suggest that the initial formation of the Fe-O-SR intermediate may be followed by heterolytic O-S cleavage, yielding the related iron-oxo species (Figure 2.1.5b). This would also tentatively explain why persulfate was not activated by Fe-TAML (Figure 2.1.1c). In the case of unreactive persulfate, the coordination of iron(III) should involve either sulfonyl or peroxy oxygen. The former may be too stable for resonance, and the corresponding  $\pi^*$  orbital of the O-S fragment would be too distant from the reducing Fe(III) center, while the latter may be sterically hindered because of the geometry of the persulfate molecule. Although this outline looks reasonable and agrees with the experimental data, further work is needed to confirm this rationalization and the related mechanisms.

## 2.1 Metabisulfite as Unconventional Reagent for Green Oxidation of Emerging Contaminants Using an Iron-based Catalyst

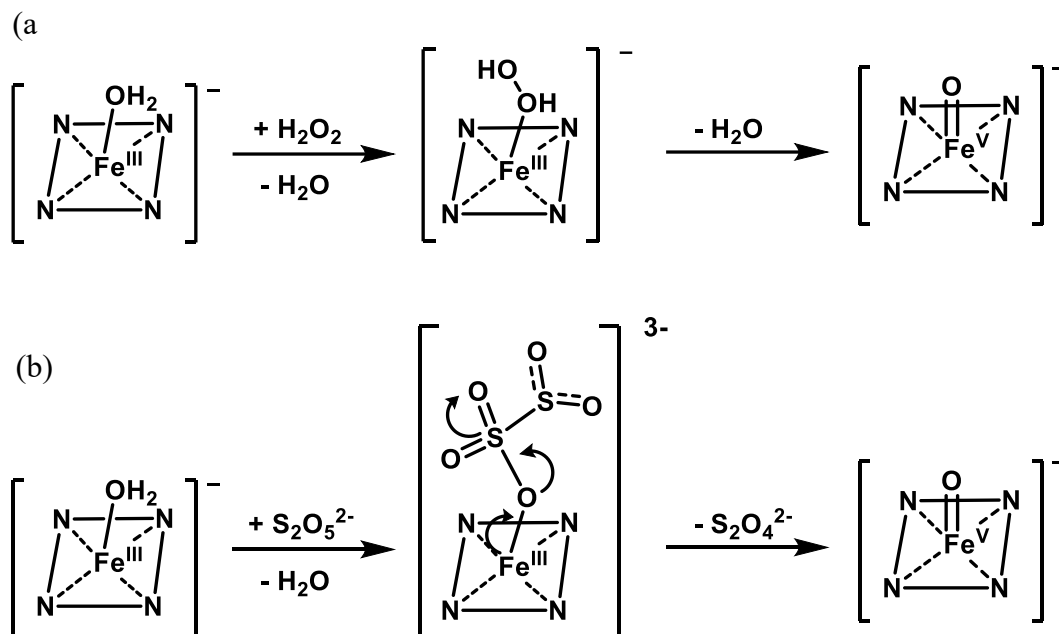


**Figure 2.1.5** Reaction pathways in the activation of reagents by Fe-TAML. (a) Established pathway for the activation of hydrogen peroxide as discussed by Ghosh et al.,<sup>98</sup> and (b) proposed pathway for the activation of metabisulfite.

The oxidation potentials recorded for the CECs studied in the present work by using the cyclic voltammetry (CV) technique (Table 2.1.1) are coherent with the mechanism here proposed. All the CECs under study have oxidation onset potentials between 0.05 and 1.75 V vs. Ag/AgCl. The reported values were obtained by averaging three CV scans (see Figure A10-A17 of the Appendix A for the raw CV data).

**Table 2.1.1** Onset potential for the oxidation of the studied contaminants of emerging concern. The onset potential is reported for both the first and the successive scans of the CVs.

Compound	Oxidation onset	Oxidation onset	Comments
ACE	0.90 V	0.90 V	Although an anodic current onset can be appreciated for acesulfame K, the oxidation current is always very low and an anodic peak is never observed. In fact, for the analytical determination of ACE, Pierini et al. <sup>130</sup> have exploited its reduction. Due to limited solubility in CH <sub>3</sub> CN, the same measurement was repeated in water at pH 10. No anodic current was observed compared with blank run.

<b>NPX</b>	0.80 V	0.25 V	An additional oxidation peak could be appreciated on the first scan only. The potential of the anodic peak observed in the successive scans corresponds with literature data. <sup>131</sup>
<b>IBU</b>	1.62 V	1.62 V	The oxidation onset potential corresponds very well to the results of Lima et al., <sup>132</sup> obtained using a boron doped diamond.
<b>DCF</b>	0.05 V	0.05 V	The results obtained are coherent with the literature. <sup>132</sup> Nevertheless, in that report, the authors reported significantly larger sensitivity in the 0 V / 0.6 V potential window, thanks to the modification of the glassy carbon electrode.
<b>ATZ</b>	1.75 V	1.75 V	Atrazine is only oxidized at very positive potential. In fact, for ATZ determination, Svorec et al. exploited its reduction. <sup>133</sup>
<b>PhOH</b>	0.70 V	0.80 V	The oxidation onset potential decreases on successive scans, because of the formation of catechol and hydroquinone. <sup>134</sup>
<b>BP3</b>	0.90 V	1.25 V	The anodic peak at 1.05 V (with corresponding oxidation onset at 0.9 V) is only observed if the potential is previously swept below 0 V. The main oxidation onset corresponds very well to the results reported by Sunyer et al. <sup>135</sup>
<b>TCS</b>	0.60 V	0.60 V	Very similar values have been found by Fotouhi et al. <sup>136</sup>

---

These results are coherent with previously published values, although the experimental conditions are not fully comparable. The radicals  $\bullet\text{OH}$  or  $\text{SO}_4^{\bullet-}$  have more positive reduction potentials (2.5 V or above vs. SHE, *i.e.*, at least 2.2 V vs. Ag/AgCl) in the pH window under investigation, thus they are able to oxidize all the CECs under study and lead to their degradation. <sup>137</sup> A less oxidant active species, such as the hypothesized iron-oxo one, could only effectively oxidize the most reducing CECs, while having negligible reactivity towards the least reducing substrates. In fact, the CECs here considered could be divided into two groups based on their redox potentials: ACE, ATZ, BP3, IBU, and NPX can only be oxidized at potentials larger than 0.8 V vs. Ag/AgCl, while DCF, PhOH, and TCS can be oxidized at potentials lower than 0.8 V. The CECs of the first group are only marginally (< 20%) abated by Fe-TAML/metabisulfite, with the notable exception of BP3. Indeed, BP3 degradation exceeded 80% at basic pH, despite an onset potential as high as 0.90 V (1.25 V for the first scan if the initial potential is more positive than 0.2 V). This implies that the redox behavior of BP3 and, consequently, its degradation with Fe-TAML/metabisulfite is hardly described by the onset potential only. In contrast, a first reduction step might trigger BP3 degradation. The compounds with oxidation potential below 0.8 V, *i.e.*, DCF, PhOH, and TCS were all significantly degraded by Fe-TAML +  $\text{S}_2\text{O}_5^{2-}$ , especially



at pH 11, in agreement with the CV data. Hence, the hypothesized iron-oxo reactive intermediate should have a redox potential of around 0.8/1 V vs. Ag/AgCl, which allows for the oxidation of compounds like DCF, PhOH and TCS, but it is insufficient to significantly degrade ACE, ATZ, IBU and NPX. Note that the CV profiles allow for a first qualitative description, but specific interactions between the active species and the substrate could activate additional mechanisms, which are not operational during the electrochemical oxidation processes at the glassy carbon electrode in CH<sub>3</sub>CN. Conversely, kinetic limitations could impede some oxidation reactions, despite their being thermodynamically possible.

### 2.1.4 Conclusions

Alternative reagents to hydrogen peroxide in the Fe-TAML activated processes were here investigated and applied towards the degradation of various micropollutants. Sulfite, metabisulfite and persulfate were initially screened: metabisulfite showed the most promising reactivity among the three reagents. The use of metabisulfite in place of hydrogen peroxide is potentially a breakthrough, as the former compound shows a lower level of health and safety risk to both users and to the aquatic environments, compared to hydrogen peroxide or other more conventional reagents; moreover, metabisulfite has lower cost than traditional reagents. The activity of metabisulfite toward the degradation of several organic contaminants was compared with that of hydrogen peroxide, and the two reagents showed generally analogous degradation yields, with a marked selectivity towards phenolic compounds (e.g., PhOH, BP3, TCS). Metabisulfite has been commonly proposed as quencher in Fenton and Fenton-like

processes. The data here reported suggest that its use with this aim must be carefully evaluated to prevent metabisulfite from promoting a further production of reactive species, rather than a quenching of the investigated process. Preliminary tests to understand the reaction mechanism with Fe-TAML + S<sub>2</sub>O<sub>5</sub><sup>2-</sup> suggested that the active species may be an iron-oxo compound, similar to that proposed when hydrogen peroxide is activated by the same catalyst. Further tests will be necessary in order to give insights into this new degradation process.

## 2.2 Fe-Chitosan Complexes for Oxidative Degradation of Emerging Contaminants in Water: Structure, Activity, and Reaction Mechanism

### 2.2.1 Introduction

Chitosan (CS) is the deacetylated form of chitin in which a number of acetamide groups have been replaced with amine ( $\text{-NH}_2$ ) groups.<sup>138</sup> Chitin is the second most abundant polysaccharide in nature, with the major source being crustacean shells.<sup>139,140</sup> The starting material for chitosan manufacturing is economical due to the extensive presence of crustacean exoskeleton, which is easily accessible as a by-product of the seafood processing industry. Some of the attractive features of this biopolymer are its biodegradability, biocompatibility, and low toxicity.<sup>141–143</sup> A distinctive feature of CS from a chemical standpoint is the high density of amine groups at the C-2 positions. This feature enables chitosan to form stable complexes with metals, a property that is exceptional among biopolymers.<sup>144–148</sup>

The ability of CS to complex elements has been mostly exploited in environmental applications for heavy metal adsorption from water streams.<sup>149–154</sup> When considering instead the degradation of organic micropollutants from water, advanced oxidation processes are established techniques, but they are not always environmentally friendly or effective at near-neutral pH.<sup>40,66,70,155,156</sup> In contrast, CS-metal complexes are promising in creating an inexpensive and sustainable organometallic catalyst, which may be applied without modifying the pH of the contaminated streams (generally near neutral pH). To date, very few literature reports have discussed the ability of CS-metal complexes to work as organometallic catalysts for the oxidative degradation of organic molecules in water (dyes, perchlorate, *etc.*).<sup>146,157–159</sup> Moreover, all these studies employed expensive and sometimes toxic metal complexes, with the obvious risks of inhibiting implementation for environmental applications.

A CS-metal complex may be used as both homogeneous and heterogeneous catalyst. Homogeneous oxidation is easily employable within a water treatment plant but with several limitations.<sup>70,92</sup> Approaches based on heterogeneous processes would circumvent difficulties related to catalyst recovery and would reduce the amount of reagents needed to implement the oxidation. Most studies on heterogeneous oxidative processes based on CS as a bio-chelating agent report the use of this material in the form of powders, flakes, or gel beads, which are not

easily deployed.<sup>157,160,161</sup> The use of films remains limited, despite the well-known ability of CS to form stable films.<sup>162</sup> Seyed Dorraji et al. reported the efficiency of wet-spun chitosan hollow fibers loaded with Fe<sub>3</sub>O<sub>4</sub> nanoparticles in the degradation of dyes in water.<sup>163</sup> However, the use of an iron ion instead of insoluble iron-based nanoparticles would allow easier regeneration of the catalytic core during applications.

Iron is the most abundant metal on Earth and its use in the ionic form in CS-based catalysts would be groundbreaking.<sup>164</sup> However, the nature of the interaction between CS and the iron, especially Fe(III), is still amply debated, thus preventing further development of these materials.<sup>165</sup> Gamblin et al. suggested the formation of a cluster between the CS polymer and the Fe(III) ions without an effective coordination.<sup>166</sup> Nevertheless, other investigations reached the opposite conclusion.<sup>167,168</sup> Bhatia and Ravi suggested the formation of a CS-Fe(III) complex that is either penta- or hexa-coordinated.<sup>169</sup> Current knowledge is also insufficient with respect to the reaction mechanism when a CS-Fe complex is used for the oxidative degradation of organic contaminants in water.

In this study, we propose CS-metal complexes both as homogeneous and heterogeneous organometallic catalysts. Specifically, we examine the detailed nature of the CS-Fe(III) complex, defining both the stoichiometry and the molecular structure of the polymer-metal complex through a combination of experiments and quantum chemical density functional theory calculations. We also evaluate the effectiveness of chitosan-metal complexes for the oxidative degradation of contaminants of emerging concern in water. The reaction mechanism is discussed and a novel CS-Fe(III) film is proposed as a cheap and sustainable heterogeneous catalyst.

### 2.2.2 Materials and Methods

#### 2.2.2.1 Chemicals

Triclosan and 3-chlorophenol were purchased from Oakwood Chemicals (Estill, SC, USA). All the other reagents were purchased from Sigma-Aldrich. The chitosan (CS) used in this study had low molecular weight and a deacetylation grade  $\geq 75\%$ . The measured CS solubility in water was 433 mg/L; more details about this determination can be found in Appendix B (Text B1).

#### 2.2.2.2 Preparation of the chitosan solid films

The protocol for the preparation of CS films was adapted from previous reports.<sup>170,171</sup> Briefly, to prepare pure CS films, a polymer solution was obtained

with 2% w/w of CS and 2% w/w of acetic acid in water. A volume of 10 mL was then poured on a petri dish and let dry at room temperature until constant weight was achieved. The film was immersed overnight in a sodium hydroxide solution (1 M) and then washed thoroughly with water. Films were also prepared in the presence of iron(III) and iron(II). Specifically, three different aqueous solutions were used: (a) 2% w/w of CS, 2% w/w of acetic acid, and  $\text{FeCl}_3$  (13.8 mM); (b) 2% w/w of CS, 2% of acetic acid, and  $\text{FeSO}_4$  (9.2 mM); (c) 2% w/w of CS, 2% w/w of acetic acid, and  $\text{FeCl}_2$  (9.2 mM). The concentration of iron was chosen based on the stoichiometric ratios defined in preliminary experiments (*vide infra*). A volume of 10 mL of each of the three solutions was poured into a separate petri dish and let dry in the oven at 80°C for 4 h. The films were left overnight in 0.1 M sodium hydroxide, then dried in the oven at 80°C for 4 h, and finally washed with ethanol. The residual ethanol was evaporated at room temperature until constant weight was achieved. All the films had a diameter of 54 mm and a thickness between 5 and 20  $\mu\text{m}$ . To assess the stability of the CS-Fe(III) film, this was immersed in 10 mL of water for 20 min under gentle stirring. Aliquots of the supernatant at initial and final times were sampled and UV-Vis spectra were compared with the spectrum obtained with a solution of iron(III) to detect any leaching of the metal into solution.

#### 2.2.2.3 Oxidation experiments: Homogeneous conditions

Six metals were tested as central ion to form complexes with CS. They were: Cu(II), Fe(III), Fe(II), Co(II), Pd(II), and Mn(II). The stoichiometry ratios between the central ion and a saturated solution of CS in water (433 mg/L) were first measured with UV-Vis titrations. The stoichiometric complexes were applied as organometallic catalysts in the oxidation of contaminants of emerging concern in water, namely, phenol (PhOH), triclosan (TCS), and 3-chlorophenol (3-CP). The oxidant was hydrogen peroxide. Initially, an appropriate amount of stock metal solution was added to 10 mL of a saturated CS solution in water. The obtained mixture was stirred for 5 min before starting the reaction in order to ensure the formation of the complex. Please note that UV titration suggested that the formation of the complex in solution occurred near instantly. Subsequently, the contaminant and the oxidant were added in this order. Preliminary oxidation tests were performed with a relative mass concentration ratio between metal, contaminant, and oxidant equal to 1:1:1. The low amount of oxidant allowed a better visualization of the relative efficiency of the different complexes. Further contaminant degradation experiments were then performed with a higher amount of oxidant (metal:contaminant:oxidant = 1:1:3 mass concentration ratio). More precisely, 1/3 of the total concentration of the oxidant was added in three separate steps, at time zero and then two more times each 20 min. The metal concentration

refers to that at the equivalence point with a saturated chitosan solution (*vide infra*). The final reaction time for all the oxidation experiments was 1 h. All the reaction occurred at room temperature, at near-neutral pH, under magnetic stirring; the pH value remained nearly constant during the reaction.

### 2.2.2.4 Oxidation experiments: Heterogeneous conditions

The CS-Fe(III, II) films obtained as described above were placed in contact with a solution of the target contaminant, PhOH. The oxidation tests occurred with a relative concentration ratio between catalyst, contaminant, and hydrogen peroxide of 1:0.5:0.5. The oxidant was added in one aliquot. The concentration of the metal salts, corresponding to the catalyst concentration, was 13.8 mM for FeCl<sub>3</sub>; 9.2 mM for FeSO<sub>4</sub>; 9.2 mM for FeCl<sub>2</sub>. The reactions were conducted for 60 min at room temperature (note that after 20 min the CS-Fe(III, II) was nearly completely dissolved in water), at near-neutral pH, under slow magnetic stirring; the pH value remained nearly constant during the reaction. CS-FeCl<sub>3</sub> and CS-FeSO<sub>4</sub> films were tested in two subsequent cycles in order to evaluate their stability and recyclability. Specifically, these films were first employed for reaction, dried in the oven (80°C for 1 h), and then used again. To rule out the possibility of phenol adsorption onto the CS-Fe(III, II) films, these films were placed in contact with a PhOH solution in the absence of hydrogen peroxide under magnetic stirring and the same environmental conditions adopted during oxidation tests. The adsorption tests occurred with a relative ratio between metal, contaminant, and oxidant of 1:1:0.5.

### 2.2.2.5 Analytical methods

UV-Vis spectrophotometric measurements were performed using a Cary 5000 Scan double-beam instrument (Varian). The concentrations of contaminants in solution were monitored by high-performance liquid chromatography coupled with a diode array detector (HPLC-DAD). The formation of by-products during the oxidation reactions was monitored with a liquid chromatography coupled with a quadrupole mass detector (LC-MS). Further information about the analytical methods can be found in Appendix B (Text B2).

### 2.2.2.6 Modeling of the chitosan dimer conformations

To explore conformations adopted by CS that could chelate Fe ions, we first pre-screened the possible conformations adopted by a CS dimer. To this end, the free energy surface along two torsional angles of the ether bond ( $\phi, \psi$ , Figure 2.2.4a) was calculated using 2D-umbrella sampling (US).<sup>172</sup> The CS model was modeled using GAFF parameters and generated using tleap.<sup>173,174</sup> Simulations were performed with NAMD 2.13,<sup>175</sup> using a generalized Born (GB) implicit solvent model ( $\epsilon=80$ ), an integration step of 1 fs with Langevin dynamics ( $\tau=5$  ps<sup>-1</sup>

<sup>1</sup>) at  $T=298$  K, and by employing a cutoff distance for non-bonded interactions of 9 Å. 50 windows for each variable was used, giving in total  $50 \times 50 = 2500$  simulations. A harmonic restraining potential with a force constant of  $0.025 \text{ kcal mol}^{-1} \text{ degree}^{-2}$  was used for the 2D-US and the dihedral space was scanned between  $-180$  and  $180$  degrees. The resulting free energy profiles were obtained using the weighted histogram analysis method (WHAM) <sup>176</sup> with 5 ns sampling for each replica. The obtained 2D-free energy profile resembled the profile by Tsereteli et al. obtained using coarse-grained models. <sup>177</sup>

#### 2.2.2.7 Modeling of the chitosan-Fe complex

To generate the  $\alpha$  and  $\beta$  chitosan-Fe complexes, an Fe(III) ion was coordinated within the chitosan framework with the amino/hydroxyl/ether groups, and the amino/hydroxyl groups, respectively (see Figure 2.2.4a). The ionic coordination spheres were saturated with water molecules (three for  $\alpha$ -chitosan, four for  $\beta$ -chitosan), and the resulting structures were optimized at the DFT level using TPSSh/def2-SVP (Fe def2-TZVP). <sup>178–180</sup> The aqueous surroundings were treated using the conductor-like screening model (COSMO) with an  $\epsilon$  set to 80. <sup>181</sup> As an intermediate step, we optimized the structures in the high spin  $S=5/2$  Fe(III) state, followed by generation of the ferryl (Fe(IV)=O) species, by deprotonating a water molecule bound to the iron, and optimizing the structure at the same theory level in the  $S=1$  and  $S=2$  states, resulting in 14 structures (3  $\alpha$  and 4  $\beta$  structures for the two respective spin states). Stable ground state structures were validated by computing the molecular Hessian, and single point energy calculations were performed at the TPSSh/def2-TZVPP/ $\epsilon=80$  level. For modeling the ferryl species, the amino groups of the CS monomers were modeled in their neutral ( $-\text{NH}_2$ ) states. All quantum chemical calculations were performed with TURBOMOLE v. 7.2. <sup>182,183</sup>

#### 2.2.2.8 Kinetic model of reaction

To interpret the results obtained from oxidation experiments and understand whether a metal-based or a free-radical oxidation mechanism is dominant, a kinetic model was applied to simulate the oxidation of an organic species (Orange II) by  $\text{H}_2\text{O}_2$  catalyzed by CS-Fe(II, III) complexes. The initial concentrations of  $\text{H}_2\text{O}_2$ , Orange II, and CS-Fe(II) or CS-Fe(III) complex were set at  $10^{-4}$  M, mimicking the experimental setup. The kinetic model was created using COPASI 4.23, <sup>184</sup> generating the system of reactions listed in Table B1. The reaction constants ( $k_i$ ) were chosen based on values reported in the literature. <sup>97,185,186</sup> The system was simulated for 150 s with a time step of 15 ms, using a deterministic (LSODA) integration method. The reactions were simulated by varying each kinetics constant,  $k_i$ , individually over an unrealistically wide range, from  $10^{-4}$  to

$10^{10} \text{ s}^{-1}$  divided by 30 logarithmic intervals and keeping all the other constants equal to the values reported in the literature (Table B1). To probe the difference in oxidation pathway promoted by Fe(II)- or Fe(III)-based catalysts, we started each model simulation with only one of the two ionic species (with two sets of simulations performed, one for each initial species), and observed the time evolution of the substrate (Orange II) and of two more products, one associated with the metal-based mechanism (referred to as “ferryl”) and the other with the free-radical mechanism (referred to as “free radical”).

### 2.2.3 Results and Discussion

#### 2.2.3.1 Chitosan-metal interaction and catalytic efficiency of the complex

When catalysis occurs through an organometallic compound, the correct metal/ligand ratio allows maximization of the catalytic efficiency while avoiding free species in solution that may negatively impact the process.<sup>187</sup> To determine the CS-metal binding stoichiometry, intended here as the ratio between the concentration of CS (g/L) and the concentration of the central ion ( $\mu\text{M}$ ), UV-Vis titrations were performed with different metals as catalytic core, namely, Cu(II), Fe(III), Fe(II), Co(II), Pd(II), and Mn(II). Figure 2.2.1a reports the concentration of the various metals associated to each equivalence point, that is, the inflection point of the titration curve, in a saturated aqueous solution of CS (433 mg/L); see Figure B1 in Appendix B for the titration curves. The equivalence point was not reached for Pd, possibly because this metal forms clusters rather than complexes with chitosan.

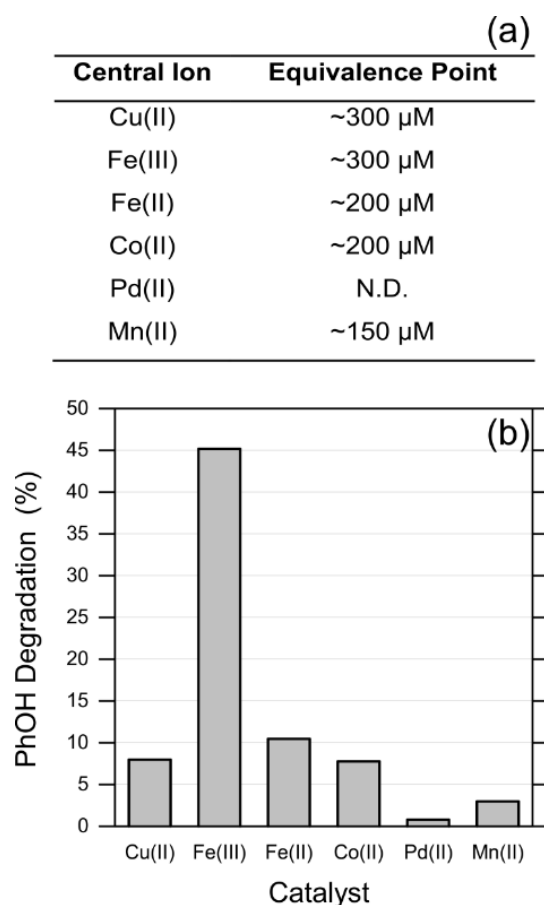


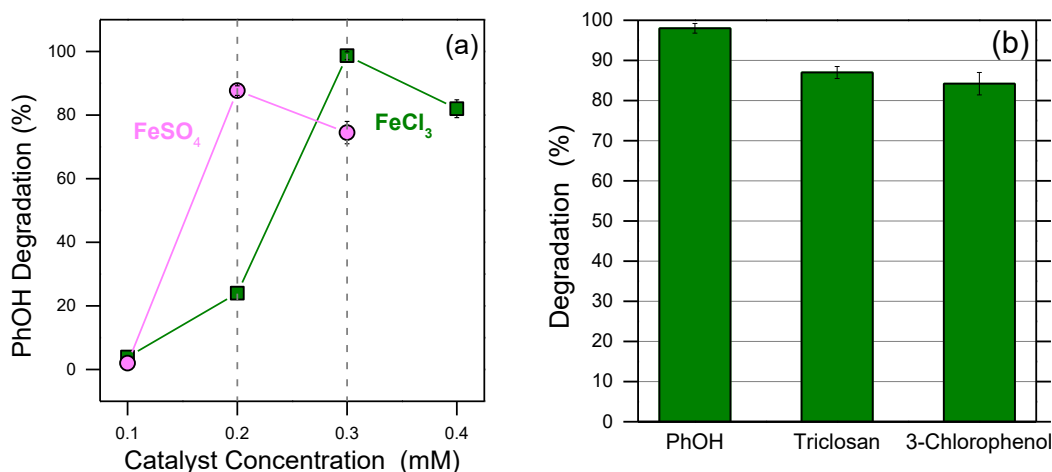
**Figure 2.2.1** Stoichiometry of the metal-chitosan complexes. (a) Metal concentration of saturation (equivalence point) in the CS-metal complexes at a chitosan concentration of 433 mg/L, from UV titration. (b) Phenol (PhOH) degradation resulting from the use of different CS-metal complexes as homogeneous catalysts after one addition of  $\text{H}_2\text{O}_2$ . The reaction was performed with metal:PhOH: $\text{H}_2\text{O}_2$  = 1:1:1 mass concentration ratio, and metal concentration as in (a).

The concentrations in Figure 2.2.1a were thus applied to prepare the catalysts employed in preliminary homogeneous oxidation reactions aimed at the degradation of phenol (PhOH) in water. Figure 2.2.1 b shows the percentage of degraded substrate after one addition of a low amount of  $\text{H}_2\text{O}_2$ , to better assess the relative efficiency of the different catalysts. The highest efficiency was obtained with the two CS-Fe systems. The different efficiency observed with the Fe(III) and Fe(II) complexes may be possibly interpreted as due to a different reaction pathway, hence a different reaction mechanism, a hypothesis that was further investigated and discussed below.



### 2.2.3.2 Homogeneous degradation of contaminants by CS-Fe complexes

The activity of the most efficient CS-Fe(III) complex and that of the CS-Fe(II) complex were further examined with the goal to gain insight into their reaction mechanisms. The results reported in Figure 2.2.2a indicate that the maximum oxidation power of both complexes indeed corresponded with the stoichiometric metal concentration, namely, 200  $\mu\text{M}$  and 300  $\mu\text{M}$  for Fe(II) and Fe(III), respectively. The lower oxidation efficiency of the super-stoichiometric conditions may be rationalized with consumption of the oxidant ( $\text{H}_2\text{O}_2$ ) by the excess species, while in the case of sub-stoichiometric metal with a low activity of the catalytic core. When the CS-Fe(III) complex at optimal CS/metal ratio was applied for the homogeneous oxidation of three contaminants of emerging concern, PhOH, triclosan (TCS), and 3-chlorophenol (3-CP), the percentage of removal was always higher than 80%; see Figure 2.2.2 b and Figure B2 in Appendix B for time trends. Please note that removal of PhOH by adsorption can be ruled out based on the result presented in Appendix B (Figure B4). The time evolution of the concentration of by-products was also analyzed during the degradation of PhOH; see Figure 2.2.2c,d. Comparison of the maximum concentration elution time ( $t_{\text{max}}$ ) of the by-products shows a strong difference between the two systems, with the Fe(III)-based system being slower than the Fe(II) one, further suggesting that two different mechanisms of reaction are at play.



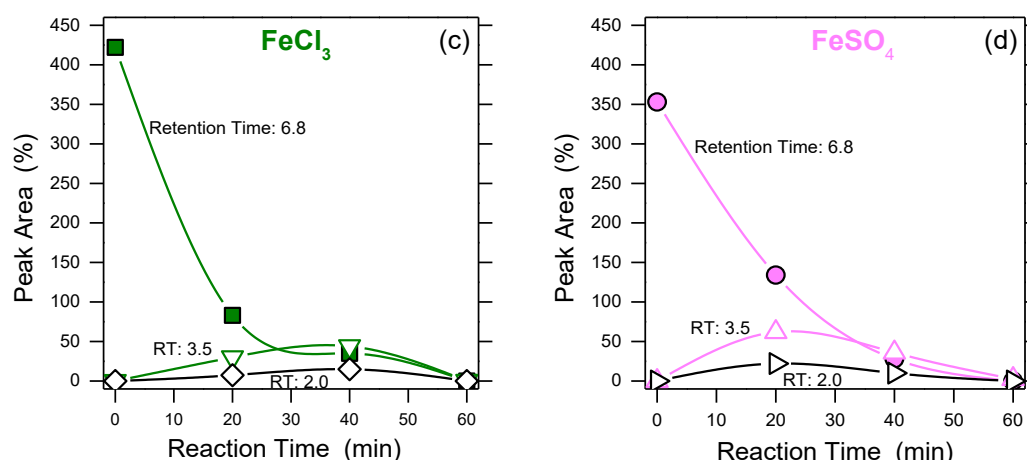


**Figure 2.2.2** Chitosan-Fe complexes in the degradation of organic contaminants. (a) Influence of metal concentration in the CS-Fe(III, II) complexes (CS concentration 433 mg/L) used as homogeneous catalysts for phenol (PhOH) degradation. (b) Degradation of three contaminants of emerging concern with the use of the CS-Fe(III) complex as homogeneous catalyst. (c,d) Degradation of PhOH and formation of byproducts (they were recognized as the mono-hydroxylated byproducts) monitored with LC-MS using (c) the CS-FeCl<sub>3</sub> complex or (d) the CS-FeSO<sub>4</sub> complex as homogeneous catalyst. The reactions were performed with metal:contaminant:H<sub>2</sub>O<sub>2</sub> = 1:1:3 mass concentration ratio, and metal concentration as in Figure 1a. The same conditions were applied to conduct the reactions using the CS-FeCl<sub>3</sub> complex related to (a-c). The reaction conditions with the CS-FeSO<sub>4</sub> complex were adjusted (metal:phenol:H<sub>2</sub>O<sub>2</sub> = 1:1:30 mass concentration ratio) to obtain the same kinetics of degradation observed in the CS-FeCl<sub>3</sub> complex. The lines connecting the data points are intended only as a guide for the eye.

### 2.2.3.3 Insights into the reaction mechanism and the nature of the active species

Figure 2.2.3 (see also Figure B3 in Appendix B for time trends) summarizes the results obtained in the homogeneous-phase degradation of PhOH using different iron salts as catalytic core in the CS-Fe. In the case of Fe(II) as central ion, a significant increase in the efficiency of degradation of phenol with SO<sub>4</sub><sup>2-</sup> as the counter-ion was observed with respect to Cl<sup>-</sup>. On the other hand, no difference was detected when Fe(III) was the central ion, regardless of the counterion. Therefore, it is possible to hypothesize that free radicals are important in the oxidation mediated by Fe(II) as the central ion, whereas the prominent mechanism related to the CS-Fe(III) system is most likely the metal-based one. Indeed, an oxidation reaction can occur either through a free-radical or a metal-based mechanism, or a combination of the two.<sup>93,185,186</sup> In the case of a free-radical mechanism similar to the Fenton reaction, chloride ions may scavenge the hydroxyl radical, while nitrate is an excellent counter-ion as (i) it does not complex ferric ions, therefore not suppressing their reaction with hydrogen

peroxide, and (ii) it does not react with hydroxyl radicals.<sup>93,188</sup> Sulfate is also a suitable counter-ion for free radical-based reactions: although this ion may slightly retard the redox reaction by coordinating to iron, the presence of other competitive ligands, such as CS itself, would thwart this effect.<sup>93,189</sup> In contrast, during a metal-based reaction, the organometallic complexes generate a ferryl (Fe(IV)=O) species, which may not be affected by the typical scavengers of a Fenton process.<sup>85,96,190</sup>

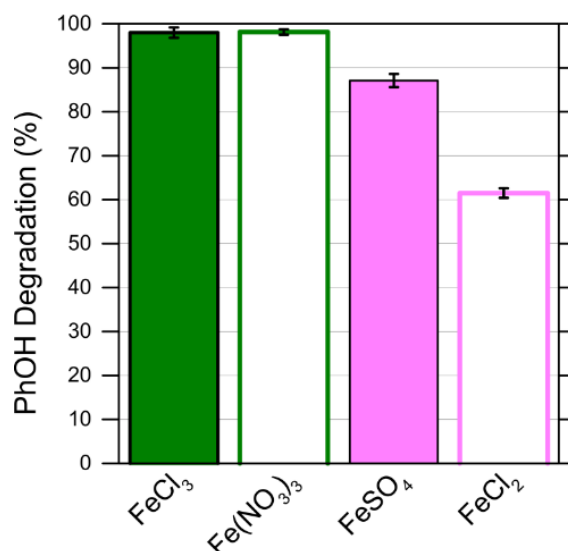


**Figure 2.2.3** Phenol degradation resulting from the use of CS-Fe(III, II) complexes applied as homogeneous catalysts obtained with different iron salts (FeCl<sub>3</sub>, Fe(NO<sub>3</sub>)<sub>3</sub>, FeSO<sub>4</sub>, FeCl<sub>2</sub>). The reactions were performed with metal:PhOH:H<sub>2</sub>O<sub>2</sub> = 1:1:3 mass concentration ratio, and metal concentration as in Figure 2.2.1 a.

If a metal-based reaction mechanism is indeed dominant, this system requires the formation of a CS-ferryl species during the reaction cycle. To derive the structure of such putative CS-bound ferryl species, we performed both classical free energy exploration of the CS-framework and quantum chemical DFT calculations to explore the electronic structure of CS-ferryl species. First, possible conformations accessible by the CS in the polymer chain were identified using a chitosan dimer. We identify three free energy minima ( $\alpha$ ,  $\beta$ ,  $\gamma$ , Figure 2.2.4a) that are similar to structures also previously described.<sup>177,191</sup> While both the  $\alpha$  and  $\beta$  CS-complexes can chelate a metal ion by their amino and hydroxyl groups, the  $\gamma$ -structure was discarded due to its inability to form stable bidentate iron-complex. Structures similar to those presented here were also adopted in previous CS-metal studies.<sup>192</sup> The two candidate conformations were thus further

employed to build a water-saturated complex of iron and optimized at the DFT level (see Materials and Methods).

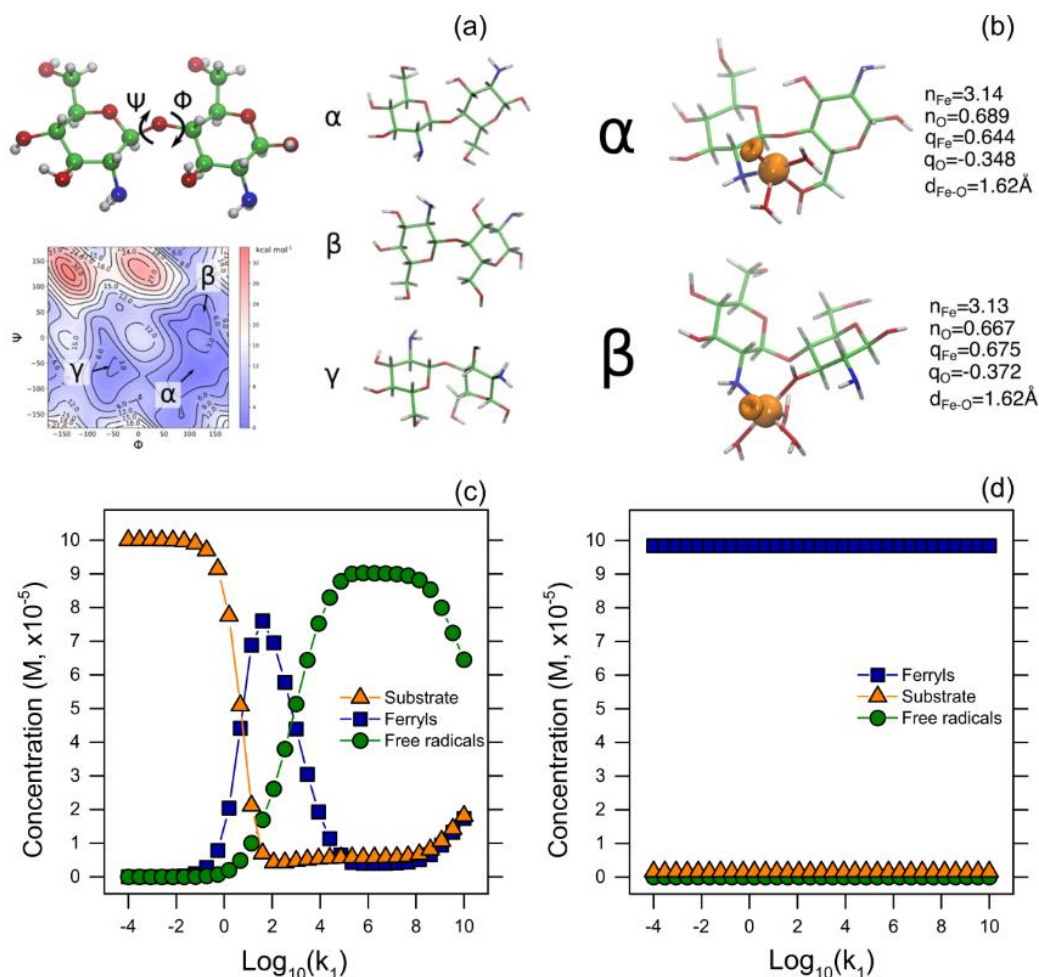


**Figure 2.2.4** Modeling of the chitosan-Fe complexes as catalysts. (a) Free-energy surface of the CS dimer along the  $\phi$  and  $\psi$  torsional angles (see Methods). Three minimum free-energy structures ( $\alpha$ ,  $\beta$ ,  $\gamma$ ) identified are indicated on the right. The  $\alpha$  and  $\beta$  CS-structures were further used to study the structure of the catalytic species. (b) Molecular structure of a ferryl species optimized at the DFT level (TPSSH/def2-TZVP) in the  $\alpha$  and  $\beta$  conformations. The spin density distribution (at the TPSSH/def2-TZVP level) is shown as in surface representation at +0.05 (-0.05) isovalue for  $\alpha$  ( $\beta$ ) spin density. Kinetic models for (c)  $Fe^{2+}$  and (d)  $Fe^{3+}$ . In c and d, the substrate, ferryl, and the free radical lines are related to the trend of Orange II, metal-based product, and free-radical product, respectively, obtained in the simulation. The lines connecting the data points are intended only as a guide for the eye.

The DFT calculations involving the dimer-iron interaction suggest that the optimized complexes have typical structures and spin distributions observed for non-heme  $Fe(IV)=O$  species,<sup>193,194</sup> corroborating the possibility of a metal-based reaction mechanism involving a ferryl species (see Figure 2.2.4b). We did not

identify a strong preference for a particular spin-state, with nearly degenerate  $S=1$  and  $S=2$  states, nor for a specific  $\text{Fe(IV)=O}$  orientation with respect to the CS polymer, suggesting an intrinsic diversity of the oxidation sites in the material (see Figure B7). However, due to the high flexibility and heterogeneity of the starting CS polymer, a large number of CS-Fe complexes are possible, for example, a complex formed by the amino groups of two non-adjacent CS units (chains). Such structural heterogeneity may further modify the properties of the oxidant species by altering the ligand field of the complex, and thus the spin and stability<sup>195</sup> with respect to the structures explored in this study that comprise a single amino group bound to the central iron. It is important to note that the DFT calculation was not used to define exclusively one of the two mechanisms (free-radical; metal-based), but only to support the experimental data previously discussed and verify the actual possibility of the presence of a ferryl species during the process.

Further support of the two reaction mechanisms involving the CS-Fe(II, III) catalysts were separately obtained with a kinetic model applied to investigate the effect of the reaction constants ( $k_i$ ) on the development of the system. Our set of reactions (see Appendix B, Table B1) involved interchange of Fe(II) and Fe(III) species through a series of potential radical-based or ferryl-based reaction pathways.<sup>97,185,186</sup> Figure 2.2.4 reports the results obtained in the two systems starting from Fe(II) or Fe(III) as a function of  $k_1$ , ( $\text{Fe(II)} + \text{H}_2\text{O}_2 \rightarrow \text{Fe(III)} + \bullet\text{OH} + \text{OH}^-$ ). Here, the products generated via metal-based or free-radical reaction are referred to as ferryl and free radical, respectively, and indicated with blue squares and green circles in Figure 2.2.4c,d. The model predicted the generation of both hydroxyl radicals and of Fe(III) ions starting from Fe(II) (see Figure 2.2.4c and Reaction 1 in Table B1). Specifically, an increase of the reaction constant,  $k_1$ , produced a switch from a metal-based to Fenton-like mechanism, with both ferryl and radical species co-existing under some conditions. In addition, by sufficiently slowing down the reaction ( $k < 1 \text{ s}^{-1}$ ), the model outcome suggests that the process would be too slow to show any oxidation in the simulation time (150 s). In stark contrast, by starting the process with Fe(III) ions, the model predicted that the system would freely oxidize the substrate via a metal-based reaction and proceed to completion within the simulation time, regardless of the value of  $k_1$  (Figure 2.2.4 d).

To account for uncertainties in the choice of reaction parameters adopted in the kinetic model, the prevailing species were monitored by scanning an ample range of nine different  $k_i$  values (Figure B5 in the Appendix B). Also, we performed additional calculations by fixing the value of  $k_1$  at  $10^4 \text{ s}^{-1}$  (instead of the most realistic value of  $53 \text{ s}^{-1}$ ), as well as testing the introduction of a direct

reaction from Fe(II) to ferryl species (Reaction 17 in Table B1). A similar pattern was found for all the reactions, with systematic differences in the species outcome using Fe(II) or Fe(III) as initial metals, thus implying a different progression of the reaction in terms of intermediates, hence mechanism of oxidation. Please note that the kinetic model was studied by taking into account general free radical and metal-based systems, and not specifically the system of this work. This model was thus deployed with the intent to evaluate the possible mechanism disagreement between systems starting with  $\text{Fe}^{2+}$  or with  $\text{Fe}^{3+}$ . The results confirmed that divergence is possible, thus supporting our hypothesis.

#### 2.2.3.4 CS-Fe(III) as heterogeneous catalytic material

Free radicals can easily degrade a polymeric material used as heterogeneous catalyst, hence degrade CS and negatively impact the process.<sup>196,197</sup> On the other hand, ferryl species are coordinated on the structure of the catalytic material itself. Therefore, a metal-based mechanism could be highly advantageous for heterogeneous catalysis. Based on the results discussed so far, the CS-Fe(III) system may thus be applied to form an effective solid-phase catalyst to support heterogeneous oxidation (see Figure B6 of Appendix B for photographic images of representative films). Figure 2.2.5a shows the degradation of phenol obtained using CS-Fe catalytic films, prepared from different iron salts (see also Figure B4a in Appendix B for time trends). The contaminant removal activity of  $\text{FeCl}_3$  or  $\text{FeSO}_4$  films was not based on adsorption but on catalytic degradation, as shown in Figure B4b of the Appendix B. The results suggest the following main conclusions: the efficiency of reaction and the effect of the counterions on the heterogeneous reaction are comparable with those observed in the homogeneous case. Therefore, (i) the most likely reaction mechanisms are the same in the two phases, namely, metal-based in the CS-Fe(III) system and free radical-based in the with CS-Fe(II) system. This assumption is further supported by the faster degradation of the film observed with CS-Fe(II) films. Moreover, Figure 2.2.5a shows that after 2 cycles, the activity of CS-Fe(III) and CS-Fe(II) dropped by ~30 and ~50 % respectively. The severe drop in the activity of the catalyst after one cycle is mostly due to its instability in the water medium. Furthermore, the larger reduction in the case of CS-Fe(II) is an additional proof of the higher instability of the CS-Fe(II) film compared to CS-Fe(III), possibly due to the free radical behavior of the process in the case of the CS-Fe(II) system. (ii) CS-Fe(III) films work as effective catalytic material for the degradation of organic contaminants in water.

## 2.2 Fe-Chitosan Complexes for Oxidative Degradation of Emerging Contaminants in Water: Structure, Activity, and Reaction Mechanism

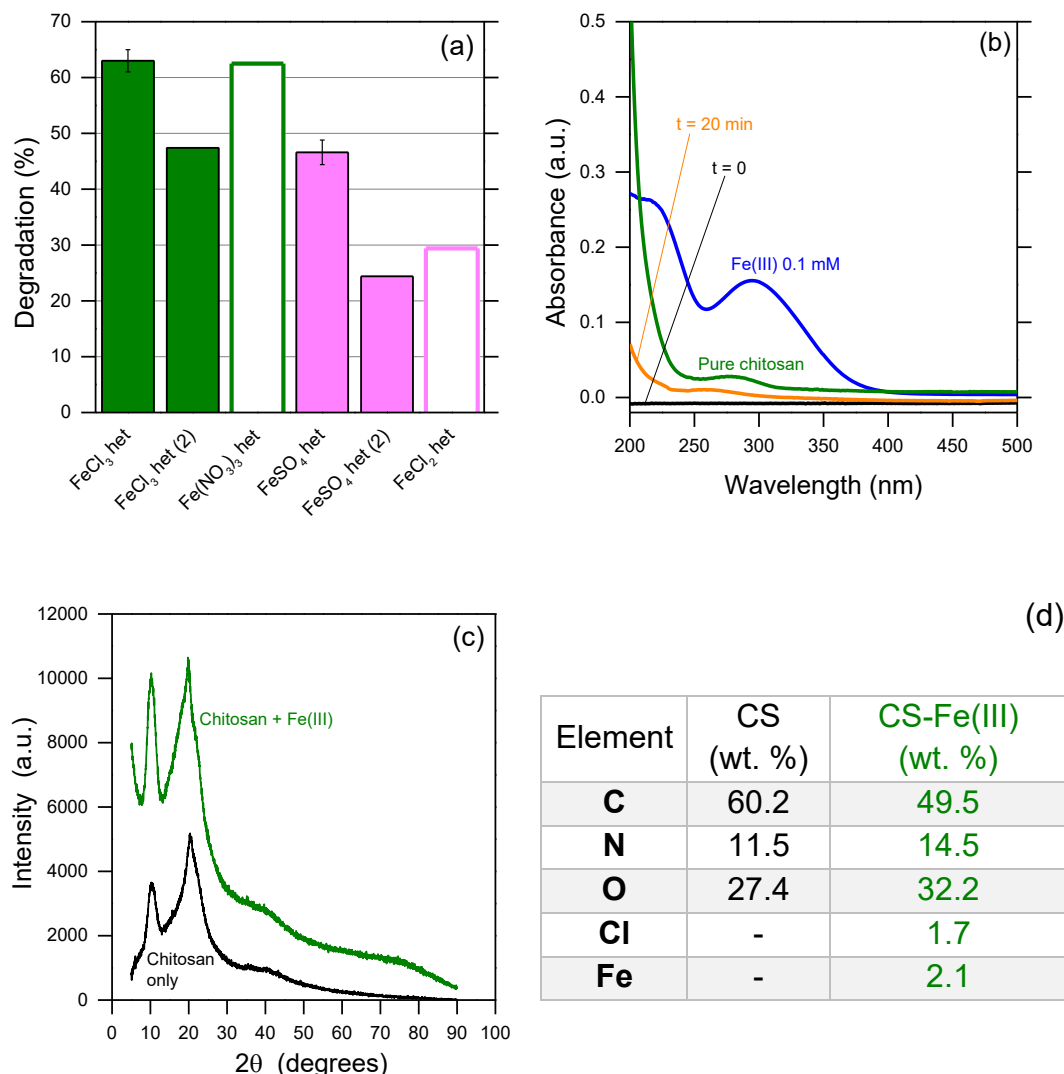


**Figure 2.2.5** Chitosan-Fe complexes as heterogeneous catalysts. (a) Phenol degradation resulting from the use of CS-Fe(III, II) films applied as heterogeneous catalysts obtained with different iron salts, *i.e.*, FeCl<sub>3</sub>, Fe(NO<sub>3</sub>)<sub>3</sub>, FeSO<sub>4</sub>, or FeCl<sub>2</sub>. CS-FeCl<sub>3</sub> and CS-FeSO<sub>4</sub> films were tested in two cycles in order to evaluate their cycling efficiency. The films were obtained from an initial solution containing 2% chitosan in the presence of FeCl<sub>3</sub>=13.8 mM, Fe(NO<sub>3</sub>)<sub>3</sub>=13.8 mM, FeSO<sub>4</sub>=9.2 mM, or FeCl<sub>2</sub>=9.2 mM. The reactions were performed with metal:PhOH:H<sub>2</sub>O<sub>2</sub> = 1:0.5:0.5 mass concentration ratio, and metal concentration as in Figure 1a. The oxidant was added in one aliquot. (b) Evaluation of leaching of Fe(III) from the surface of the CS-Fe(III) film. The blue and the green line represent the reference spectra of Fe(III) 0.1 mM and CS. (c) XRD and (d) EDX analyses of the surface of a pure chitosan film and of a CS-Fe(III) film.

To preliminarily assess the stability of the catalytic films, leaching experiments were performed, indicating that some CS was released into solution; see Figure 2.2.5b. While this observation implies that the polymeric matrix should

be stabilized, the absence of iron leaching suggests that the CS-Fe(III) coordination was strong and any parasitic reactions during the degradation tests due to free iron in solution can be ruled out. On the other hand, it is not possible to discard a priori the concomitance of homogeneous reactions. However, the leaching of the CS-Fe(III) complex is too low to imagine a major role of the homogeneous process in the degradation of PhOH. Fe(III) may also be oxidized to  $\text{Fe}_n\text{O}_x$  during the preparation of the material or during the oxidation reaction. The potential presence of iron oxide nanoparticles may thus affect the results. Figure 2.2.5 c shows the XRD characterization of a simple CS film (black line) and the CS-Fe(III) film (green line) after the oxidation reaction. Both lines display only the two characteristic peaks of CS.<sup>171,198</sup> This implies that no other solid compounds are present in the material and that the oxidation was thus promoted uniquely by the CS-Fe(III) coordination. From SEM analysis (see Figure B6 in Appendix B) both the CS and the CS-Fe(III) materials appeared as dense films composed by the overlap of thin layers. Figure 2.2.5d summarizes the elemental composition, which confirmed the presence of the iron ion in the CS-Fe(III) film.

## 2.2.4 Conclusions

Chitosan-metal coordination systems with different metallic cores were tested as potential organometallic catalysts for the degradation of phenol in water. Fe(III) was found to form an effective catalytic complex, and promising candidate for practical applications by virtue of the low cost and environmental impact of Fe(III). The CS-Fe(III) catalyst was also able to degrade (>80% removal) triclosan and 3-chlorophenol in the homogeneous phase. An in-depth investigation combining experiments, simulations of the complex structure, and a kinetic reaction model, suggested that the CS-Fe(III) system is a robust polymer-metal complex that promotes oxidation through a metal-based (ferryl mediated) mechanism. On the other hand, the CS-Fe(II) system likely works through a mixed free radical and metal-based reaction mechanisms.

The CS-Fe(III) system was also tested as a solid catalytic film for heterogeneous reaction. The results suggest that the solid catalyst also works through a metal-based mechanism, which is necessary to perform a stable heterogeneous catalytic process, and that its catalytic effectiveness has significant potential for the removal of organic contaminants in water. In conclusion, this work proved the ability of a biodegradable, environmentally friendly, cheap and easy-to-use system (CS-Fe(III) system) to work as both a homogeneous and a heterogeneous catalyst toward the degradation of contaminants of emerging concern in water. This catalyst is active at near-neutral pH and promotes oxidation



via ferryl species: these conditions are particularly advantageous as they allow the elimination of pH-adjusting chemicals before and after oxidation and as they provide better control over the degradation products compared to traditional free radical-based oxidation. To develop the heterogeneous catalyst, further optimization of the material should be directed toward the synthesis of a more stable catalytic film in water.

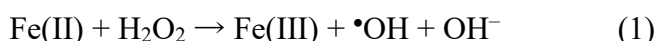
## 2.3 Natural Iron Ligands Promote a Metal-Based Oxidation Mechanism for the Fenton Reaction in Water Environments.

### 2.3.1 Introduction

The limitations of classic Fenton process were already thoroughly discussed above.<sup>70</sup> As stated, a possible solution to tackle these limitations is the use of iron ligands, in analogy with the biological oxidations catalyzed by iron complexes, e.g., Cytochrome P450 (Cyt P450) or Taurine Dioxygenase (TauD).<sup>199</sup> The use of similar iron(II) complexes as engineered catalysts is a promising variation of the traditional Fenton process, because it permits the degradation of persistent contaminants at near-neutral pH, while reducing the sludge production by keeping iron in solution.<sup>200–202</sup> Moreover, the use of an iron ligand can eventually promote a more selective action toward the oxidation, which can increase the efficiency of the treatment and give a control on by-products formation. Nevertheless, the afore stated perspective depends on the reaction mechanism, namely the active species of the system, but little is known regarding the reaction pathway in these systems. For these reason in this section, we are addressing the application of a simple method to investigate the reaction pathway when iron ligands are involved.

The reaction mechanism is widely debated both in the classic Fenton process and in the chelated modified one.<sup>203</sup>

The classic description of the traditional Fenton process is based on the first reaction of the Haber-Weiss mechanism proposal (eq. 1):<sup>55</sup>



More recent investigations also proposed a mechanism that includes the formation of a transient species where iron has a formal redox state of IV.<sup>50,57</sup> The presence of other superoxidized iron species (not only  $\text{Fe}^{\text{IV}}_{(\text{aq})}$ , but also  $\text{Fe}^{\text{V}}_{(\text{aq})}$ )

and  $\text{Fe}^{\text{VI}}_{(\text{aq})}$ ) has been additionally proven by stopped-flow experiments and UV-Vis spectroscopy.<sup>61</sup> However, the reactivity, role, and the stability of such species is only partially known. Essential contributions were provided in the works by Bossmann et al. (1998) and Pignatello et al. (1999) who highlighted the different reactivity of ferryl and hydroxyl radicals. In particular, Bossmann and co-workers compared the products of the reaction of 2,4-xylydine in genuine  $\bullet\text{OH}$  generation processes ( $\text{H}_2\text{O}_2$  photolysis) with those obtained from Fenton reactions, showing the formation of different reactive species.<sup>57</sup> Pignatello et al. provided evidence of alternative oxidants to  $\bullet\text{OH}$ .<sup>59</sup> More recently, Minero and co-workers concluded that  $\bullet\text{OH}$  (60% yield) and other species (e.g.,  $\text{FeO}^{2+}$ ) (40% yield) are formed simultaneously.<sup>60</sup>

As afore mentioned, the oxidation mechanism is amply debated also when the system comprises iron complexes, e.g., in the presence of iron ligands. Rush and Koppenol investigated a variety of chelated iron complexes, concluding that a metal-oxo species was generated in neutral solutions, while  $\bullet\text{OH}$  species dominated the process in acidic solutions of non-chelated iron.<sup>90</sup> Sutton et al. reached a different conclusion, proposing that free iron generates a metal-oxo species as the primary oxidant while  $\bullet\text{OH}$  is dominant when chelated iron is present.<sup>91</sup> A reasonable rationalization of this apparent discrepancy is that metal-oxo species and  $\bullet\text{OH}$  can both be generated concurrently in Fenton systems. Indeed, Yamazaki and Piette suggested that more than one type of oxidizing intermediate is present, and that the stoichiometry  $\bullet\text{OH}:\text{Fe}(\text{II})$  is also a function of the nature of the prevailing iron chelators.<sup>204</sup> Different chelating agents for  $\text{Fe}(\text{II})$  have been reported to promote the formation of oxoiron (ferryl) species in addition to, or instead of,  $\bullet\text{OH}$ , thus accelerating (e.g., with fulvic acid,<sup>205</sup> oxalate,<sup>206</sup> and EDTA<sup>207</sup>) or suppressing (e.g., with phosphates) the Fenton reaction.<sup>208</sup>

Because the direct experimental observation of the key intermediates involved in the oxidation pathways is challenging, indirect probes were developed.<sup>5,71,209,210</sup> Cyclohexane (Cy) was used in previous studies as an advantageous tool to discriminate between the different pathways of the Fenton reaction in organic solvents, by following the selective production of two products, namely cyclohexanol and cyclohexanone in different ratios.<sup>71</sup> Reactions initiated by hydroxyl radicals produce long-lived alkyl radical intermediates. These intermediates may react with dissolved molecular oxygen at diffusion-controlled rates to produce alkylperoxyl radicals, whose subsequent reaction is a Russell-type termination that gives equimolar quantities of alcohol (A) and ketone (K) (Figure 2.3.1 A).<sup>211</sup> Therefore,  $\text{A/K} \sim 1$  suggests the occurrence of hydroxyl radical-based reaction pathways. In contrast, an A/K ratio different than 1 is indicative of a non-free radical mechanism of oxidation, *i.e.*, the presence of

## 2.3 Natural Iron Ligands Promote a Metal-Based Oxidation Mechanism for the Fenton Reaction in Water Environments.

metal-based oxidant species (Figure 2.3.1 B). Hence, Cy oxidation may be used as a probe to clarify in a systematic way the mechanism of the Fenton reactions in water.

By using this mechanistic tool based on Cy oxidation, in this section we (i) support previous findings that (a) the classic  $\text{Fe}^{2+} + \text{H}_2\text{O}_2$  process yields  $\bullet\text{OH}$  in acidic conditions, but the reactant shifts from  $\bullet\text{OH}$  to ferryl at neutral pH values, and (b) the process combining the commercial iron tetra-amido macrocyclic ligand compound (Fe-TAML) and  $\text{H}_2\text{O}_2$  operates through a ferryl species.

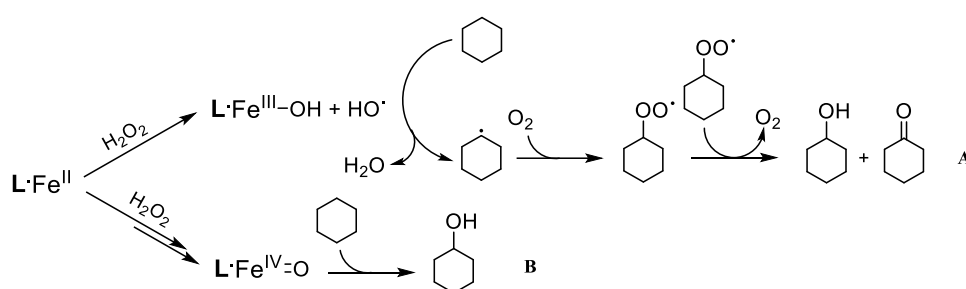


**Figure 2.3.1** Proposed mechanism for cyclohexane oxidation. A: free radical path with Russel termination type. B: a metal-based path.

One of the hypotheses of this investigation is that many iron ligands can promote a metal-based reaction process. As such, eight ligands were tested, namely, citric acid, tartaric acid, malic acid, quinic acid, EDTA, EDDS, and NTA, as well as Fe-TAML (see Figure B1 in Appendix B for its molecular structure). Therefore, we (ii) developed a method easy to use to provide evidence of the nature of Fenton reactive species in the presence of several common Fe(II) ligands, also as a function of ligand concentration to control the reaction pathway. The first seven ligands are well-known iron chelators, applied to perform oxidation reactions in water at near-neutral pH. Fe-TAML and the classic Fenton reagents (pH 3) are studied as standard controls for a metal-based and (supposed) free radical process, respectively.<sup>82,98,120</sup> Through an active species linked to the iron-ligand complex, a metal-based mechanism can modulate the path of the reaction and generate fewer and more predictable by-products. Therefore, by verifying the involvement of a metal-based mechanism during a classic or modified Fenton process in water, one can open the route toward a safer oxidation of hazardous substances, e.g., phenols, pharmaceuticals, and pesticides. In conclusion, in this investigation we validated an easy-to-use method by using the Cy as a mechanistic probe in order to investigate on the reaction mechanism of the

classic Fenton process and the chelated modified one. Moreover, the A/K ratio was used as a selectivity parameter in order to correlate a structural parameter of the iron ligands (binding constants) and their influence on the reaction.

## 2.3.2 Materials and Methods

### 2.3.2.1 Chemicals

Fe(III)-TAML was purchased from GreenOx Catalysts Inc. (Pittsburgh, PA, U.S.A.). Sodium phosphate tribasic was obtained from Carlo Erba (Italy). All the other reagents, buffer solutions, and solvents were purchased from Sigma-Aldrich. Water was of Milli-Q quality (TOC 2 ppb, resistivity  $\geq 18.2 \text{ M}\Omega \text{ cm}$ ).

### 2.3.2.2 Reaction conditions

The reaction experiments were carried out at room temperature in a 20 mL solution for 10 min under continuous stirring and were performed within 40 mL vials equipped by caps provided with septum. The concentrations of the catalyst (computed in terms of iron concentration), reagent (hydrogen peroxide), and substrate (cyclohexane) were  $10^{-7}$ ,  $10^{-6}$ , and  $10^{-4} \text{ mol/L}$ , respectively, resulting in a relative ratio of 1:10:1000. While a 1:10 catalyst:oxidant ratio is typical of engineered applications, an excess of substrate was used here to avoid the subsequent oxidation of one of the major by-products, namely, cyclohexanol. Phosphate buffer (10 mM) or perchloric acid were used to fix the pH. Because the value of the solubility constant of phosphate with iron is approximately  $10^{-16}$ , significant formation of iron phosphate can be ruled out in favor of the formation of iron-ligand complexes. All the reactions were quenched by using *tert*-butyl alcohol (t-BuOH) as scavenger of reactive species (excess concentration of 30 mM, thus 300:1 compared to cyclohexane) for subsequent analysis.<sup>212,213</sup> The iron-ligand complexes were prepared in equimolar ratio in a concentrated stock solution (0.01 mM) by stirring the mixture of the iron and ligand for 5 min, and were then diluted to 0.1  $\mu\text{M}$ .

### 2.3.2.3 Analytical conditions

The headspace, solid phase microextraction technique (HS-SPME) was chosen as extraction method before carrying out GC-MS analysis. This technique does not require solvents and allows for highly sensitive analyses. Following each reaction experiment, the vials were left in a thermostatic bath at 50 °C for 10 min to promote the transfer of all the relevant compounds into the gas-phase headspace. Then, a SPME fiber (df 75  $\mu\text{m}$ , fiber assembly carboxen/polydimethylsiloxane) was injected through the septum of the cap and

was left in the headspace for 10 min, before withdrawing it for the subsequent GC-MS analysis. Samples were analyzed on an Agilent 6890 GC system coupled with an Agilent 5973N mass selective detector (MSD). For the chromatographic separation, a Zebron-5MS capillary column (30 m  $\times$  250 mm  $\times$  0.25  $\mu$ m) was used. The injection port temperature was 280 °C, and the oven temperature program was set as follows: 40°C for 5 min, then an increase to 310°C at a rate of 15 °C/min (total run time 28.00 min). Helium was used as carrier gas at a constant flow of 1.2 mL/min, and the injector was held in splitless mode. The interface temperature was 280°C, the ionization energy was 70 eV, and the mass spectrometer operated in SIM mode acquiring the following fragments: 84, 56, 41 (cyclohexane); 82, 67, 57 (cyclohexanol); 98, 55, 42 (cyclohexanone). Duplicate experiments for some of the tests discussed in this study indicated high repeatability of the results; the error associated to the data and presented below is related to the intrinsic uncertainty of the SPME technique, computed as the average among the standard deviations reported in the 525.2 method provided by the EPA.

A few control experiments were carried out to study the Fenton degradation of phenol (by both  $\text{Fe}^{2+} + \text{H}_2\text{O}_2$  and  $\text{Fe}^{\text{III}}$ -TAML +  $\text{H}_2\text{O}_2$ ) using t-BuOH as scavenger, to take advantage of the ability of this compound to react with  $\bullet\text{OH}$  faster than with electron-capture oxidants, such as ferryl.<sup>127,213</sup> The time evolution of phenol was monitored by liquid chromatography (see the Appendix B for additional details).

### 2.3.3 Results and Discussion

#### 2.3.3.1 Iron ligands promote the preferential formation of cyclohexanol

Eight widely available ligands able to complex iron in a stable fashion were tested, namely: citric acid, tartaric acid, malic acid, quinic acid, EDTA (ethylenediaminetetraacetic acid), EDDS (ethylenediamine-N,N'-disuccinic acid), NTA (nitrilotriacetate), and TAML (tetraamidomacrocyclic ligand). These ligands belong to two macro-categories: natural (citric, tartaric, malic, quinic acid) and artificial ligands (EDTA, EDDS, NTA, TAML). This choice was provisionally made to gain insight into any possible correlation between the two categories, or among ligands in the same category. The Fe-TAML system is well-known to induce a metal-based oxidation process via a ferryl species, thus we expected an alcohol/ketone (A/K) product ratio different from 1 upon oxidation of cyclohexane.<sup>82,120</sup> Conversely, the Fenton process at pH 3 generates mostly hydroxyl radicals, or at least the hydroxyl radical is the most reactive (although

not the only one) species in the system. Therefore, the reaction should proceed mostly via a free radical mechanism, with an A/K ratio around 1.<sup>60</sup>

Figure 2.3.2 shows the A/K ratio values obtained with all the investigated ligands and in the absence of ligands, *i.e.*, classic Fenton. The results obtained from oxidation tests performed with Fe-TAML and in the classic Fenton process are in line with expectations, namely, an A/K ratio higher than 1 and around 1 in the case of Fe-TAML and classic Fenton, respectively, thus attesting to the validity of the method. Since an A/K ratio significantly higher than 1 was obtained with all the investigated ligands, it is reasonable to hypothesize that the presence of an iron ligand in water promotes a metal-based oxidation.

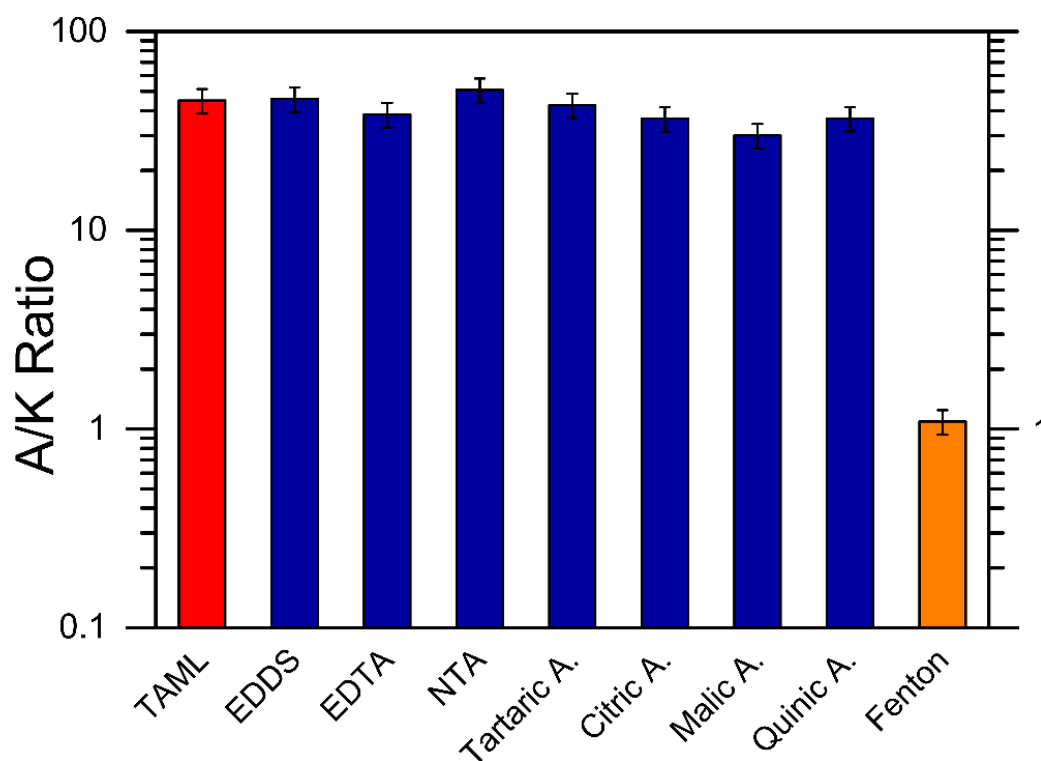


**Figure 2.3.2** A/K ratio observed in the oxidation of cyclohexane with different iron ligands at pH 7 (phosphate buffer) and with the classic Fenton process at pH 3 (perchloric acid) after 30 min of reaction.

These conclusions are confirmed by the results of the degradation of phenol, with  $\text{Fe}^{2+} + \text{H}_2\text{O}_2$  at pH 3 and with Fe-TAML +  $\text{H}_2\text{O}_2$  (see Figure C2 in Appendix C, as well as the related text). We carried out these experiments both in the absence and in the presence of t-BuOH, which reacts with  $\cdot\text{OH}$  faster than with ferryl.<sup>127,213</sup> However, to avoid total quenching of the system by t-BuOH, the t-BuOH:phenol ratio was 40:1 and not 300:1 as per the Cy experiments. In the case of  $\text{Fe}^{2+} + \text{H}_2\text{O}_2$ , t-BuOH strongly inhibited phenol degradation, while in the case

of Fe-TAML the effect of the alcohol was practically negligible. These findings are consistent with  $\bullet\text{OH}$  being involved in phenol degradation by  $\text{Fe}^{2+} + \text{H}_2\text{O}_2$  at pH 3, and with ferryl playing the same role with Fe-TAML +  $\text{H}_2\text{O}_2$ . Indeed, the t-BuOH scavenging experiments agree with the A/K ratios derived from the Cy degradation experiments (Figure 2.3.2).

It is important to check for possible variations of the A/K ratio with reaction time, to ensure that unbiased conclusions are obtained. Figure 2.3.3 shows the kinetics of Cy degradation with citric acid (Figure 2.3.3a), malic acid (Figure 2.3.3b), and quinic acid (Figure 2.3.3c) as iron ligands (left Y-axis: A/K ratio, right Y-axis: Cy degradation). Cy degradation with citric and quinic acids was very fast and the process reached completion after roughly 2 min of reaction. The corresponding A/K ratio remained stable and significantly larger than 1 during the entire duration of the test (30 min). On the other hand, Figure 2.3.3

b (malic acid) shows slower kinetics of degradation, with an A/K ratio reaching a peak value after 10 min of reaction. This slower degradation allowed for an easier monitoring of the initial preferred formation of the alcohol species ( $\text{A/K} > 1$ ) and the subsequent oxidation of the alcohol into the ketone, which caused a slight A/K reduction following the peak. The large excess of the initial Cy consumed almost all the reactive species, thereby limiting their availability for alcohol oxidation. By monitoring the A/K time evolution, one can thus be confident that there is negligible bias linked to the further evolution of the system ( $\text{A} \rightarrow \text{K}$  oxidation, or further Fenton processes involving, e.g., Fe(III) after total Fe(II) consumption) after the initial reaction step.<sup>211</sup>

The fact that the A/K ratio did not change much after the initial step suggests that the mechanistic conditions reflect those of the initial reaction between Fe(II) and  $\text{H}_2\text{O}_2$ . Under our experimental conditions and based on the stoichiometry of reaction (1), this process would entail total consumption of Fe(II) that would be oxidized to Fe(III), and 10% degradation of  $\text{H}_2\text{O}_2$ . Afterwards, Fe(III) would be recycled to Fe(II) at the expense of the remaining  $\text{H}_2\text{O}_2$ .

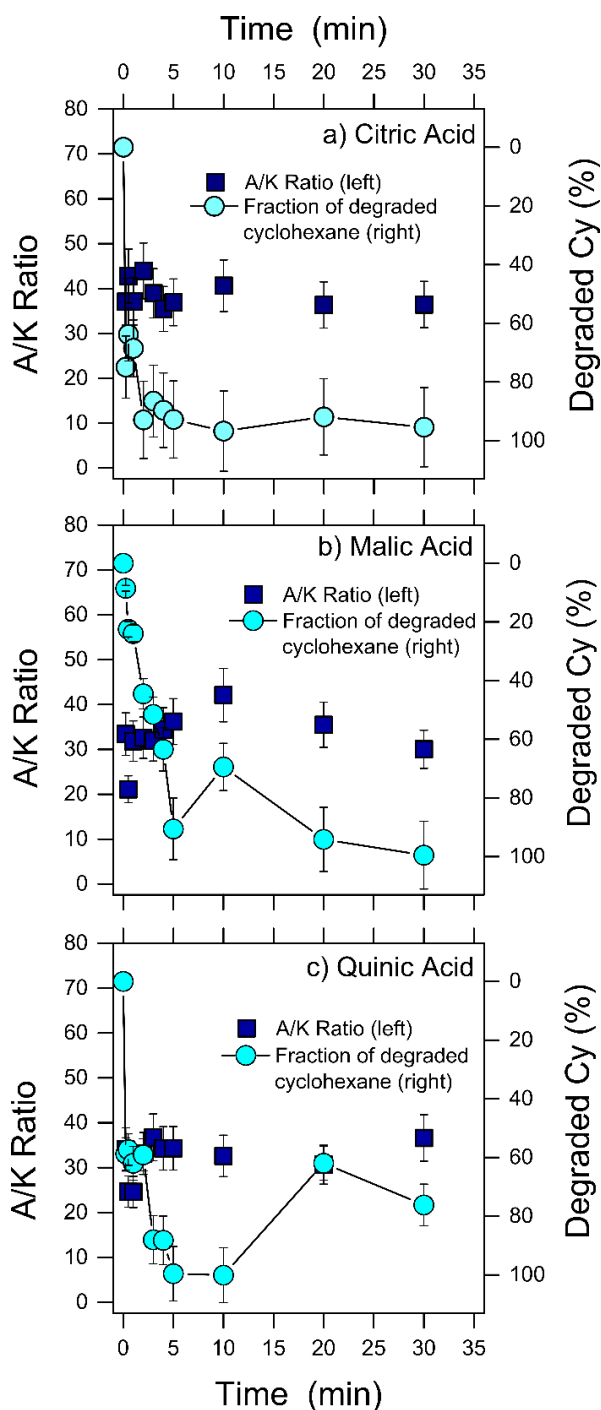


**Figure 2.3.3** Fraction of degraded cyclohexane with respect to the total degraded amount (circles, right axis) and trend of selectivity, *i.e.*, A/K ratio (squares, left axis), as a function of time in a system containing hydrogen peroxide as reactant and a) citric acid, b) malic acid, or c) quinic acid as iron ligands. The pH of the aqueous system was buffered at 7 (phosphate buffer). The solid lines connecting the circles are only intended as a guide for the eye.



## 2.3 Natural Iron Ligands Promote a Metal-Based Oxidation Mechanism for the Fenton Reaction in Water Environments.

The influence of the reaction environment was also studied by following the A/K ratio in the oxidation of Cy at different pH values (3-7) (Table 2.3.1). All the individual concentrations of alcohol and ketone products obtained during the experiments are presented in the Appendix C (Tables C1-C3). Citric, malic, and quinic acid were chosen as iron ligands because the iron binding constant of these compounds would not change significantly within the explored pH range, thereby allowing for the pH value to solely affect the Fenton process (Appendix C, Figure C3). Phosphate (10 mM) was used to buffer the pH at values of 5, 6, and 7, while perchloric acid (1.16 M stock solution) was employed in tests performed at pH 3. In all these cases, the A/K ratios were higher than 1, independently of the pH values. This finding suggests that a metal-based mechanism in the presence of the three ligands was observed regardless of the acidity of the solution. Although acidity has no direct effect on the mechanistic path, the conditional binding constant may be function of the pH and this indirect effect of the solution acidity is discussed below.

**Table 2.3.1** A/K ratio for the oxidation of cyclohexane at different pH values with citric, malic and quinic acid as iron ligands. The pH was fixed with phosphate buffer except for pH 3 (HClO<sub>4</sub>). The reaction time was 30 min.

	pH 3	pH 5	pH 6	pH 7
<b>Citric acid</b>	10±1	7.4±1.0	8.5±1.2	8.6±1.2
<b>Malic acid</b>	18±3	15±2	16±2	15±2
<b>Quinic acid</b>	28±4	31±4	23±3	28±4

### 2.3.3.2 Switching the mechanism from free radical to metal-based catalysis

In the previous part, we hypothesized that the mechanistic degradation path depends on the presence of the ligand, and possibly on its concentration and conditional binding constant. In order to investigate the influence of the ligand concentration and of its conditional binding constant with the metal (*i.e.*, the value of the binding constant that takes into account the protonation of the ligand at the given pH value), EDTA and EDDS were chosen as iron ligands and applied at acidic pH. Despite their structural similarity, these two ligands behave differently in terms of their conditional binding constant as a function of pH (reasons are well described in the paper of Martell et. al). Specifically, while the conditional binding constant at pH 7 is high for both EDTA and EDDS ( $\sim 10^{11}$  and  $10^6$ , respectively), at pH 3 EDDS features a low conditional binding constant ( $10^{-3}$ ),

while that of EDTA is still relatively high ( $\sim 10^4$ ) (see Appendix C, Figure C3). Therefore, when using EDDS as iron ligand at pH 3, one expects a high amount of free iron to occur in solution, which could reasonably induce a classic Fenton process (free radical mechanism). In this series of experiments, the pH value was fixed at a value of 3 by addition of perchloric acid.

Figure 2.3.4 reports the A/K ratios observed when EDDS and EDTA were used as ligands at pH 3, at various [Ligand]:[Fe(II)] ratios. All the individual concentrations of alcohol and ketone products obtained during the experiments are presented in the Appendix C (Tables C4-C5). Please note that Figure 2.3.2 summarized instead the A/K ratios measured at 1:1 [Ligand]:[Fe(II)] ratio and at pH 7. Consistently with the hypotheses, at 0:1 ligand:iron ratio (*i.e.*, with no ligand in solution) we observed the classic Fenton process and the A/K ratio was close to 1. The A/K ratio remained always close to 1 with EDDS, regardless of its concentration. Based on the conditional binding constants, when using EDDS as iron ligand at pH 3, one expects free iron to occur in solution, which could reasonably promote a process similar to a classic  $\bullet$ OH-based Fenton reaction. In contrast, with EDTA the reaction clearly switched from a free radical mechanism to a metal-based one when the ligand concentration increased. These results strongly suggest that the presence of a bonded Fe(II)-ligand complex plays a crucial role in the direction of the mechanistic path. This parameter is a strong function of the concentration of the ligand as well as of the conditional binding constant of the complex metal/ligand. Therefore, one can generalize that the mechanistic path may be mostly imputable to the concentration and to the conditional binding constant of the ligand, and that the environmental conditions have importance only if they affect complex formation.

### 2.3 Natural Iron Ligands Promote a Metal-Based Oxidation Mechanism for the Fenton Reaction in Water Environments.

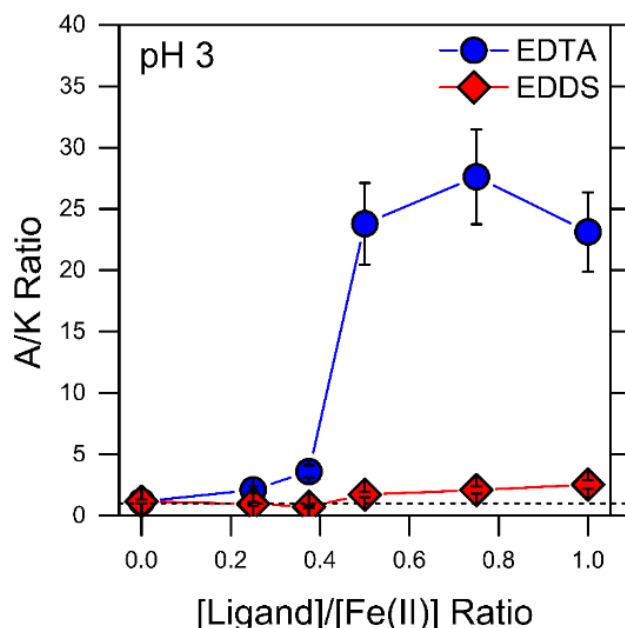


**Figure 2.3.4** A/K ratio observed after 30 min of reaction in the oxidation of cyclohexane with EDTA and EDDS as iron ligands, added at different concentrations. The runs were carried out at pH 3. The condition of no added Ligand ( $[\text{Ligand}]/[\text{Fe(II)}] = 0$ ) corresponds to the classic Fenton process. The solid lines are only intended as a guide for the eye. The dashed line depicts the expected A/K ratio for a pure free radicals-based catalysis.

#### 2.3.3.3 Evidence of the effect of pH on the traditional Fenton process

Finally, we provide some insight into the Fenton mechanism at different pH values. Figure 2.3.5 shows the A/K ratio obtained with the classic Fenton process in the 3-7 pH range, fixed by use of phosphate buffer solution (PBS). Additional experiments were also conducted by fixing the pH at 3 and 4 using perchloric acid instead of phosphate buffer. Please note that Fe(II) was dosed at low concentration (0.1  $\mu\text{M}$ ) to avoid its precipitation as hydroxide, which would otherwise take place at near-neutral pH ( $\text{pKs}^{\text{Fe(OH)}_2} = 15.1$ <sup>214</sup>). The results obtained in the absence of ligands imply that the classic Fenton reaction proceeds through a free radical or mixed mechanism up to pH 5. Above this value, the mechanism switched to a preferential metal-based one. This result is supported by previous reports proposing that a ferryl species is involved in the Fenton reaction at near-neutral pH.<sup>58,89,215</sup> The presence of a ferryl species at pH 6-7 means that the classic Fenton reaction will be less reactive under near-neutral conditions, since the non-coordinated ferryl species is considered less reactive than the hydroxyl radical.<sup>215</sup>

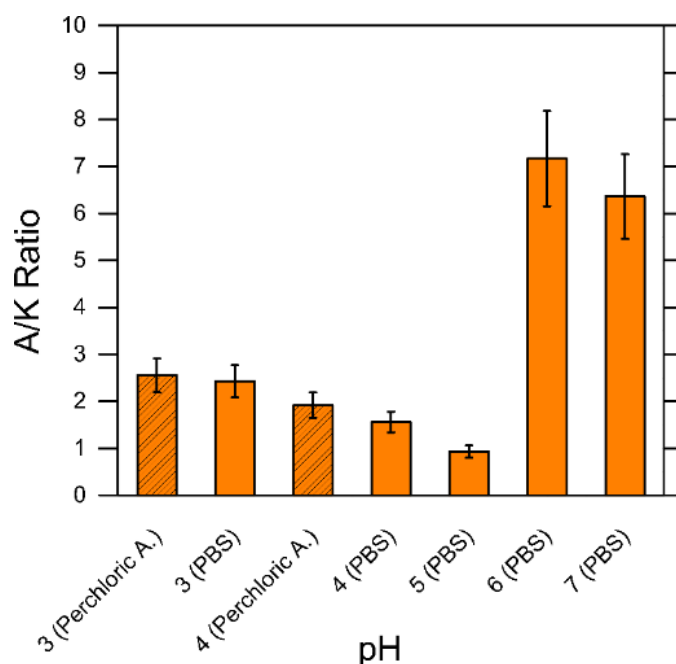


**Figure 2.3.5** A/K ratio observed in the classic Fenton process performed at different pH values.

### 2.3.4 Conclusions

The oxidation mechanism of the Fenton reaction was here investigated with and without iron ligands in solution. Eight widely common ligands that are able to complex iron(II) were studied, namely, citric acid, tartaric acid, malic acid, quinic acid, EDTA, EDDS, and NTA, plus the Fe-TAML system. The ligand performance was tested toward the oxidation of cyclohexane by following the formation of the main products, namely, cyclohexanol (A) and cyclohexanone (K). Measurement of the concentration ratio between these two species (A/K ratio parameter) during the reaction was used to provide evidence of the mechanisms involved in the oxidation of the substrate.

All the tested ligands showed high A/K ratios, which is a proper index of a metal-based behavior, including the well-known Fe-TAML system that was expected to behave in this fashion. Also expected was the fact that the classic Fenton process was associated with an A/K ratio of approximately 1, evidence of a free radical process, which adds further evidence in favor of cyclohexane as suitable probe when coupled with the A/K ratio.

This work proves the ability of simple iron ligands to drive the reaction pathway towards selective metal-based catalysis, as opposed to the activity of free radicals that promote undifferentiated oxidation of substrates in solution. Selective

catalysis allows for better control of the degradation pathway of harmful contaminants, to avoid the formation of toxic by-products. The ubiquitous character of the Fenton process in nature and of iron complexes formed in water (e.g., citrate), alongside the generation of  $\text{H}_2\text{O}_2$  in illuminated NOM-containing environments, lead to (photo)Fenton reactions during the diurnal cycles. As such, the present study holds important implications also in the elucidation of the Fenton process that occurs both in nature and in engineering applications and sets the basis for further investigation concerning the effectiveness of ligand-mediated oxidation of natural and anthropogenic contaminants.

## 2.4 Summary

Metabisulfite is suggested as an effective alternative to conventional hydrogen peroxide, if used as reactant in oxidations mediated by Fe-TAML. Fe-TAML promotes highly selective and efficient degradations, in particular toward phenolic compounds. The feasibility of processes promoted by Fe-TAML would gain from the use of metabisulfite, as this reactant shows a lower level of health and safety risks to both users and to the aquatic environments compared to hydrogen peroxide or other conventional oxidants.

The CS-Fe system was demonstrated to be a new effective and environmentally friendly catalyst for the oxidative degradation of organic contaminants. This system was preliminary used as both homogeneous and heterogeneous catalyst. It is highly effective at near-neutral pH and is cheaper and easier to handle than Fe-TAML since it does not require a cumbersome synthesis protocol. Moreover, preliminary mechanistic study showed the prominent metal-based behavior of the system, hinting to a probable high selective oxidation process.

Also, a new analytical strategy was developed and validated to discriminate metal-based and free radical mechanisms. The method is an easy mechanistic tool, although still indirect in the identification of the ferryl species. The experiments showed that the presence of an iron ligand induces a metal-based process, hence a more selective oxidative process.

The use of effective iron ligands is the general strategy here proposed to overcome some the limitations of the Fenton process. Using an environmentally friendly iron ligand and reactants, it is possible to promote the sustainability of the oxidation process, to avoid the production of large amounts of sludge, to perform oxidations at near-neutral pH, hence avoiding the use of acids and bases, to induce a selective catalytic process, hence gain efficiency in multi-contaminated waters,

and eventually to limit the formation of undesirable by-products. Moreover, the catalytic process allows recycling the reagents through the catalytic cycle, hence limiting waste.

## Chapter 3

### 3 Impact of oxidative and non-oxidative processes in disinfection

Water disinfection strategies have undoubtedly contributed to dramatically increase the quality of life of people worldwide, widening the pool of potential sources of water. The most used biocides work through oxidative processes. Indeed, the most common biocide worldwide is an oxidant species, namely, hypochlorite.<sup>216</sup> Its low cost and its high efficiency toward a wide spectrum of biological contaminants explain its extensive use as disinfectant.<sup>216</sup> However, chlorination by-products are potential carcinogenic compounds.<sup>39</sup> Numerous other biocides working through different disinfection mechanisms (*e.g.*, oxidative, lytic, electrophilic), have been identified and developed.<sup>46</sup> Every biocide has advantages and disadvantages in terms of harmful DBPs formation, cost of implementation, and environmental impact. Therefore, it is unhelpful, if not impossible, to define the perfect biocide for all and any circumstance. It would rather be more constructive to develop a general strategy to evaluate the feasibility of various disinfection approaches to be applied in specific cases. The link among the disinfection mechanism and the mechanism of DBPs generation may be the key to determine a generalized strategy of biocide implementation according to each circumstance, for example, the main physico-chemical features of the target water effluent and the disinfection objectives.

In the first part of this section, the activity of 9 biocides acting through three different mechanisms is discussed against both algae and *E. coli* in a highly representative real wastewater. Their safety and environmental impact are

assessed by evaluating the formation of halogenated by-products. The disinfection mechanisms already proposed in the literature for each biocide and the results of DBPs formation discussed in this section help to define preliminary hypotheses on the mechanisms of generation of DBPs, hence guide biocide selection.

In the second part, the ability of PAA to generate DBPs is specifically assessed both in presence and absence of DOM, hence in simplified synthetic waters and in the same real wastewater employed to screen among the 9 biocides. PAA is quickly gaining ground in water treatments although its behavior in water is not completely clarified and its ability to generate harmful DBPs is still controversial. Specific experiments are thus discussed aimed at defining the full process of DBPs generation, hence eventually identifying other harmful intermediates during disinfection process in the presence of PAA.

### **3.1 Evaluation of the Effectiveness, Safety, and Feasibility of 9 Potential Biocides to Disinfect Acidic Landfill Leachate from Algae and Bacteria**

#### **3.1.1 Introduction**

The European Union defines biocides as substances “intended to destroy, deter, render harmless, prevent the action of, or otherwise exert a controlling effect on any harmful organism”. Despite the potential risks for humans and for the environment, biocides are deployed in a variety of activities, including sanitation, the textile industries, and water treatment.<sup>46,217–219</sup> Within the water treatment industry, they are usually applied as antifouling additives and disinfectants.<sup>220–223</sup> However, disinfection processes may lead to the formation of harmful disinfection by-products (DBPs), such as halogenated compounds (*e.g.*, trihalomethanes, THMs) and bromate, which are often known or suspected carcinogenic compounds.<sup>43,69,224</sup> Therefore, the correct application and management of biocides is crucial for the implementation of safe water technologies.

Well-established solutions include processes like ozonation. Ozone must be produced in situ and it is thus associated with higher operational costs; also, it can generate bromate, a carcinogenic DBP, in the presence of bromide.<sup>43</sup> The other commonly employed biocides have each advantages and disadvantages. For example, owing to its optimum cost-efficiency ratio, hypochlorite represents one



of the most applied bactericidal compounds.<sup>225</sup> Nevertheless,  $\text{ClO}^-$  leads to the formation of THMs and it is an irritant for the mucous membranes when concentrated in water.<sup>225–227</sup> Promising alternatives were developed during the last decade, among which chlorine dioxide and peracetic acid are the most successful examples. Even if these two compounds are effective biocides against a wide spectrum of microorganisms, recent studies demonstrated that the former could generate chlorite and chlorate, both harmful DBPs, together with traces of tribromomethane, while the latter represents a potential source of THMs in the presence of bromide and NOM in water.<sup>44,228–231</sup> All the above-mentioned compounds rely on oxidative processes in order to attain disinfection. Other compounds can work as biocides through different mechanisms, for example, the couple methylisothiazolinone / chloro-methylisothiazolinone (MIT), as well the 2,2-dibromo-2-cyanoacetamide (DBNPA).<sup>46</sup> Nevertheless, the literature lacks studies related to these compounds and to the formation of DBPs once they are used for disinfection of contaminated water streams.

In addition to the compounds discussed so far, reductants may find an application in water disinfection. For instance, they can potentially affect the photosynthetic mechanism, thus limiting the growth of algae species.<sup>232–235</sup> Reducing agents include sulfuric compounds, such as sulfur dioxide, bisulfite, and sulfite. Moreover, the ability of sulfites to inhibit the growth of some bacterial groups has been reported.<sup>47</sup> In particular, sulfites are promising compounds for industrial applications, owing to their ease of storage, safety (they are not as explosive as oxidants), lack of toxicity for humans and the environment, and low capital and operational costs.<sup>236</sup>

Finding an inexpensive and easy-to-deploy biocide, which concurrently is effective, eco-friendly, and does not contribute to DBPs generation, is a challenging task. This is especially true in the treatment of complex water and wastewater streams, such as those laden with organic materials and dissolved solids. Relevant examples of such effluents are landfill leachate and mine drainage. For example, the leachate of phosphogypsum landfills create an acidic environment, rich of phosphate nutrients and halides.<sup>237</sup> Acidophilic microalgae can easily adapt and grow in this environment.<sup>238,239</sup> Although acidic conditions generally kill bacteria, Gut et al. observed that a significant salt concentration in the water matrix, chloride content in particular, plays a key role in the activity of proton membrane pumps that allows the survival of bacteria.<sup>240</sup> Moreover, Jordan et al. and de Jonge et al. showed that some *Escherichia coli* (*E. coli*) sub-populations can reach physiological equilibrium even at pH values as low as 2–3.<sup>241,242</sup> The possible presence of different microorganisms and the complexity of

such matrix make this type of contaminated water a perfect target for an investigation aimed at the evaluation of traditional as well as innovative biocides.

In this investigation, the disinfection effectiveness of different biocides is evaluated against both microalgae and *E. coli*, while their safety is assessed by quantifying the formation of harmful halogenated by-products. Specifically, 9 biocides acting through three different disinfection mechanisms are evaluated. Along with the most common biocides commercially available, exploiting mainly oxidation, a detailed discussion is reported for electrophilic biocides, while a new disinfection route exploiting reducing agents is assessed for the first time. In order to evaluate the applicability of the studied solutions, the biocide behavior is evaluated in real groundwater contaminated with phosphogypsum landfill leachate. A brief discussion of the disinfection mechanism is provided for each biocide, with the goal to help the interpretation of the biocidal action and the consequent formation of halogenated compounds in the target water matrix. Finally, the most promising biocides are evaluated in terms of environmental impacts and cost of application.

### 3.1.2 Materials and Methods

#### 3.1.2.1 Chemicals, reagents, and water matrices used in the study

The biocides investigated in this study were: (i) oxidants, namely, hypochlorite ( $\text{HClO}$ ), peracetic acid (PAA), chlorine dioxide ( $\text{ClO}_2$ ), hydrogen peroxide ( $\text{H}_2\text{O}_2$ ), and persulfate ( $\text{K}_2\text{S}_2\text{O}_8$ ); (ii) electrophilic, namely, DBNPA and MIT; (iii) reductants, specifically, sulfite and metabisulfite. All the chemicals were used as received. Except for chlorine dioxide, which was purchased from Apura Srl (Brescia, Italy), all the other compounds were purchased from Sigma-Aldrich (Milano, Italy). MIT was prepared by mixing methylisothiazolinone and chloro-methylisothiazolinone at the appropriate concentration in an aqueous solution in a volume ratio of 1 to 3. For disinfection and DBP generation experiments, individual biocides were dosed at the target concentrations (*vide infra*) in 15 mL of water samples. All the water chemistry analyses were performed at a private external laboratory (Natura Srl, Naples, Italy).

Groundwater receiving leachate from a phosphogypsum landfill was directly obtained from the pumping wells in a contaminated site in the south of Italy and used as is. The main characteristics of the contaminated groundwater are summarized in Table 3.2.1. A significant concentration of microalgae is present, but with a low level of organic matter. The contaminated water did not contain trihalomethanes or other halogenated organic compounds at detectable

### 3.1 Evaluation of the Effectiveness, Safety, and Feasibility of 9 Potential Biocides to Disinfect Acidic Landfill Leachate from Algae and Bacteria

---

concentrations. Disinfection of this wastewater is required as a first stage in the existing treatment train, to protect and enhance the subsequent coagulation process, accomplished through addition of polyelectrolytes, ferric chloride, and calcium hydroxide for the removal of a large part of heavy metals, radionuclides, phosphate, sulfate, and fluoride. A second disinfection phase is then present to reduce fouling and biofouling in the following ultrafiltration and reverse osmosis filtrations aimed at final effluent desalination. <sup>220,222,223</sup>

**Table 3.1.1** Main characteristics of the contaminated groundwater from analysis of the samples and historical data obtained from the treatment plant management.

Parameter	Units	Average Value or Range
Chloride	mg/L	2690
Bromide	mg/L	6.4
Fluoride	mg/L	220-320
Sulfate	mg/L	3130
Phosphate	mg/L	2400
Nitrate	mg/L	60
Bicarbonate	mg/L	10
N-NH <sub>4</sub> <sup>+</sup>	mg/L	480-590
Iron	mg/L	5.4
Manganese	mg/L	6.2
TOC	mg/L	58 ± 12
Microalgae	cells/mL	1.76 ± 0.6 × 10 <sup>6</sup>
pH		2.8

---

#### 3.1.2.2 *Microalgae sampling and counting*

Samples for microalgae quantification were collected in real water samples before disinfection and 2 h after the addition of each disinfectant. To quantify the algae concentration, a counting chamber was employed (Paul Marienfield GmbH & Co, Lauda-Königshofen, Germany). The chamber is equipped with an optical microscope (Renishaw, UK). The concentration of algae cells suspended in the samples was determined by multiplying the average number of cells observed in the microscope images by the relevant area, the chamber depth, and the dilution factor.

#### 3.1.2.3 *Bacterial methods: LB, saline solution, and bacterial suspension preparation*

Luria Bertani (LB) broth was prepared by completely dissolving tryptone (10 g), yeast extract (5 g), and sodium chloride (10 g) in 1 L of deionized water. A slightly hypertonic saline medium was also prepared by dissolving sodium chloride (8 g) and potassium chloride (0.8 g) in 1 L of deionized water; the pH of this solution was adjusted to a value between 7 and 7.5 with 0.1 M NaOH and 0.1 M HCl. Before use, the LB and saline mixtures were autoclaved for 15 min at 15 psi at a temperature of 121 °C.

To prepare the bacterial suspension, a volume of 5 mL LB was pipetted into a 15 mL falcon tube. The working *E. coli* strain is a wild-type isolate from urban secondary wastewater, obtained by isolation and selection of the microorganism on selective growth media. The *E. coli* bacterial inoculum was made from a pre-prepared master plate; a colony was dispersed in 5 mL LB by mixing in a vortex machine for 30 s. Following this step, the falcon tube was placed in a temperature-controlled incubator at 37 °C for 8 h under gentle agitation by circular motion. Subsequently, 2.5 mL of the suspension was diluted in 250 mL of LB and left for 15 h in the incubator to achieve stationary growth phase (3.5-5.5 OD<sub>600</sub>) and a concentration of roughly 10<sup>9</sup> colony forming units (CFU)/mL; the detailed procedure of bacterial preparation and purification was published elsewhere.<sup>243</sup>

#### 3.1.2.4 *Determination of the minimum inhibitory concentration (MIC) of E. coli, and determination of bacterial disinfection kinetics by biocides*

The minimum inhibitory concentration (MIC) represents the lowest concentration of biocide in water, above which no significant visible growth of bacteria occurs. It is an intrinsic characteristic of each biocide and depends also on the type of bacteria. To determine this parameter for the different biocides investigated in this study, a falcon tube was filled with a 10<sup>6</sup> CFU/mL suspension of *E. coli* in LB. Each biocide was spiked in the suspension at the target concentration and the falcon tube was then incubated for 24 h at 37 °C. Both

positive and negative controls (*i.e.*, no biocide, and no bacteria, respectively) were always performed to ensure that no contamination occurred. The absorbance at 600 nm wavelength was then measured to determine the bacterial concentration, following calibration with suspensions of known concentrations determined by plating and counting.

Furthermore, kinetics disinfection experiments were performed in real contaminated groundwater by addition of the various biocides. An appropriate amount of LB *E. coli* suspension was added to the matrix to obtain a concentration of bacteria of roughly  $10^6$  CFU/mL. The biocides were added individually to the matrix and samples were collected at regular intervals. Upon sampling, serial dilutions were immediately made in saline medium and the resulting suspensions were spread onto agar plates. After 1 day of incubation at 37 °C, the CFUs were counted to determine the concentration of cultivable cells. A concentration of biocides equal to 0.03 mM was chosen for kinetics disinfection tests, this being the lowest value determined for the removal of microalgae from real groundwater samples (*vide infra*). The same disinfection experiments were also performed with metabisulfite and hydrogen peroxide at each respective MIC (*vide infra* for MIC values determined by experiments).

#### 3.1.2.5 Methodology of life cycle analysis (LCA)

The environmental burden from the production of 1 kg of the three most interesting biocides (*i.e.*, MIT, hydrogen peroxide, and metabisulfite; *vide infra*) were evaluated by life cycle analysis using OpenLCA 1.10 software, which incorporates the Ecoinvent 3.5 database. Three different methodologies were employed to conduct the environmental assessments: ReCiPe, Cumulative Energy Demand (CED), and IPCC2013. In the case of ReCiPe, the environmental analysis was modeled on both the endpoints and the midpoints, the latter presented as normalized values on the total impact. Midpoints are representative of the cause-effect chain (environmental mechanism) of an impact category, such as ozone depletion potentials, global warming potentials, and photochemical ozone (smog) creation potentials. The endpoints are indicators of the social implication of midpoints. They are divided into: (i) human health, which represents the years that are lost or during which a person is disabled due to a disease or accident; (ii) the unit for ecosystem quality, which represents the local species loss integrated over time; (iii) resource scarcity, which represents the extra costs involved for future mineral and fossil resource extraction. The Cumulative Energy Demand (CED) approach was applied to assess the required energy expressed as the primary energy demand, while Intergovernmental Panel on Climate Change (IPCC2013) analysis with a timeframe of 20 years was performed to assess the global warming potential of the production of the three

biocides. While hydrogen peroxide is present in the Ecoinvent database, the impacts of metabisulfite and MIT were determined by modeling their most common synthesis approach. For metabisulfite, the reaction between  $\text{SO}_2$  and NaOH was considered, while the protocol for MIT production was based on literature reports.<sup>244</sup>

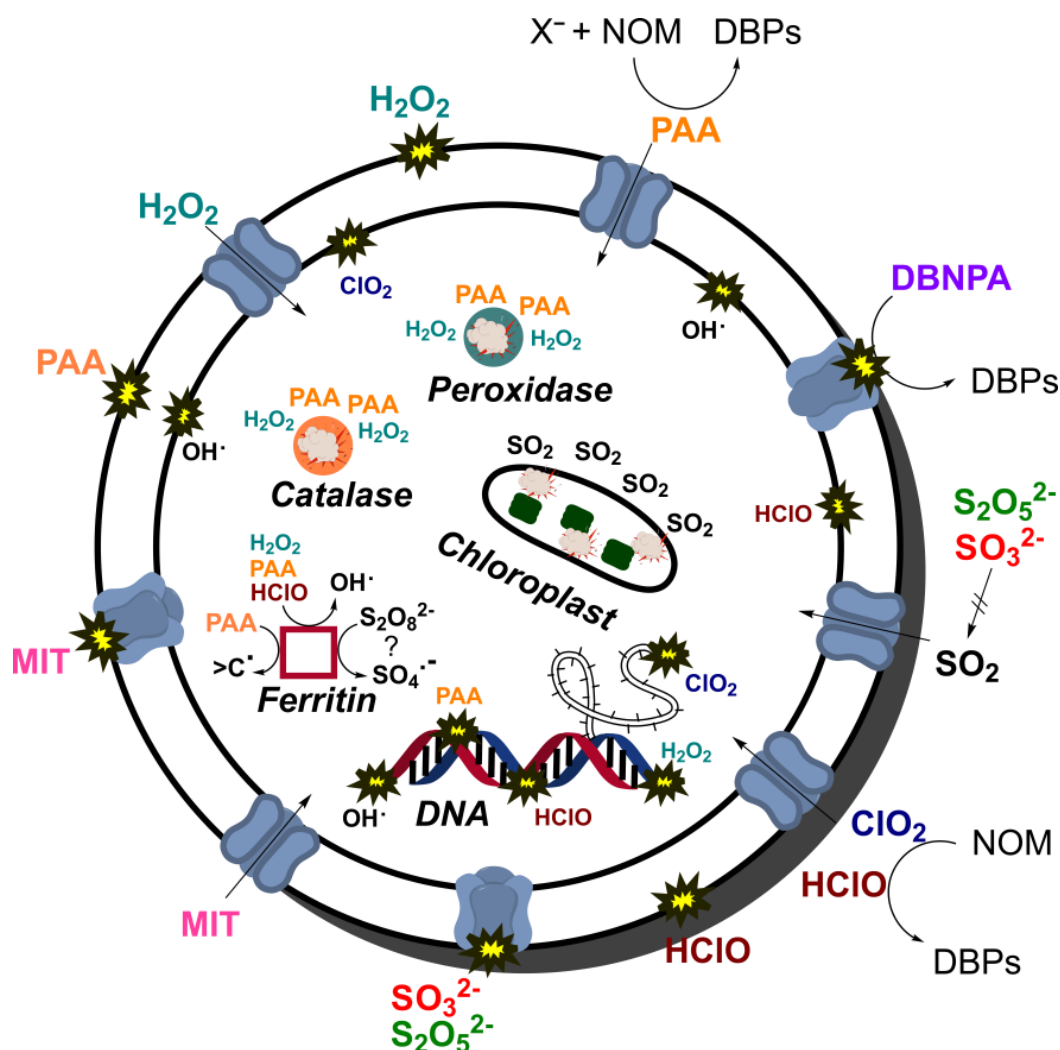
### 3.1.3 Results and Discussion

#### 3.1.3.1 Disinfection targets and principal characteristics of the studied biocides

Before the analysis of the efficacy of each disinfectant, we present a succinct summary of their main characteristics. The mode of action of the 9 biocides investigated in this work is depicted in Figure 3.1.1 and briefly summarized in Table 3.1.1 together with each molecular structure.  $\text{HClO}$ ,  $\text{ClO}_2$ ,  $\text{H}_2\text{O}_2$ , and PAA can penetrate the phospholipidic membrane through passive diffusion, thus these biocides disinfect through an intracellular action by acting on enzymatic processes and by attacking the DNA purine bases and the internal cytoplasmic membrane.<sup>202,225,245–250</sup> Moreover  $\text{HClO}$ ,  $\text{ClO}_2$ ,  $\text{H}_2\text{O}_2$ , and PAA can also damage the outer cellular membrane.<sup>225,245,251</sup> Persulfate is active toward microorganism disinfection mostly if activated by transition metals.<sup>249,252</sup> An estimation of the oxidation efficiency of an oxidant biocide can be estimated from a thermodynamic standpoint by comparing the redox potential of the reagent with that of bacteria strains (the *E. coli* redox potential is generally +0.45 to +0.72 V at pH 7 vs. SHE).<sup>253</sup> Therefore, all the biocides with a redox potential higher than +0.45 to +0.72 V at pH 7 will be able to damage *E. coli* bacteria through oxidation.

The two electrophilic biocides, namely, DBNPA and MIT, disinfect by means of both extracellular and intracellular actions. DBNPA is mostly active by damaging the external cellular membrane through an electrophilic addition to the nucleophilic groups of membrane proteins. MIT is active also by inhibiting internal enzymatic processes.<sup>45,46,246,254</sup> Literature lacks a detailed explanation on the disinfection mechanism of metabisulfite. On the basis of previous reports and of its molecular structure, it is reasonable to assume that metabisulfite can potentially alter the photosynthetic process of microalgae by releasing  $\text{SO}_2$  in solution and that it can damage the cellular membrane in the same fashion of an electrophilic biocide, but its intracellular activity is still under debate.<sup>232–235</sup> A more exhaustive discussion of the mechanism of disinfection and DBPs generation mode for each of the 9 biocides is provided in Appendix D.

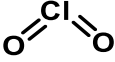
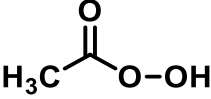
### 3.1 Evaluation of the Effectiveness, Safety, and Feasibility of 9 Potential Biocides to Disinfect Acidic Landfill Leachate from Algae and Bacteria



**Figure 3.1.1** Mode of action of the biocides investigated in this study. Please note that chloroplasts are present only in algae.

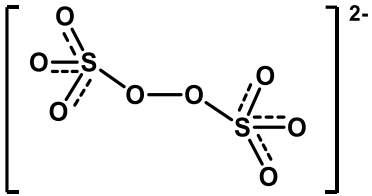
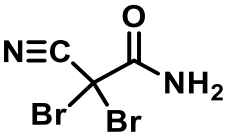
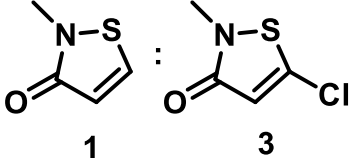
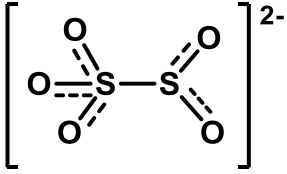
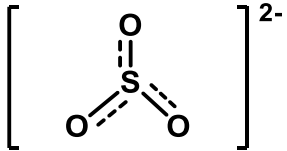
**Table 3.1.1** Molecular structure, mode of action (MOA), and mechanism of DBPs generation for each biocide investigated in this study. In the fourth column, “oxidizing” (O), “electrophilic” (E), and “reductant” (R) refer to the main MOA of each biocide. The last column presents the redox potential for each oxidant biocide.

Biocide	Molecular structure	Mechanisms of disinfection and of DBPs generation	MOA	$E_0$ (V vs. SHE; pH 7)
Hypochlorite ( $\text{HClO}$ )	$\text{Cl}-\text{OH}$	<ul style="list-style-type: none"> <li><math>\text{HClO}</math> prevails at pH 2.8.</li> <li>Intracellular/Extracellular action.</li> </ul>	O	1.4

		<ul style="list-style-type: none"> <li>Internal "Fenton-like" process  <math>(\text{HClO} + \text{Fe}^{2+} \rightarrow \text{HO}^\cdot + \text{Cl}^- + \text{Fe}^{3+})</math></li> <li>Addition to purine base of DNA and nucleophilic sites of internal organelles.</li> <li>THMs and HACs generation through electrophilic addition to organic material.</li> </ul>		
Chlorine dioxide ( $\text{ClO}_2$ )		<ul style="list-style-type: none"> <li>Intracellular action (and possible extracellular action).</li> <li>Inhibition of protein synthesis and enzymatic processes.</li> <li>Addition to internal cytoplasmic membrane</li> <li><math>\text{ClO}_2^-</math>, <math>\text{ClO}_3^-</math> generation through oxidation of <math>\text{Cl}^-</math>.</li> <li>Slight THMs generation through electrophilic addition to NOM.</li> </ul>	O	0.95
Hydrogen peroxide ( $\text{H}_2\text{O}_2$ )	HO-OH	<ul style="list-style-type: none"> <li>Intracellular/Extracellular action.</li> <li>Inhibition of peroxidase activity.</li> <li>Internal Fenton process.  <math>(\text{H}_2\text{O}_2 + \text{Fe}^{2+} \rightarrow \text{HO}^\cdot + \text{OH}^- + \text{Fe}^{3+})</math></li> </ul>	O	1.8
Peracetic acid (PAA)		<ul style="list-style-type: none"> <li>Intracellular/Extracellular action.</li> <li>Inhibition of peroxidase activity.</li> <li>Internal "Fenton"-type process  <math>(\text{C}_2\text{H}_4\text{O}_3 + \text{Fe}^{2+} \rightarrow \text{HO}^\cdot + \text{C}_2\text{H}_3\text{O}_2^- + \text{Fe}^{3+})</math></li> <li>Easier generation of <math>\text{OH}^\cdot</math> than <math>\text{H}_2\text{O}_2</math>.</li> <li>Possible THMs &amp; HACs generation through oxidation of <math>\text{Cl}^-</math> (or <math>\text{Br}^-</math>) to <math>\text{HClO}</math> (or <math>\text{HBrO}</math>) which binds NOM.</li> </ul>	O	1.4



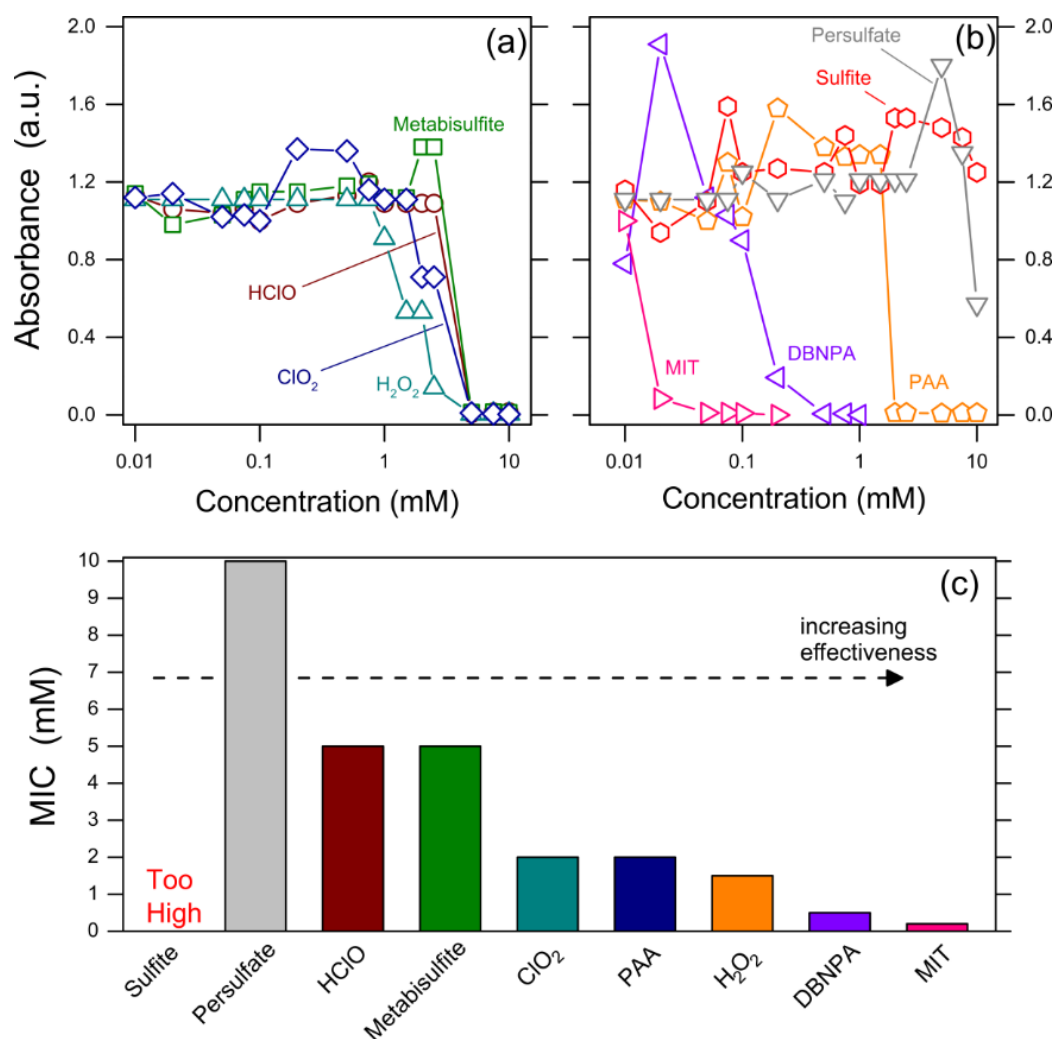
### 3.1 Evaluation of the Effectiveness, Safety, and Feasibility of 9 Potential Biocides to Disinfect Acidic Landfill Leachate from Algae and Bacteria

Persulfate ( $S_2O_8^{2-}$ )		<ul style="list-style-type: none"> <li>Extracellular action (and possible intracellular action until otherwise proven).</li> <li>Activated in presence of transition metals (<i>i.e.</i>, Fe, Mn and Cu) or light.</li> <li>Sulfate radical generation (<math>SO_4^{\cdot-}</math>).</li> <li>Possible THMs &amp; HACs generation through radical processes.</li> </ul>	O	2.1
DBNPA		<ul style="list-style-type: none"> <li>Extracellular action.</li> <li>Addition to -SH and -NH groups of membrane proteins.</li> <li>THMs release through nucleophilic acyclic substitution reaction.</li> </ul>	E	N.A.
MIT		<ul style="list-style-type: none"> <li>Extracellular and intracellular action.</li> <li>Addition to -SH and -NH groups of membrane proteins.</li> <li>Inhibition of enzymatic processes.</li> <li>Internal radical processes.</li> <li>No THMs &amp; HACs generation mechanism detected.</li> </ul>	E	N.A.
Metabisulfite ( $S_2O_5^{2-}$ )		<ul style="list-style-type: none"> <li>Extracellular and possible intracellular action through reductant activity.</li> <li>Possible extracellular action electrophilic addition.</li> <li>No THMs &amp; HACs generation mechanism detected.</li> </ul>	R/E	N.A.
Sulfite ( $SO_3^{2-}$ )		<ul style="list-style-type: none"> <li>Extracellular</li> <li>and possible intracellular action through reductant activity.</li> <li>Possible extracellular action electrophilic addition.</li> <li>No THMs &amp; HACs generation mechanism detected.</li> </ul>	R/E	N.A.

### 3.1.3.2 Disinfection efficacy

As a first step to understand the capability of the various biocides to inactivate *E. coli* bacteria, we benchmarked their efficacy at the most unfavorable conditions by assessing their minimum inhibitory concentration (MIC), with the main results summarized in Figure 3.1.2. In Figure 3.1.2a,b, the values of light absorbance at 600nm (OD<sub>600</sub>) are plotted as a proxy of bacterial growth, vs. the biocide concentration in water. A drop in absorbance indicates the MIC, namely, the lowest concentration of a compound that prevents visible growth of bacteria. No MIC value was found for sulfite in the biocide concentration range investigated in this study, that is, 0-10 mM, and a high MIC value (~10 mM) was found for persulfate. Therefore, these compounds were not used for further investigation on disinfection against *E. coli*. The most effective biocides were MIT, DBNPA, H<sub>2</sub>O<sub>2</sub>, and PAA, in this order, as they required the lowest concentrations to inhibit bacterial growth. Figure 3.1.2c summarizes the MIC values determined for all the biocides.

### 3.1 Evaluation of the Effectiveness, Safety, and Feasibility of 9 Potential Biocides to Disinfect Acidic Landfill Leachate from Algae and Bacteria



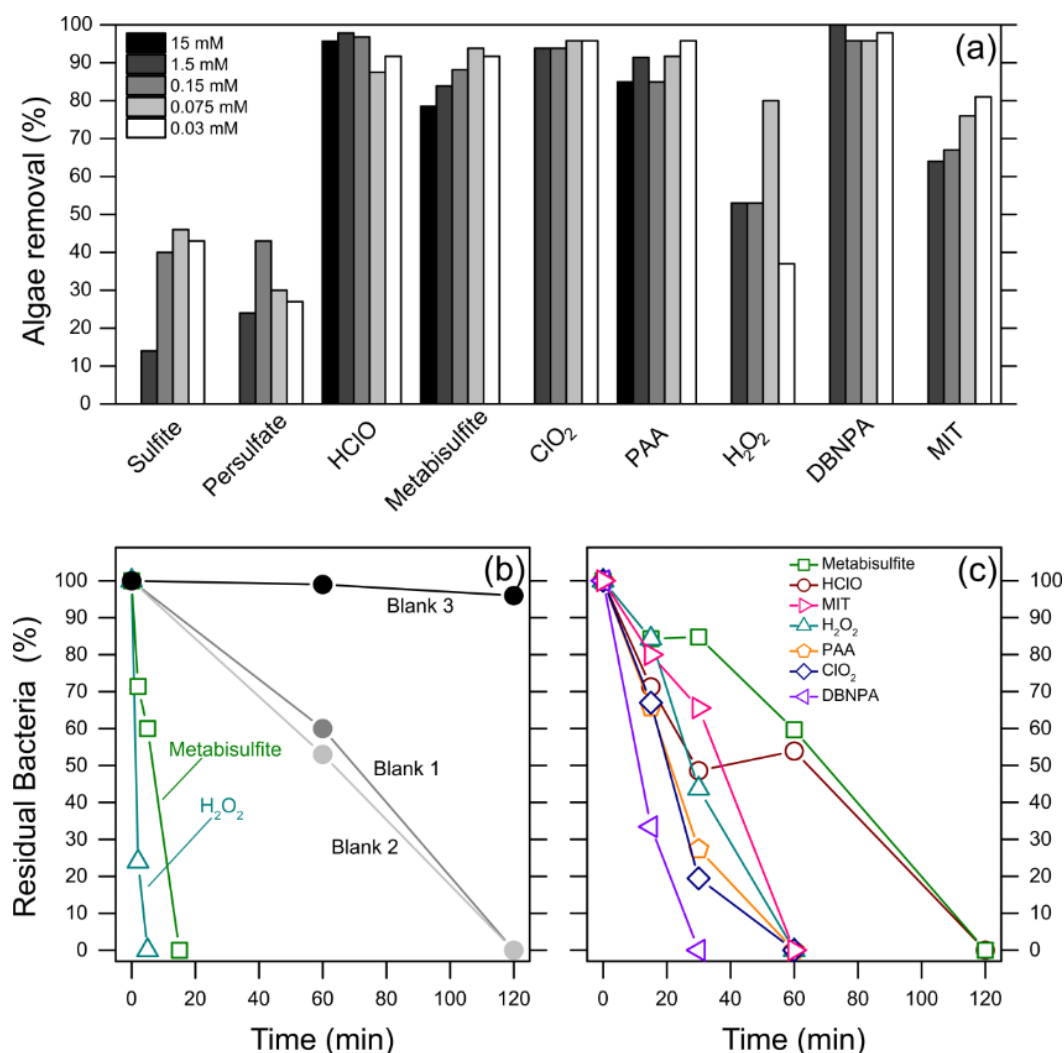
**Figure 3.1.2** Minimum inhibitory concentration (MIC) of the biocides toward *E. coli* inactivation. (a, b) Results of light absorbance of the *E. coli* suspension as a function of biocide concentration. The lines are only intended as guides for the eye. The control values of the stationary phase resulted in the OD<sub>600</sub> range 3.5-5.5, from which solution spiking to OD<sub>600</sub> 1 ± 0.1 was carried out. The standard deviation is 20% for each result. (c) Summary of MIC values. No MIC values could be determined for sulfite and persulfate up to 10 mM biocide concentration.

Figure 3.1.3a reports the values of microalgae removal percentage achieved by employing the different biocides at varying concentrations in the real groundwater samples. Consistent with the results observed with bacteria and presented in Figure 3.1.2, sulfite and persulfate showed the lowest biocidal activity also towards microalgae. Indeed, the activity of persulfate for both microbiological and chemical decontamination has been clearly shown only if this reagent is activated by transition metals.<sup>129,249,252,255</sup> The literature instead lacks reports about the disinfection efficacy of sulfite. In general, no evident increase in

algae removal rate was observed by increasing the concentrations of biocides. Actually, metabisulfite and sulfite showed a similar, inverse trend of increasing disinfection efficacy by reducing the reagent concentration, which suggests that these reagents may undergo “suicidal”, self-inhibition reactions at large concentrations. Furthermore, MIT showed the same inverse trend with concentration. This compound is known to have a slow biocidal activity; moreover, it is highly susceptible to oxidation.<sup>254</sup> It is thus possible that, at high concentration, this biocide reacted faster with the oxygen freely present in the solution (~0.3 mM) than with the microbiological target. Overall, it was found that the lowest concentration of 0.03 mM would allow near maximization of algae removal while minimizing the amount of required reagent.

Several algae species, such as *Chlorella*, adapt well in acidic environments.<sup>238,239</sup> On the contrary, *E. coli* cannot typically survive below pH 4.<sup>256</sup> The water matrix effect on *E. coli* viability was investigated to understand this behavior and to isolate the effect of biocides from that of pH. The results of *E. coli* cultivability from the three blanks indicate that the acidity of the contaminated groundwater (pH 2.8) is responsible for bacterial inactivation within 2 h (Figure 3.1.3a). Therefore, a biocide can only be considered effective toward bacteria disinfection in this matrix if it inactivates *E. coli* faster than 2 h. Clearly, metabisulfite and hydrogen peroxide were able to quickly inactivate *E. coli* at their respective MIC. On the other hand, metabisulfite was not as quickly effective at a low concentration of 0.03 mM (Figure 3.1.3c). Except also for HClO, all the other biocides were instead able to inactivate bacteria at a fast rate even at this low dose, which was found to be the optimal concentration for microalgae removal (Figure 3.1.3a).

### 3.1 Evaluation of the Effectiveness, Safety, and Feasibility of 9 Potential Biocides to Disinfect Acidic Landfill Leachate from Algae and Bacteria



**Figure 3.1.3** Disinfection of microalgae and *E. coli* in the real contaminated groundwater matrix. (a) Removal rates of microalgae at varying biocide concentration. (b, c) Bacteria disinfection kinetics. In (b), metabisulfite and hydrogen peroxide were added at their MIC. Blank 1 shows the matrix effect on *E. coli* viability; blank 2 shows the matrix effect on *E. coli* viability by buffering the suspension at pH 7 before plating; blank 3 shows the matrix effect on *E. coli* viability by buffering the suspension at pH 7 before biocide addition. In (c), *E. coli* disinfection results obtained with a biocide concentration of 0.03 mM are shown. The lines are only intended as guides for the eye.

These data lead to an important conclusion: when working with a complex water matrix such as that examined in this study, each of the following biocide may be employed at low dose when only microalgae removal is required: PAA, H<sub>2</sub>O<sub>2</sub>, ClO<sub>2</sub>, DBNPA, MIT, HClO, and metabisulfite. On the other hand, in the presence of *E. coli* or other persistent/surviving bacteria behaving in a similar way, the utilization of HClO and metabisulfite requires larger concentration to achieve both an effective algae removal and a suitable antibacterial activity.

### 3.1.3.3 Generation of disinfection by-products

The formation of disinfection by-products was determined following addition of biocides in the real groundwater matrix. As expected,  $\text{ClO}_2$  generated THMs, and in particular tribromomethane (a carcinogenic compound), at all the investigated concentrations. The formation of this halogenated compound upon employment of  $\text{ClO}_2$  is consistent with reports in the literature.<sup>44,226</sup> As expected, also the use  $\text{HClO}$  and PAA induced the formation of halogenated by-products,<sup>228,230,257,258</sup> specifically at biocide concentrations of 15, 1.5, and 0.15 mM (see Table 2.1.1 and Appendix D for the complete set of analysis). Tribromomethane was detected as the most prevalent DBP. In particular, in the case of PAA, the concentration of halogenated by-products sharply increased with increasing disinfectant. This behavior indicates the involvement of PAA itself as a primary source in halogenated by-products formation (Table 3.1. and Appendix D provide a more exhaustive discussion on the generation of DBPs related to the nine biocides). However, THMs or other halogenated compounds were not detected at concentrations of 0.075 or 0.03 mM, even though both  $\text{HClO}$  and PAA still maintained a suitable disinfectant efficiency. Therefore, 0.075 mM represents the threshold safety-related dose for  $\text{HClO}$  and PAA application to the water matrix in examination. These results suggest that it should be possible to find a threshold dose for any matrix at which adequate disinfection occurs without the detectable formation of halogenated compounds when employing of  $\text{HClO}$  and PAA.

**Table 3.1.2** Concentration of total THMs and other halogenated compounds upon disinfection of the contaminated groundwater through addition of the various biocides at different dosage.

	Sulfite	Persulfate	$\text{HClO}$	Metabisulfite	$\text{ClO}_2$	PAA	$\text{H}_2\text{O}_2$	DBNPA	MIT
	Total THMs								
15 mM	<i>N.A.</i>	<i>N.A.</i>	<b>312</b>	< LoQ	<i>N.A.</i>	<b>588</b>	< LoQ	<i>N.A.</i>	<i>N.A.</i>
1.5 mM	< LoQ	< LoQ	<b>329</b>	< LoQ	<b>335</b>	<b>12</b>	< LoQ	<b>54</b>	< LoQ
0.15 mM	< LoQ	< LoQ	<b>303</b>	< LoQ	<b>220</b>	< LoQ	< LoQ	<b>5.8</b>	< LoQ
0.075 mM	< LoQ	< LoQ	< LoQ	< LoQ	<b>13</b>	< LoQ	< LoQ	<b>5.4</b>	< LoQ
0.03 mM	< LoQ	< LoQ	< LoQ	< LoQ	<b>10</b>	< LoQ	< LoQ	< LoQ	< LoQ
	Other halogenated organic compounds								

### 3.1 Evaluation of the Effectiveness, Safety, and Feasibility of 9 Potential Biocides to Disinfect Acidic Landfill Leachate from Algae and Bacteria

15 mM	N.A.	N.A.	< LoQ	< LoQ	N.A.	<b>84</b>	< LoQ	N.A.	N.A.
1.5 mM	< LoQ	< LoQ	< LoQ	< LoQ	< LoQ	<b>13</b>	< LoQ	< LoQ	< LoQ
0.15 mM	< LoQ	< LoQ	< LoQ	< LoQ	< LoQ	<b>10</b>	< LoQ	< LoQ	< LoQ
0.075 mM	< LoQ	< LoQ	< LoQ	< LoQ	< LoQ	< LoQ	< LoQ	< LoQ	< LoQ
0.03 mM	< LoQ	< LoQ	< LoQ	< LoQ	< LoQ	< LoQ	< LoQ	< LoQ	< LoQ

“N.A.”: test not performed. “LoQ”: limit of reliable detection.

Notably, metabisulfite, H<sub>2</sub>O<sub>2</sub>, MIT, sulfite, and persulfate did not generate any trace of halogenated compounds, even at the upper limits of the biocide concentration range. The behavior of sulfite and persulfate may be merely ascribed to their low disinfection activity toward bacteria and algae, which limited the formation of by-products and prevented the formation of halogenated compounds. Ultimately, we surmise that metabisulfite, H<sub>2</sub>O<sub>2</sub>, and MIT are the most interesting biocides of the study, since they maintain high disinfection efficiency toward microorganisms, without generating DBPs.

Another interesting result obtained in this study is the behavior of DBNPA and the formation of tribromomethane as a disinfection by-product. Specifically, the concentration of tribromomethane in water increased linearly with the dose of DBNPA (see Figure 3.1.4a), suggesting that the disinfectant itself is an important source of the related by-product. The formation of tribromomethane may be ascribed to the molecular structure of the biocide: it is reasonable to consider the release of a 2,2-dibromo-2-cyanomethyl group after the nucleophilic acyl substitution between the thiol or aminic residues of the membrane proteins and the disinfectant (see section on electrophilic biocides in Appendix D).<sup>45,46</sup> Once in solution, the cyano- group can be replaced by a bromide present in the aqueous environment (~6.4 ppm, see Table 3.1.1), thus forming the most stable by-product, that is, tribromomethane (Figure 3.1.4b). At 0.03 mM biocide concentration, the formation of halogenated by-products was not detected. Given the reaction mechanism of the disinfectant, however, it is reasonable to assume that 2,2-dibromo-2-cyanomethane was still released, but in quantities that were too modest to react with the bromide and generate tribromomethane at detectable concentration. It is interesting to note that MIT belongs to the same biocide category of DBNPA (*i.e.*, electrophilic biocides), but that its employment was not associated with the formation of halogenated by-products (Figure 3.1.4a), potentially by virtue of the different molecular structure of the two biocides.

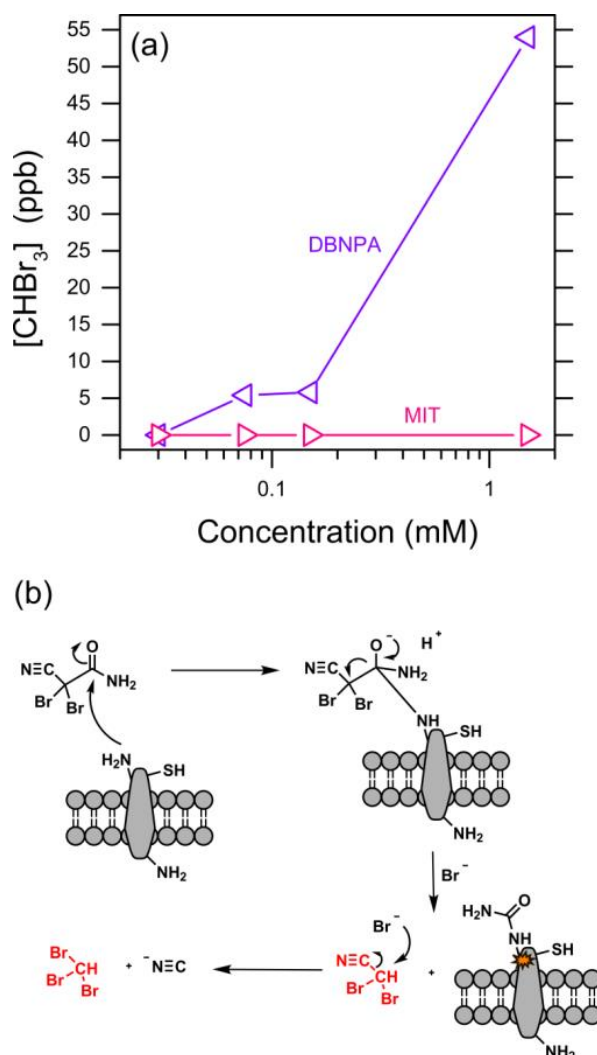


**Figure 3.1.4** (a) Trend of tribromomethane concentration in water as a function of DBNPA and MIT concentrations. The lines are only intended as guides for the eye. (b) Proposed scheme of DBNPA disinfection mechanism and tribromomethane generation.

### 3.1.3.4 Metabisulfite, $H_2O_2$ , and MIT: logistics of implementation

Metabisulfite,  $H_2O_2$ , and MIT resulted equally safe in terms of DBPs generation, but they are different in terms practical utilization (*e.g.*, storage, security). Indeed,  $H_2O_2$  and MIT are well known in the literature as effective disinfectants;<sup>46,202,254</sup> however, they present some practical limitations compared to metabisulfite. Firstly, the storage of large amounts of  $H_2O_2$  is dangerous because of its explosive characteristics.<sup>42</sup> Besides, the utilization of hydrogen peroxide is strongly discouraged before membrane desalination systems, due to the possible degradation of the membrane when exposed to oxidizing agents.<sup>259,260</sup> On the other hand, MIT is at the same time an allergenic and cytotoxic



compound.<sup>261–263</sup> Metabisulfite, although rarely studied for applications similar to that of this study, may be the safest biocide overall, also consistent with the hypothesis of its disinfection mechanism; see Table 3.1.1 and Figure 3.1.1.

#### 3.1.3.5 *Environmental impacts, economic analysis, and overall review of biocides*

A summary of the efficacy and DBPs generation potential of the biocides used for the disinfection of leachate-contaminated groundwater is reported in Figure 3.1.5a. In this three-dimensional plot, a dot is associated with each biocide, with the exclusion of persulfate and sulfite. The values of MIC, microalgae removal rate at biocide concentration of 1.5 mM, and average formation of halogenated compounds were considered to perform this summary analysis. An ideal biocide that is both highly effective and does not induce the production of harmful DBPs would sit in the top left corner of the graph. Chlorine-based disinfectants are instead found on the right side of the graph because they are associated with the production of a significant concentration of harmful DBPs. The safest biocides in this respect were MIT, hydrogen peroxide, and metabisulfite. Of these three, MIT was found to be highly effective against *E. coli* (*i.e.*, low MIC) and less so to remove microalgae, while the opposite conclusion may be drawn regarding H<sub>2</sub>O<sub>2</sub>. A larger concentration of metabisulfite may be necessary to achieve the same disinfection efficacy of the other two biocides against both algae and bacteria.

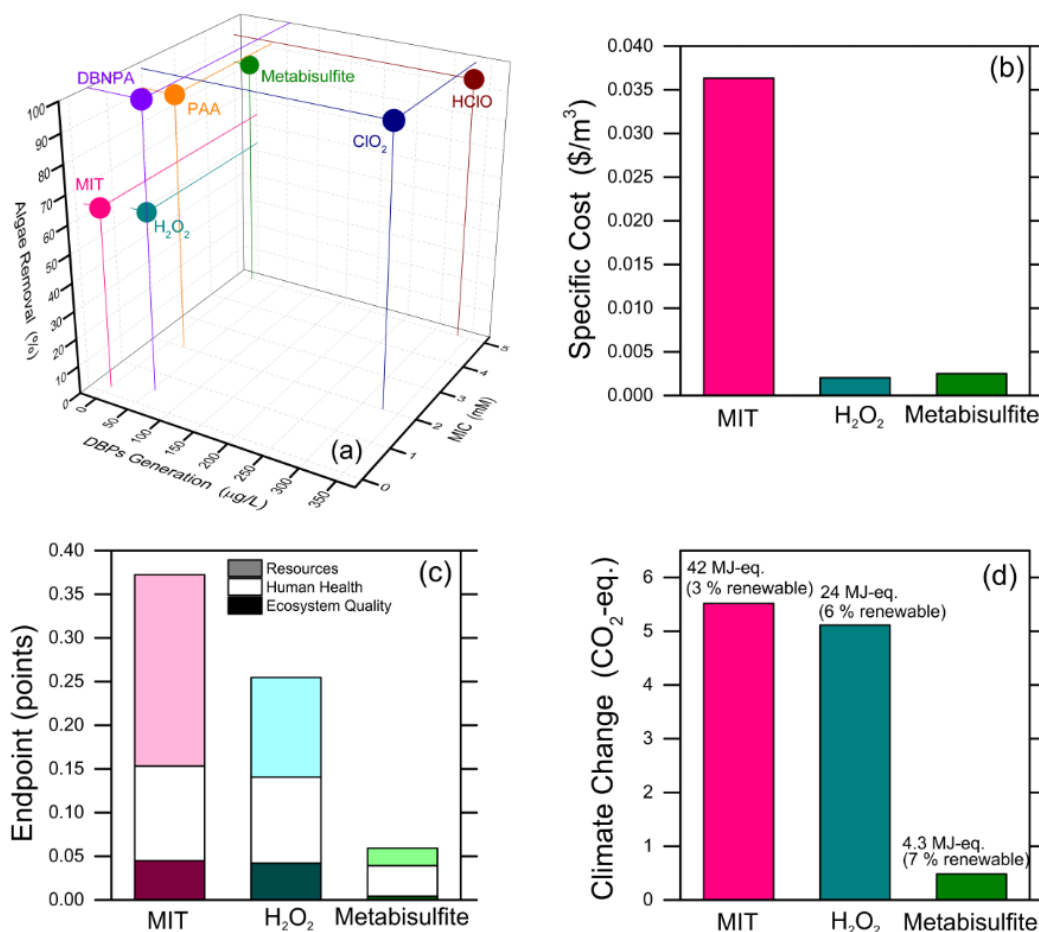


**Figure 3.1.5** Evaluation of the biocides in terms of performance, environmental impacts, and cost of use. (a) Summary of safety and disinfection efficacy expressed as (x axis) DBP generation, (y axis) MIC, and (z axis) microalgae removal (at dosage of 1.5 mM). (b) Cost of deployment to treat one m<sup>3</sup> of wastewater, based on the optimal dosage found in this study. (c) Endpoint results of ReCiPe methodology in LCA; light shade, white, and dark shade colors refer to the categories “resources”, “human health”, and “ecosystem quality”, respectively. (d) Results of IPCC2013 analysis and indication of the energy costs from CED analysis. In (b-d), only the three most promising biocides are presented, namely, MIT, hydrogen peroxide, and metabisulfite.

On the basis of these observations, the economic and environmental impacts associated with the use of MIT, hydrogen peroxide, and metabisulfite were evaluated. Wholesale cost of reagents was assumed, and in particular 1200, 400, and 200 \$/ton for, respectively, MIT (14% w/w solution in water),  $\text{H}_2\text{O}_2$  (50% v/v solution in water), and sodium metabisulfite (97% purity). To calculate the cost of application to disinfect one cubic meter of contaminated groundwater, concentrations of 0.03 mM, 0.075 mM, and 0.075 mM were considered in the effluent matrix, for the three biocides, respectively. These values are based on the results presented in Figure 3.1.3a and are thus associated with their effect against

microalgae. Despite MIT should be dosed at the lowest concentration, the cost of its application would be the largest among the three biocides owing to its high market price; see Figure 3.1.5 b. The use of hydrogen peroxide and metabisulfite would be economical ( $\sim 0.0025$   $\$/\text{m}^3$ ) due to a combination of low price and medium concentration required in the matrix.

Considering the environmental impacts of the three biocides, MIT is associated with the largest burdens, mainly because this substance is toxic for the environment and for humans;<sup>262,264,265</sup> see also Figure 3.1.5c and Figure D1 in Appendix D. Its production involves the reaction of five compounds, namely, acrylic acid, hydrogen sulfide, methanol, methylamine, and hydrogen chloride, thus the exploitation of a large amount of environmental resources. The extraction, processing, and production of each single compound necessary for the synthesis of MIT also has a higher energy needs than the production of the other two biocides and is associated with a more notable production of  $\text{CO}_2$  (Figure 3.1.5d). The production of  $\text{H}_2\text{O}_2$  also involves a relatively large amount of  $\text{CO}_2$  release, as it takes place through anthraquinone auto-oxidation. In addition, the use of hydrogen peroxide poses problems of transport and storage, because this substance is unstable and may cause fire or explosion. On the contrary, metabisulfite does not involve particularly high energy expenditures or environmental impacts. This result stems from the fact that the electrolytic process behind the production of  $\text{NaOH}$  is well established, while  $\text{SO}_2$  is a waste element resulting from metal extraction processes and its reuse implies a gain in terms of life cycle. Figure D1 shows the midpoints related to the three best biocides selected in this study. MIT presents a substantial impact in each midpoint category, with the highest values for terrestrial ecotoxicology, ozone depletion, and fossil depletion. Indeed, the production of MIT utilizes only 3% of renewable resources, while 50% of renewable resources are used for the production of  $\text{H}_2\text{O}_2$  and metabisulfite (see Figure 3.1.5d).  $\text{H}_2\text{O}_2$ , similar to MIT, presents a significant impact in all the midpoints categories, with the highest impact in the categories related with water matrix, namely, marine ecotoxicity and freshwater eutrophication. Metabisulfite is associated with the lowest impacts, with the largest ones in the terrestrial acidification category and in the formation of particulate matter. However, its impact was low for all the other categories.

#### 3.1.4 Conclusion

This study investigated the performance and safety of 9 different biocides ( $\text{HClO}$ ;  $\text{PAA}$ ;  $\text{ClO}_2$ ;  $\text{H}_2\text{O}_2$ ; persulfate; DBNPA; MIT; sulfite; metabisulfite) when employed for the abatement of algae and bacteria (*E. coli*) in a complex aqueous

solution, specifically, leachate from a phosphogypsum landfill. Overall, the following conclusions can be drawn:

- (i) Various biocides are effective in the removal of algae in acidic wastewater, including oxidizing compounds, electrophilic biocides, and reducing agents. In particular, algae disinfection rates larger than 80% were achieved even with a low addition (0.03 mM) of HClO, PAA, ClO<sub>2</sub>, DBNPA, MIT, or metabisulfite. H<sub>2</sub>O<sub>2</sub> required 0.075 mM to disinfect with a rate equal or larger than 80%.
- (ii) Due to the possible generation of harmful disinfection by-products, HClO and PAA may not be employed for water disinfection with concentrations above a threshold value. Below this value, likely specific for each water matrix, these two biocides may represent effective and clean compounds for the abatement of algae and bacteria. In the complex water matrix investigated in this study, this threshold value was 0.075 mM.
- (iii) The molecular structure of each biocide plays a key role in the disinfection process. A chief example is represented by DBNPA and MIT. Despite their analogous disinfection mechanisms (they are both electrophilic biocides), DBNPA induced the formation of tribromomethane during disinfection, while MIT acted as an effective biocide without generating halogenated compounds.
- (iv) The most favorable biocides within the water matrix analyzed in this study, considering simultaneously safety and effectiveness, were H<sub>2</sub>O<sub>2</sub>, MIT, and metabisulfite.
- (v) In particular, metabisulfite represents a highly promising new biocide due to its low cost, low environmental impacts, and adequate efficacy against both microalgae and bacteria.

## **3.2 Formation of Halogenated By-products upon Water Treatment with Peracetic Acid**

### **3.2.1 Introduction**

The antimicrobial properties of peracetic acid (PAA) were reported as far back as 1902,<sup>266</sup> and over the last century PAA has been recognized as an extremely efficient disinfectant toward a wide spectrum of microorganisms.

<sup>245,267,268</sup> This feature promoted the application of PAA in many industrial fields, such as food and beverages, healthcare, textile, as well as the pulp and paper industries. <sup>245,266</sup> In the early '80s, PAA also gained a position in the wastewater treatment industry, where it found the most fertile market. <sup>52,245,269–271</sup> This success is mostly due to the increased mandate to reduce chlorine usage, which is associated to the formation of carcinogenic chlorination by-products. <sup>44,227,272</sup> The larger oxidation potential compared to chlorine and chlorine dioxide and the higher antimicrobial efficiency with respect to H<sub>2</sub>O<sub>2</sub> explain the increasing demand of PAA in the water disinfection field. <sup>245,268,271,273</sup> However, the chemical behavior of PAA in an aqueous medium is complex, since this compound is added in the form of a quaternary equilibrium mixture containing acetic acid (AA), H<sub>2</sub>O<sub>2</sub>, and PAA. Indeed, PAA is synthesized according to the reaction between acetic acid and H<sub>2</sub>O<sub>2</sub>, catalyzed by sulfuric acid: <sup>274,275</sup>



Both AA and H<sub>2</sub>O<sub>2</sub> play major roles in the disinfection process when the PAA mixture (PAAM) is employed. AA can potentially allow bacteria to regrow. <sup>276</sup> Conversely, H<sub>2</sub>O<sub>2</sub> can compete in the disinfection process acting as primary disinfectant, <sup>277</sup> hence consuming PAA by virtue of Le Chatelier principle. For these reasons, the mode of disinfection of PAA has not been entirely clarified so far <sup>245</sup> and the scientific community has encountered difficulties describing the PAAM disinfection by-products (DBPs) and their mechanism of generation. Initially, no halogenated DBPs were noticed in PAA-treated surface water. <sup>278</sup> Shortly after, the same authors and other researchers corroborated the initial results and reported the formation of aldehydes in the order of ppbs. <sup>279–281</sup> On the contrary, later studies remarked that in the presence of chloride and phenol, PAAM is able to generate chlorophenol, potentially through a radical mechanism, since it was proven that PAAM does not seem capable of oxidizing chloride to hypochlorite. <sup>282</sup> However, the competition between PAA and H<sub>2</sub>O<sub>2</sub> was not considered in those studies.

Despite the observation that PAAM cannot oxidize chloride, this mixture has been shown to oxidize bromide to hypobromite and to potentially generate brominated by-products. <sup>43,245,258</sup> Bromide is present in virtually all water sources at concentrations ranging from ~10 to 1000 µg/L in fresh waters and of roughly 67 mg/L in seawater. <sup>41</sup> Therefore, its role in the PAAM system may be significant. Shah *et al.* gained insight into the chemical behavior of PAAM in saline waters and discriminated the reactivity of H<sub>2</sub>O<sub>2</sub> from that of PAA, thus noting the formation of mostly bromoform and haloacetic acids (HAAs). <sup>43,258</sup> The authors ascribed the formation of halogenated by-products to the reaction between hypobromite (formed by PAA and bromide) and dissolved organic matter (DOM).

<sup>258</sup> The formation of halogenated by-products in the absence of DOM and the DBP formation mechanism have not been discussed or explained so far. Indeed, if hypobromite can react with DOM, one may be prone to hypothesize that it might also react with acetic acid already present in PAAM or formed after the oxidation of bromide by PAA, or even with the acetyl group of PAA.

This study investigates the possible ability of PAAM and PAA to work as primary sources of halogenated compounds in the presence of halides. Moreover, specific experiments are discussed that provide a likely interpretation of the reaction mechanism, and that give insight into the role of pH and reactants concentration. The chemical behavior is studied in both simplified synthetic waters and in a real wastewater. Therefore, the main objectives of this work are: (i) theoretical, by proposing a mechanistic interpretation of the prevailing reaction as well as a method of quantitative speciation between PAA and H<sub>2</sub>O<sub>2</sub> in the PAAM mixture; and (ii) consequential for PAA application, to understand when and how safely dosing PAA in a wastewater effluent.

### **3.2.2 Materials and Methods**

#### *3.2.2.1 Chemicals and real wastewater*

The PAA mixture (PAAM) was purchased from Acros Organics (Rodano, MI, Italy). The solution of hypobromite was provided by Farm Srl (Guidonia-Montecelio, RM, Italy). All the other reagents were purchased from Sigma-Aldrich (Milan, Italy). Groundwater receiving leachate from a phosphogypsum landfill was directly obtained from the pumping wells in a contaminated site in the south of Italy and used as is. The main characteristics of the contaminated groundwater are summarized in previous section of this chapter. Disinfection of this wastewater is performed in the treatment plant as a preliminary step and, specifically, the PAAM is added at a concentration of approximately 1.5 mM.

#### *3.2.2.2 Analytical Methods*

Halomethanes formation in synthetic waters was determined with a GC-MS analyzer (HP 6890 Series GC system equipped with a HP 5973 Mass Selective Detector). An aliquot of sample was taken when the total oxidant  $c/c_0$  ratio was near 0 (total oxidant is intended as the sum of all the possible oxidant species in the target solution); see Figure 3.2.1 below. The sample was diluted 1:50 in a 50 mL volumetric flask containing an aqueous solution with 0.5 g of NaOH. Halomethanes were initially extracted through a purge and trap system (P&T Tekmar LSC 2000 coupled to an Entech 7000 focuser) in a 1 mL volume aliquot. The purge time was 11 min, followed by 4 min of purge drying. Then, volatile compounds were cryofocused at -200 °C. The focusing program lasted 3.5 min,

after which the sample was injected into the GC system. An Agilent CP-SIL 5 CB column (length 60 m, internal diameter 0.32 mm, film width 1  $\mu\text{m}$ ) was used for the chromatographic separation. The carrier gas was Helium 6.0 (Sapio, Italy). The injector temperature was 280  $^{\circ}\text{C}$ , and the oven temperature program of the chromatographic system was: 35  $^{\circ}\text{C}$  from 0 to 5 minutes, 5  $^{\circ}\text{C}/\text{min}$  ramp up to 140  $^{\circ}\text{C}$ , 15  $^{\circ}\text{C}/\text{min}$  ramp up to 240  $^{\circ}\text{C}$ , and 15 min at 240  $^{\circ}\text{C}$  (total run time 47.7 minutes). The MS detector operated in scan mode. Monitored halomethanes were: bromomethane ( $t_r$  = 5.16 min, peaks at 15 and 94  $m/z$ ), dibromomethane ( $t_r$  = 13.60 min, peaks at 93 and 174  $m/z$ ), tribromomethane ( $t_r$  = 21.54 min, peaks at 91 and 173  $m/z$ ), chloromethane ( $t_r$  = 4.44 min, peaks at 15 and 50  $m/z$ ), dichloromethane ( $t_r$  = 7.25 min, peaks at 49 and 84  $m/z$ ), trichloromethane ( $t_r$  = 10.27 min, peaks at 47 and 83  $m/z$ ), and dibromochloromethane ( $t_r$  = 17.76 min, peaks at 48 and 129  $m/z$ ). The halomethanes generated in the real water upon PAAM addition were analyzed at a private external laboratory (Chelab srl – Merieux Nutrisciences, Volpiano (TO), Italy) using the method EPA 5030 C 2003 + EPA 8260 D 2018. All the analyses for the determination of the oxidant concentration (*i.e.*,  $\text{H}_2\text{O}_2$  or the sum of PAA and  $\text{H}_2\text{O}_2$ ) were performed with a spectrophotometer using an analytical wavelength of 350 nm (*vide infra*).

#### 3.2.2.3 PAA solution characterization

The PAAM mixture consists of the following partial concentrations, as indicated by the manufacturer: PAA 34-39%; AA 46-55%;  $\text{H}_2\text{O}_2$  11-15% (*i.e.*, PAA 5.05-5.79 M; AA 8.66-10.35 M;  $\text{H}_2\text{O}_2$  3.65-4.98 M). A volumetric titration of the PAA solution allows verification of the partial concentration of AA. The titration was performed after 50x dilution and the result was a concentration of AA equal to 9.81 M, consistent with the data provided by the supplier. Please note that PAA does not compete with the titration due to its  $\text{pK}_a$  of 8.2, while the  $\text{pK}_a$  of AA is 4.75.<sup>117</sup> The combination of iodide and iodine (triiodide method) was used to quantify the concentration of total oxidants in PAAM, which mostly include PAA and  $\text{H}_2\text{O}_2$ . The method was adapted from previous studies.<sup>258,283</sup> A volume of 3 mL of sample (composed of 2.9 mL of MilliQ water and 0.1 mL of PAAM), 1 mL of solution A (KI 66 g/L; NaOH 2 g/L; 0.2 g/L ammonium heptamolybdate), and 1 mL of solution B (40 g/L potassium hydrogenphthalate) were added in a 5 mL volumetric flask. Then, the absorbance of this solution was measured at the wavelength of 350 nm. The total concentration of oxidants in the PAAM was estimated as 9.3 M, in accordance with the data provided by the supplier (*vide supra*).

In order to define the concentrations of PAA and  $\text{H}_2\text{O}_2$  separately, the enzyme catalase from bovine liver was used to quench  $\text{H}_2\text{O}_2$  and the triiodide method was used to quantify the residual oxidant, namely, PAA. The difference between the

total concentration of oxidants and the PAA concentration allows for finally estimating the  $\text{H}_2\text{O}_2$  concentration. This approach is enabled by the fact that the equilibrium reaction (1) has very slow interconversion kinetics, thus PAA takes a lot of time to regenerate  $\text{H}_2\text{O}_2$  degraded by catalase. Catalase only reacts with  $\text{H}_2\text{O}_2$ , even if other peroxides are present.<sup>284,285</sup> To quantify the correct amount of catalase (catalase: $\text{H}_2\text{O}_2$  4:1 wt.) and the time (5 min) needed to quench  $\text{H}_2\text{O}_2$ , preliminary experiments were performed and the results are shown in Appendix E (Figure E1a, E1b). Specifically, Figure E1a shows the volume of a solution of catalase (6.7 mg/L) needed to completely quench  $\text{H}_2\text{O}_2$  concentration (1.5 mM). Figure S1b shows the time needed to completely quench  $\text{H}_2\text{O}_2$ , namely 5 min. Figure S1c shows the effect of catalase on  $\text{H}_2\text{O}_2$  in a solution where PAAM was dosed to obtain PAA 1.5 mM in solution. The results additionally imply that a slightly acidic pH does not affect the function of catalase; these latter experiments were performed at pH 5.2, that is, the natural pH of the PAAM solution after dilution, which was adopted in all the experiments of this study, unless otherwise stated.

### 3.2.3 Results and Discussion

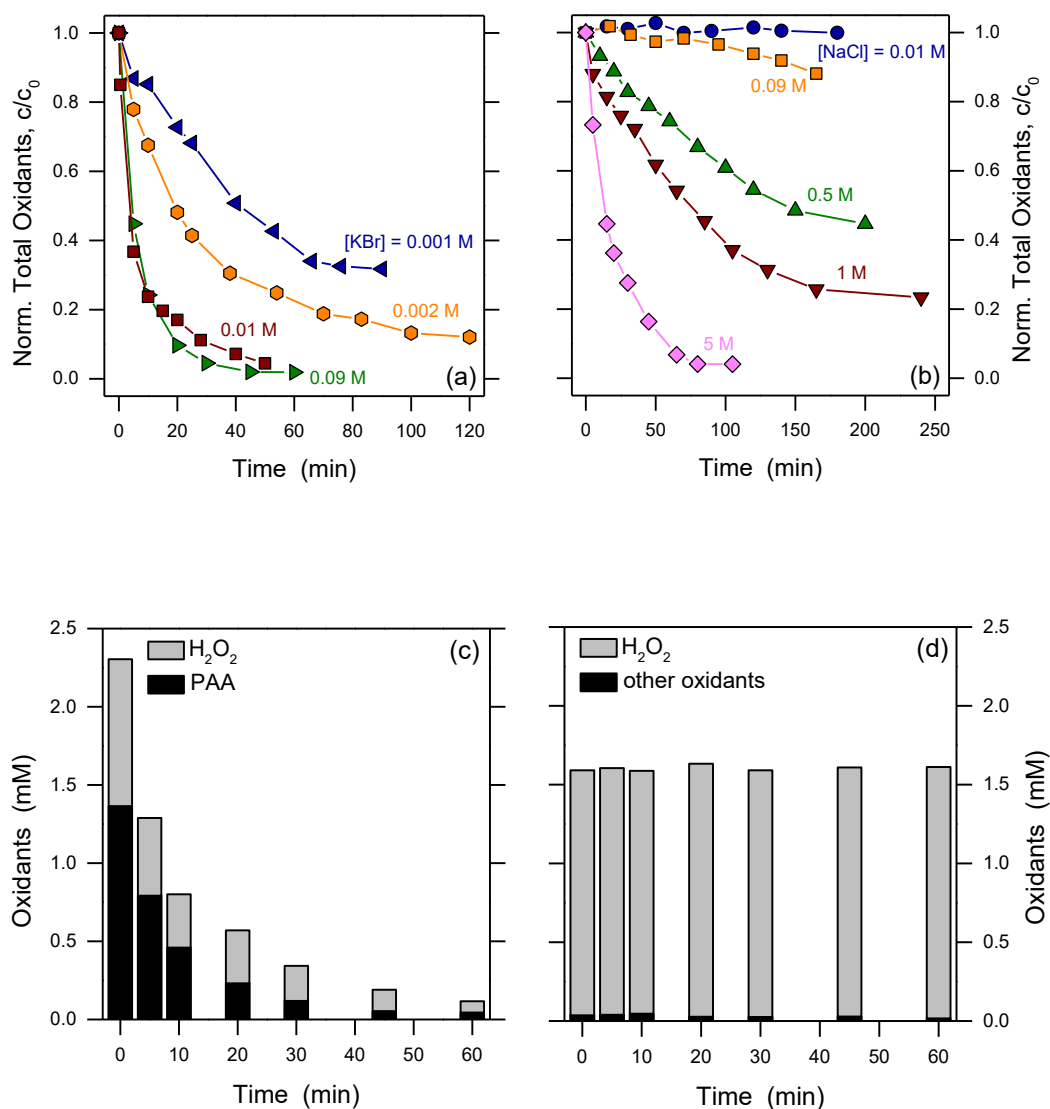
#### 3.2.3.1 Stability of the peracetic acid mixture in the presence of halides

Figure 3.2.1 shows the consumption of the total oxidants present in PAAM (dosed to achieve 1.5 mM PAA in solution) at varying concentration of KBr and NaCl. When bromide was present, the total oxidants were consumed rapidly even at a low KBr concentration of 1 mM (Figure 3.2.1a). This process reached saturation at 10 mM KBr, since only marginal increases in the total oxidant degradation kinetics were observed when the concentration of KBr was further increased up to 90 mM. This observation is consistent with previous studies, which proved the ability of PAA to oxidize bromide to hypobromite in water.<sup>43,258</sup> On the contrary, the results reported in Figure 3.2.1 b indicate that 10 mM of NaCl did not have significant effects on the stability of PAAM. The consumption of total oxidants became visible in 90 mM NaCl, then proceeding more and more rapidly at larger concentrations. The need for high concentration of chloride, namely, 5 M, to produce the same consumption effects observed in the presence of 10 mM KBr, suggests that the activity of chloride toward oxidants contained in PAAM is low from a kinetic standpoint. Indeed, PAA should be able to oxidize both bromide and chloride from a thermodynamic standpoint ( $E_0$  PAA/AA = 1.81 V vs. NHE at pH 7;  $E_0$   $\text{Br}^-/\text{Br}_2$  = 1 V vs NHE;  $E_0$   $\text{Cl}^-/\text{Cl}_2$  = 1.36 V vs NHE).<sup>273</sup> However, on the basis on the data presented in Figure 3.2.1b, we surmise that the process involving chloride does not take place with perceptible kinetics in the absence of other forms of dissolved organics and/or catalysts, only at high



### 3.2 Formation of Halogenated By-products upon Water Treatment with Peracetic Acid

chloride concentrations ( $\text{Cl}^- \geq 0.5 \text{ M}$ ).<sup>286,287</sup> Indeed, Booth and Lester proposed that PAA promotes the generation of halogenated products upon reaction between PAA-induced free chlorine radicals and the organic substrates, probably organic matter present in the effluent, without generation of hypochlorite.<sup>282</sup> Crathorne *et al.* corroborated those results by observing the absence of chlorinated by-products when PAA was added to a solution of humic acids enriched with chloride.<sup>288</sup>

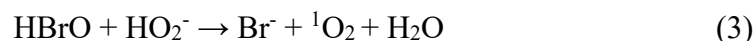


**Figure 3.2.1** Consumption of total oxidants in the presence of halides. (a) Consumption in a solution of PAA (1.5 mM) with KBr present at different concentrations. (b) Consumption in a solution of PAA (1.5 mM) with NaCl present at different concentrations. Lines connecting the data points are only intended as guides for the eye. (c) Consumption in a solution of PAA (1.5 mM) and KBr (10 mM). (d) Consumption in a solution of  $\text{H}_2\text{O}_2$  (1.5 mM) and KBr (10 mM). In (c, d), a solution of catalase (6.7 ppm)

allowed for discrimination between PAA and H<sub>2</sub>O<sub>2</sub>. The results imply that H<sub>2</sub>O<sub>2</sub> is not consumed by KBr, while PAA is.

Shah *et al.* observed only brominated by-products when PAA was dosed in brackish water containing both chloride and bromide.<sup>43</sup> The same authors observed the formation of chlorophenols,<sup>258</sup> which would suggest a role of chloride in the reaction with PAA; however, chlorinated phenol can also be formed through a free radical process without the requirement of hypochlorite occurrence, according to the previous literature.<sup>282,288</sup> Moreover, while chloride is well known to be less reactive than bromide in such processes,<sup>282,288</sup> it should be remarked that the [Cl<sup>-</sup>]/[Br<sup>-</sup>] ratio found here to produce comparable chloride and bromide effects, is of the same order of magnitude of the [Cl<sup>-</sup>]/[Br<sup>-</sup>] ratio in seawater, namely, ~300. Therefore, in high-salinity streams one might expect that naturally occurring bromide and chloride could be involved in similar PAAM consumption. On the other hand, in typical wastewaters and in all bromide-rich aqueous streams the consumption of PAAM could be mostly accounted for by bromide.

As far as the oxidant consumption pathway in the presence of Br<sup>-</sup> is concerned, our data suggests that H<sub>2</sub>O<sub>2</sub> does not react with bromide to generate hypobromite; see Figure 3.2.1d. This result is consistent with previous literature, which indicated that the oxybromination reaction (HBr + H<sub>2</sub>O<sub>2</sub> → HBrO + H<sub>2</sub>O) needs a catalyst to occur<sup>289</sup> (the process can also be triggered in acidic solution, where the catalyst would be H<sup>+</sup>). The consumption of H<sub>2</sub>O<sub>2</sub> observed in Figure 3.2.1c can be justified by virtue of the reaction reported in the literature, according to which H<sub>2</sub>O<sub>2</sub> reacts with hypobromite to produce bromide.<sup>258</sup> In turn, the occurrence of HBrO in the system would be accounted for by the well-known oxidation process of Br<sup>-</sup> by PAA<sup>258</sup>:



Our results thus show that PAAM is not stable in a solution containing bromide, and it will be consumed even at low (mM) Br<sup>-</sup> concentrations. According to reactions (2,3), Br<sup>-</sup> would have a catalytic role in inducing PAAM consumption.

### 3.2.3.2 Formation of trihalomethanes.

Bromoform was the only halomethane detected in the presence of PAA + NaCl + KBr, regardless of the initial concentration of the reactants (see

### 3.2 Formation of Halogenated By-products upon Water Treatment with Peracetic Acid

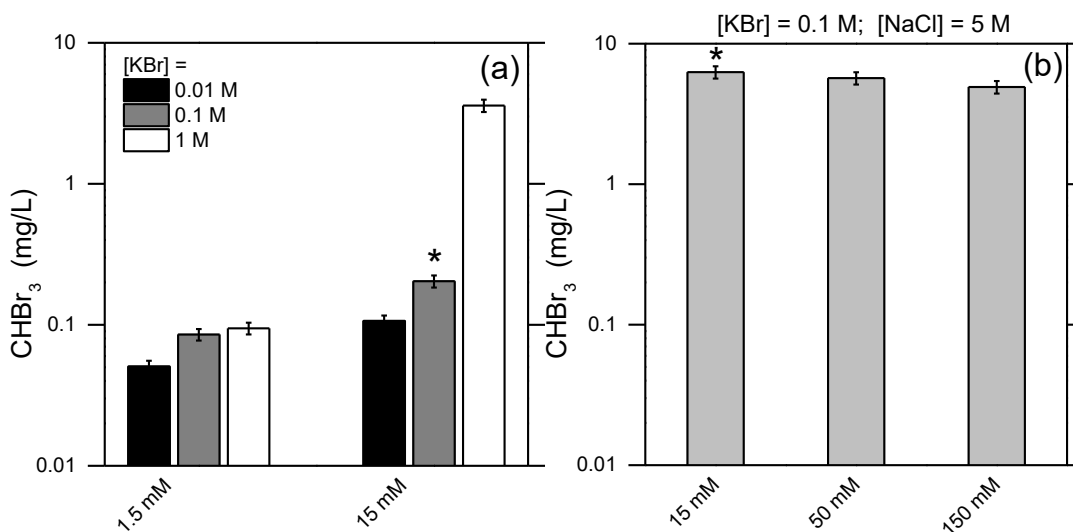


Figure 3.2.2). Experiments were performed at different PAAM doses and by varying the  $\text{PAA}/\text{Br}^-$  ratio.

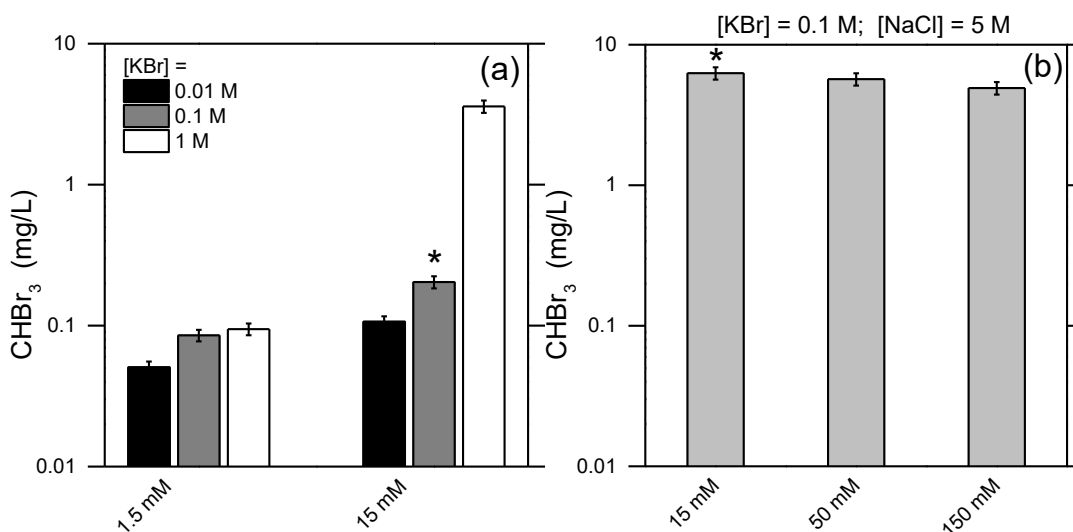


Figure 3.2.2a presents the concentration of  $\text{CHBr}_3$  upon PAAM addition to reach a PAA concentration of 1.5 or 15 mM, at varying levels of KBr (0.01-1 M). The observed increase of bromoform concentration following the increase of PAA and/or bromide concentration corroborates the results discussed above and suggests that PAA (or its derivatives) and bromide (or its derivatives) are the species responsible for  $\text{CHBr}_3$  generation (with yields in the range of 0.03-0.08% of the initial PAA). While previous studies have discussed the formation of brominated by-products only with the presence of other organic components upon

oxidation with PAA, <sup>43,227,228,230,245,258,282,288</sup> this work provides evidence of PAA (or its derivatives) as a substrate for  $\text{CHBr}_3$  generation.

The data summarized in

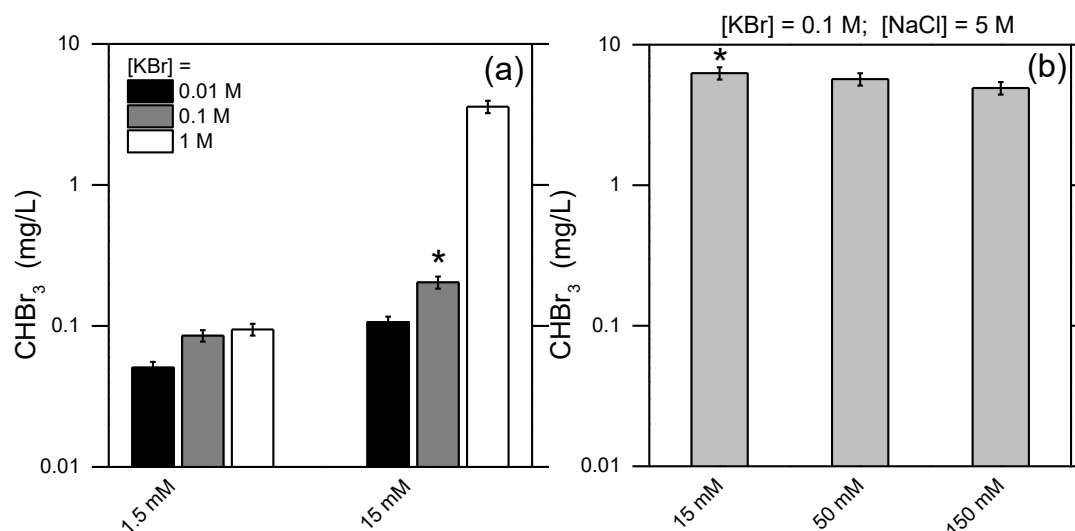
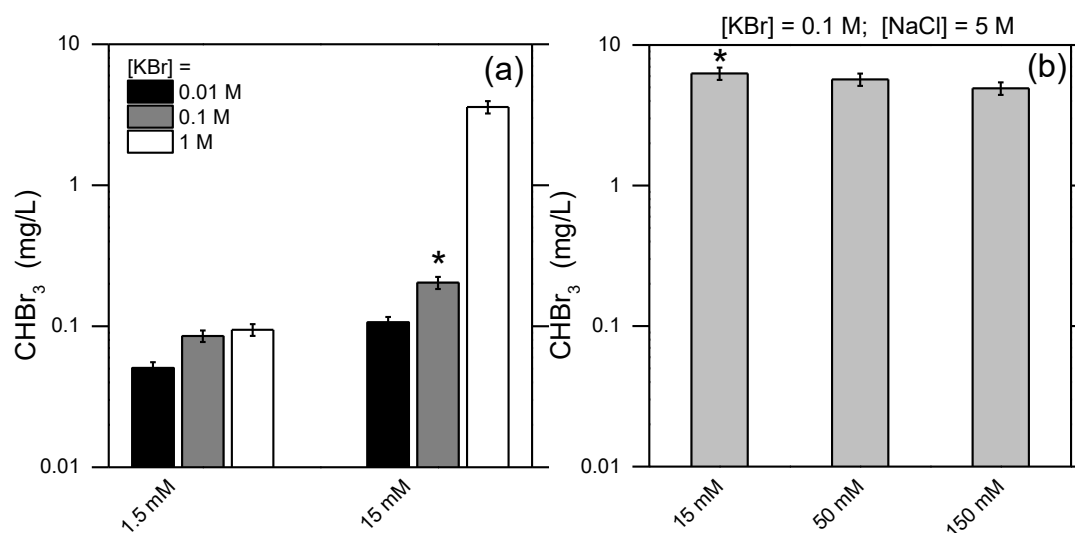


Figure 3.2.2b further corroborate the low activity of chloride toward PAA consumption and halomethane generation. By increasing the concentration of PAA ranging from 15 to 150 mM in a solution with  $\text{KBr}$  0.1 M and  $\text{NaCl}$  5 M, bromoform remained the only detected halogenated organic by-product.



**Figure 3.2.2** Formation of  $\text{CHBr}_3$  in the presence of PAA and halides. (a)  $\text{CHBr}_3$  measured in solution as a function of  $\text{KBr}$  (10; 100; 1000 mM) and PAA (1.5; 15 mM). (b)  $\text{CHBr}_3$  measured in solution in the presence of PAA, at different initial concentrations

### 3.2 Formation of Halogenated By-products upon Water Treatment with Peracetic Acid

---

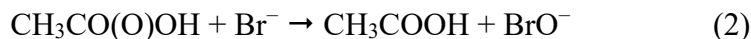
of PAA (15; 50; 150 mM) in a solution consisting of KBr (0.1 M) and NaCl (5 M). Only CHBr<sub>3</sub> was detected among the possible trihalomethanes. The star symbol (\*) over the bars indicates experiments at equivalent concentrations of PAA and KBr, (a) without and (b) with NaCl.

However, when comparing the results of Figure 3.22a and b, a significantly higher concentration of bromoform was formed in the solution prepared by dissolving both KBr and NaCl (Figure 3.22b) with respect to that containing only KBr (Figure 3.22a), at the same concentration values of PAA and KBr. It is important to mention that no bromoform or chloroform were detected when PAA at 15, 50, and 150 mM was present in a solution of NaCl 5 M. The higher formation of bromoform in Figure 3.22b might suggest cooperative phenomena among bromide and chloride when simultaneously present in solution.

Overall, the evidence discussed so far frames one component of PAAM, namely, PAA or AA, as the organic substrate consumed to form CHBr<sub>3</sub>.

#### 3.2.3.3 Reaction mechanism and prevailing species.

To gain insight into the previously described phenomenon, it is crucial to further define the prevailing species involved in the process. Previous studies have widely proven the ability of PAA to oxidize bromide generating hypobromite and AA.



The results reported in Figure 3.2.3 describe the participation of AA in the process. The formation of bromoform was monitored as a function of pH (ranging from 2 to 6) in two different systems. In the first system, PAA and bromide reacted at the optimized PAA : Br<sup>-</sup> ratio for the consumption of PAA, namely, [PAA] = 1.5 mM and [KBr] = 10 mM; see Figure 3.2.1a. The second system was instead obtained by directly dissolving the products of reaction 2, namely, AA and hypobromite. AA was dosed according to its percentage in PAAM when PAA is 1.5 mM, that is, [AA] = 2.8 mM, while [HBrO] = 2 mM was chosen by considering the oxidation of bromide to hypobromite when [PAA] = 1.5 mM.

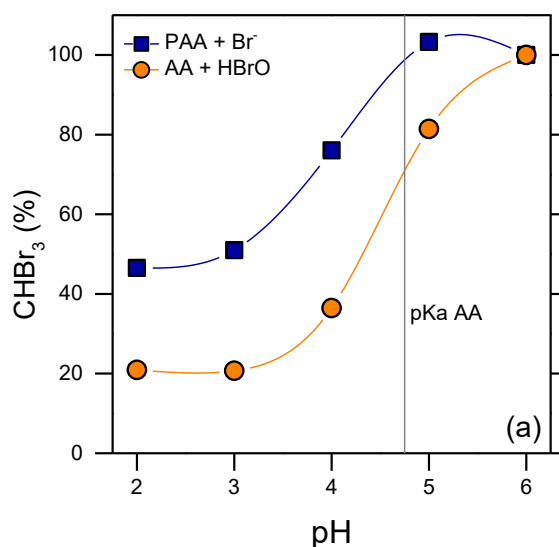


**Figure 3.2.3** Formation of CHBr<sub>3</sub> as a function of pH. CHBr<sub>3</sub> produced in solutions of varying pH, starting with: (blue) a solution containing PAA (1.5 mM) and KBr (10 mM); (orange) a solution containing AA (2.8 mM) and HBrO (2 mM).

The system AA-HBrO also generated bromoform, with analogous pH trend as the PAA-Br<sup>-</sup> system, which implies that the same reaction mechanism occurred in both cases. Moreover, the flex point of the curves lied around the pK<sub>a</sub> value of AA (4.75). These results suggest that AA is the organic substrate responsible for the formation of bromoform when PAA reacts with bromide, and that bromoform formation is higher when AA is deprotonated. According to the results summarized in Table 2.1.1 it is reasonable to conclude that HBrO is directly involved in the process. In a system containing AA, H<sub>2</sub>O<sub>2</sub>, and KBr, no bromoform was detected, as oxybromination needs a catalyst.<sup>289</sup> On the contrary AA and HBrO together promoted the formation of bromoform, the concentration of which increased with increasing HBrO. In conclusion, AA and HBrO are the most probable species that are responsible for the generation of bromoform in the system PAAM-Br<sup>-</sup>.

**Table 3.2.1** Formation of CHBr<sub>3</sub> in solutions consisting of: AA (2.8 mM) and HBrO at different concentrations (2; 10 mM); AA (2.8 mM), H<sub>2</sub>O<sub>2</sub> (1.5 mM), and KBr (10 mM).

AA (mM)	HBrO (mM)	H <sub>2</sub> O <sub>2</sub> (mM)	KBr (mM)	CHBr <sub>3</sub> (mg/L)
---------	-----------	------------------------------------	----------	--------------------------

### 3.2 Formation of Halogenated By-products upon Water Treatment with Peracetic Acid

2.8	-	1.5	10	<LOQ
2.8	2	-	-	1.01 ± 0.05
2.8	10	-	-	3.98 ± 1.54

LOQ: limit of quantification

In this framework, the  $\alpha$ -bromination of carboxylic acids (known as Hell-Volhard-Zelinsky reaction) is the likely mechanism of bromoform formation. Figure 3.2.4 represents the mechanism of the reaction reported for the first time between 1880 and 1887.<sup>290,291</sup> This reaction occurs in aqueous mediums owing to a keto-enolic tautomerization, which can also take place with carboxylic acids, as well as esters and amides, and not solely with ketones.<sup>292</sup> The enolate would represent the nucleophile that is able to react with the electrophile (in this case, HBrO). Following the first addition of bromine, the monobrominated methyl group becomes more electronegative, hence it is more prone to accept other two equivalents of bromine to produce  $\text{CBr}_3^-$ , which is a stable exit group. A basic environment can help both the tautomerization process and the electrophilic addition. This rationalization would explain why pH played a role and why a higher  $\text{CHBr}_3$  formation occurred in our study when AA was deprotonated. When  $\text{CBr}_3^-$  exits, it regenerates the basic environment forming  $\text{CHBr}_3 + \text{OH}^-$ . The formation of stable  $\text{CHBr}_3$  breaks the reversible condition of the process and pushes the reaction toward bromoform formation. Indeed,  $\text{CHBr}_3$  is a typical by-product of the  $\alpha$ -bromination of carboxylic acids.

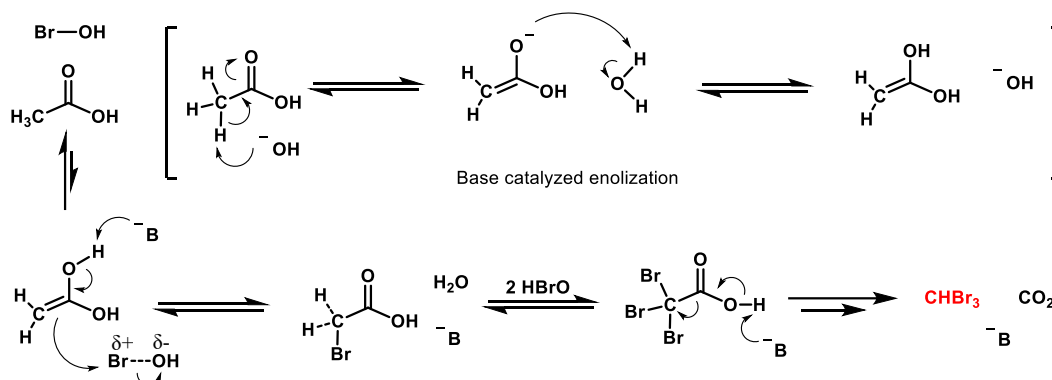


**Figure 3.2.4** Rationalization of the possible reaction mechanism causing the formation of  $\text{CHBr}_3$  in the presence of PAAM and  $\text{Br}^-$ . The proposed mechanism is based on the Hell-Volhard-Zelinsky reaction.

The results summarized in Table 3.2.2 corroborate this hypothesis over the reaction pathway. According to the Hell-Volhard-Zelinsky mechanism, the formation of  $\text{CHBr}_3$  would be contemplated only when AA is the carboxylic organic substrate. In the case of other carboxylic acids, such as propionic and butyric acid, the possible exit groups would be 1,1-dibromoethane and 1,1-dibromopropane, respectively. However, these groups are too non-polar to be stabilized by an aqueous medium (see Scheme E1 in the Appendix E for further details). Indeed, no evidence of  $\text{CHBr}_3$  formation was found and no traces of 1,1-dibromoethane or 1,1-dibromopropane were detected during the tests with propionic and butyric acids instead of AA.

**Table 3.2.2** Formation of  $\text{CHBr}_3$  in solutions with  $\text{HBrO}$  2 mM and different organic substrates (AcOH; Propionic acid; Butyric acid) at 2 mM.

Substrate (2.8 mM)	HBrO (mM)	$\text{CHBr}_3$ (mg/L)
Acetic acid (AA)	2	$1.01 \pm 0.05$
Propionic acid	2	<LOQ
Butyric acid	2	<LOQ

LOQ: limit of quantification

Another evidence of this mechanism was provided by Shah *et al.*, who observed the sole formation of bromoform and brominated acetic acids in an aqueous medium rich in bromide and treated with PAAM, even in the presence of DOM.<sup>43</sup> According to the results of this work, Figure 3.2.5 is proposed to summarize the overall process involved in the formation of bromoform when PAAM and bromide are in the same bulk.

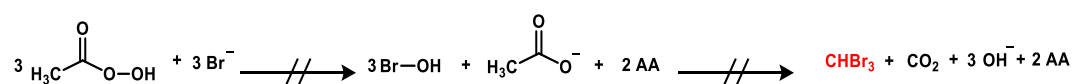


**Figure 3.2.5** Final rationalization of the steps occurring to produce  $\text{CHBr}_3$  in a solution containing PAA and bromide.



### 3.2.3.4 Implications for PAAM use in real waters.

In the last decades, the interest in using PAAM in water treatment industry has substantially grown.<sup>227,245,266,279,281</sup> However, this study suggests that the use of PAAM should be considered carefully in the presence of bromide. Aiming to verify the output of PAAM addition in a real and complex environment, we tested a real wastewater (see previous section for further details). The selected matrix contains 6.4 mg/L of bromide (80  $\mu$ M), around 3 g/L of chloride (0.09 M), and the PAA concentration was 1.5 mM upon addition of the oxidant mixture. Figure 3.2.6 shows that also in a highly complex matrix with multi-contamination parameters and in the presence of a quite high concentration of TOC, bromoform is the major by-product of the PAAM treatment. As far as the chlorine-containing by-products are concerned, chloromethane may be generated through the substitution of chloride on methanol,<sup>293</sup> while chloro-dibromomethane may be generated through the substitution of chloride on bromoform. The results summarized in Figure 3.2.6 imply that when the same amount of PAAM dosed in the real groundwater (1.5 mM) was spiked to a synthetic groundwater with the same ionic composition (including 80  $\mu$ M Br<sup>-</sup> and 0.09 M Cl<sup>-</sup>) and same pH (2.8), but in absence of DOM or other biological material, a significant albeit lower concentration of bromoform was detected in solution (2.6  $\mu$ g/L). The value of bromoform detected in the synthetic groundwater was around 50% of the value detected in the real groundwater, hence PAA had possibly an equivalent activity as DOM and other organic compounds as source of bromoform upon addition of PAAM. Therefore, even in a complex matrix containing a substantial concentration of DOM, PAA may play an important role in the production of brominated by-products.

Finally, this study corroborates the slow oxidative activity of H<sub>2</sub>O<sub>2</sub> toward halides to generate more reactive species, such as HBrO and HClO.<sup>289</sup> This phenomenon would thwart the generation of THMs in presence of DOM during a disinfection process mediated by hydrogen peroxide. Indeed, in the previous section, H<sub>2</sub>O<sub>2</sub> was tested as a potential disinfectant in the same real groundwater tested in this work, showing no traces of THMs upon treatment, differently from PAA (see Figure 3.2.6).

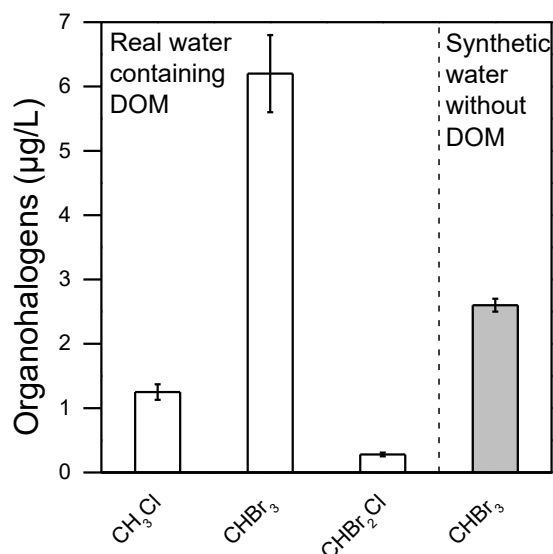


**Figure 3.2.6** Organohalogens detected upon addition of PAAM in a (white bars) real contaminated groundwater and in a (grey bar) synthetic water consisting of the same ionic composition and pH of the real groundwater but in the absence of DOM and other biological material.

### 3.3 Summary

In this section, the effectiveness of biocides and the DBPs generation associated with their use were investigated in both synthetic wastewaters and a specific contaminated matrix, namely, leachate of a phosphogypsum landfill. Due to the possible presence of different microorganisms and the complexity of such matrix, this contaminated water was a perfect target for an investigation aimed at the evaluation of traditional as well as innovative biocides. However, the results of this study may be used as guidelines for the choice of the best biocide in different wastewaters. Oxidizing agents, such as PAA, should not be employed in water matrices with large concentrations of halides, especially bromide, due to the consequent likely generation of halogenated compounds. Specifically, PAA was identified as the primary substrate for the generation of harmful brominated by-products. Moreover, this study indicated that an optimal biocide dosage exists to find a balance between disinfection and safety. Finally, our results suggest that unconventional reagents may be applied effectively for the abatement of microorganisms, such as microalgae and *E. coli*, within complex water sources. In particular, metabisulfite is a promising new disinfectant, safer and more eco-friendly than traditional biocides. However, further studies are required to understand its disinfection mechanism in detail. A cost-benefit analysis was

performed for the most promising biocides tested in the selected matrix, namely, metabisulfite, hydrogen peroxide, and MIT. The benefit of biocides was evaluated through both the efficiency toward biological contaminants and their environmental impacts, evaluated with an LCA analysis.

## Chapter 4

### 4 Final conclusion and perspectives

The rise in the efficiency of industrial and agricultural productions has led to quick population growth worldwide in the last decades. Population growth has in turn increased the pressure on ecosystems and tilted the balance between human activities and natural resources. The pursuit of a sustainable development is the gold rush of our time, which should be undertaken with an eco-friendlier and more equitable implementation of technological solutions. Two of the major challenges of both the urban and the rural water cycle of the future are the increase of recalcitrant organic contaminants and microbiological contaminations. Oxidations and advanced oxidation processes represent effective opportunities in the portfolio of tools to face these challenges. Oxidative processes need improvements specifically to eliminate the use of unsafe and hazardous reactants, to decrease costs of implementation and management, and to increase their selectivity for a better control on the oxidation by-products.

The investigations presented in this thesis aimed to increase the sustainability of oxidation processes in water treatment applications. In the first section, AOPs were investigated to improve their application in the degradation of CECs. The classic Fenton chemistry was modified and enhanced with the specific goal to induce a more selective catalytic process that would also be efficient at near-neutral pH, using safe and greener compounds. Moreover, an analytical method was developed to determine the selective behavior of a modified-Fenton process. The second section of this thesis focused on the behavior of oxidative biocides and their potential alternatives in the disinfection of wastewaters. The results can increase awareness over the application of different biocides, aimed at limiting the

formation of harmful DBPs. The connection among disinfection mechanism and DBPs generation mechanism guided the identification of safer biocides and their best mode of use.

Investigation of the reaction mechanisms, even if at preliminary stage, represented in this work a fundamental ground of knowledge to evaluate the potential of the oxidation processes and to promote their further developments and optimizations.

The following conclusions can be drawn from the work presented in the first part of this thesis:

1. Fe-TAML, and likely other similar ligand-iron complexes, can effectively activate metabisulfite to promote modified Fenton oxidations. Current systems deploy oxidant species as activators, such as hydrogen peroxide, oxone, and hypochlorite. Metabisulfite is a highly promising reactant since it is safer and easier to handle than these classic oxidants. Moreover, preliminary mechanistic investigation showed that the metabisulfite/Fe-TAML system may induce a metal-based process, hence a more selective one, if compared to traditional Fenton and Fenton-like reactions. The system showed a clear preference toward the degradation of phenolic compounds.
2. The presence of an effective iron ligand generally promoted a metal-based mechanism of oxidation. A metal-based chemistry can thus be obtained with the use of inexpensive and easy-to-handle carboxyl acids. A metal-based mechanism is the necessary condition to allow control on the reaction pathway by means of the molecular structure of the ligand-iron complex.
3. Cyclohexane is an effective mechanistic probe to discriminate between a free radical and a metal-based oxidation process. Determination of its major oxidation by-products allows discrimination between the two mechanisms of reaction.
4. Polymeric systems, such as that based on chitosan, are also capable of effectively binding iron, as well as other metals, thus catalysing a metal-based oxidation toward organic contaminants in water with high degradation yields. Chitosan is a particularly promising iron ligand since it is widely accessible, inexpensive, and biodegradable. The potential ability of chitosan and other polymers to form stable films allows the synthesis of both homogeneous and heterogeneous catalysts for the oxidation of organic contaminants in water.

This thesis proposes that a modified-Fenton process by means of effective iron ligands can drastically increase the feasibility of classic AOPs, and in

particular of the Fenton process. A so called modified-Fenton may still be characterized by the low cost and the ease of the treatment that characterize traditional Fenton processes, but at the same time: (i) avoiding unnecessary waste of reactants by recycling them through a catalytic cycle; (ii) inducing a more selective oxidation pathway, hence limiting undesirable by-products; (iii) increasing the efficiency of the process in multi-contaminated water effluents; and (iv) allowing reaction at near-neutral pH. It is possible to assume that promoting an oxidation through efficient catalytic cycles is the preferable direction in terms of circular economy.

In the same way that Leon Battista Alberti defined the artistic representation as an “open window to the world”, as it focuses on a singular object, but it allows the simultaneous imagination of the landscape all around, this thesis focused on a few main study objects through which we can imagine a plethora of further potential routes of development. For instance, metabisulfite is proposed as a highly promising alternative to hydrogen peroxide in modified-Fenton processes; however, only Fe-TAML was tested as activator of metabisulfite. Fe-TAML, although biodegradable, is still a highly expensive catalyst and its synthetic path complex and not green, thus it is necessary to find a cheaper and eco-friendlier catalyst able to activate metabisulfite in the same fashion of Fe-TAML. Moreover, a specific investigation on the degradation path and the active transient species of the metabisulfite/Fe-ligand system should be performed. Since both natural iron ligands as well as chitosan are able to promote a metal-based mechanism in the same fashion of Fe-TAML, they are promising candidates as activators of metabisulfite in solution.

Fe(III)/CS complex works as a highly effective catalyst in CECs degradation at circumneutral pH in the homogeneous phase. However, in the homogeneous phase, other species of a real wastewater may compete with chitosan (and other ligands) on iron complexation, impairing the effect of the catalyst. Two solutions may be possible: (i) the development of a highly stable iron complex, such as Fe-TAML, which would limit the chances of a green synthesis of the ligand or to the use of a natural material; (ii) the development of a heterogeneous process, generally more resilient in water effluents. A heterogeneous process may also be able to limit the suicidal reactions typical of a homogeneous process. With this respect, a catalytic film of chitosan and iron was manufactured. Despite the film showed preliminary promise in the oxidation of phenol, its stability in water needs to be drastically increased. Increasing the crosslinking grade of the film is a possible strategy to enhance the stability of the catalyst. The investigations toward an effective heterogeneous process promoted by a polymeric material like

chitosan necessarily require a metal-based reaction mechanism, in order to avoid the presence of free radicals in solution which may degrade the catalyst itself.

While cyclohexane was demonstrated as a useful mechanistic probe to discriminate between a metal-based and a free-radical pathway, its solubility in water is low. Therefore, the detection of its main by-products, namely, cyclohexanol and cyclohexanone, may be difficult according to the yield of cyclohexane degradation. Following the same rationale behind the choice of cyclohexane as mechanistic probe, further investigations are required to identify other probes that are more soluble in water.

The following conclusions can be drawn from the work presented in the second part of this thesis:

5. As shown for a specific wastewater, it may be possible to determine a biocide threshold dose at which an effective disinfection is performed avoiding harmful halogenated by-products for each water matrix. Therefore, in the absence of feasible alternatives to potential harmful disinfectants, such as hypochlorite, it should be possible to optimize its dosage in order to perform a safe disinfection.
6. When peracetic acid is used as a disinfectant, this compound is the primary organic substrate for the formation of brominated by-products, if bromide is present in the effluent. The same conclusion can be drawn for 2,2-dibromo-3-nitrilopropionamide.
7. Methylisothiazolinone-based compounds,  $H_2O_2$ , and metabisulfite are promising biocides to achieve an effective disinfection while avoiding formation of halogenated by-products. Specifically, metabisulfite was identified as a new and highly promising potential water disinfectant.

This thesis underlines the need of a case-by-case selection of the disinfection strategy. A preliminary assessment is presented, which should work as starting point for the critical evaluation of the most suitable fit-for-purpose biocide and its dosage according to the effluent features. The discussion was widened to inquire upon the specific behavior of DBNPA and PAA biocides, which are both able to work as primary source of bromoform and should thus be used with caution in all aqueous environment rich in bromide.

For further development, more detailed studies may be required for each biocide, in the same fashion of what was presented for PAA. While metabisulfite is proposed as new and highly promising disinfectant, investigations should clarify its real efficiency toward biological contaminants and eventually its disinfection mechanism. There are also issues related to the possible generation of

acid fumes of sulphur dioxide during treatment through metabisulfite that should be addressed.



## 5 References

- (1) Leasor, J. *The Plague and the Fire*; House of Stratus, 2001.
- (2) McNaught, A. D.; internationale de chimie pure et appliquée, U.; Wilkinson, A.; Jenkins, A. D.; of Pure, I. U.; Chemistry, A. *IUPAC Compendium of Chemical Terminology: The Gold Book*; International Union of Pure and Applied Chemistry, 2006.
- (3) Kim, S. J.; Kim, H. S.; Seo, Y. R. Understanding of ROS-Inducing Strategy in Anticancer Therapy. *Oxid. Med. Cell. Longev.* **2019**, 2019, 5381692. <https://doi.org/10.1155/2019/5381692>.
- (4) Yang, H.; Villani, R. M.; Wang, H.; Simpson, M. J.; Roberts, M. S.; Tang, M.; Liang, X. The Role of Cellular Reactive Oxygen Species in Cancer Chemotherapy. *J. Exp. Clin. Cancer Res.* **2018**, 37 (1), 266. <https://doi.org/10.1186/s13046-018-0909-x>.
- (5) Sun, H.; Zhang, C.; Cao, S.; Sheng, T.; Dong, N.; Xu, Y. Fenton Reactions Drive Nucleotide and ATP Syntheses in Cancer. *J. Mol. Cell Biol.* **2018**, 10 (5), 448–459. <https://doi.org/10.1093/jmcb/mjy039>.
- (6) Stevens, R. G.; Kalkwarf, D. R. Iron , Radiation , and Cancer. **1990**, 87 (15), 291–300.
- (7) Toyokuni, S. Role of Iron in Carcinogenesis: Cancer as a Ferrotoxic Disease. *Cancer Sci.* **2009**, 100 (1), 9–16. <https://doi.org/https://doi.org/10.1111/j.1349-7006.2008.01001.x>.
- (8) Akatsuka, S.; Yamashita, Y.; Ohara, H.; Liu, Y.-T.; Izumiya, M.; Abe, K.; Ochiai, M.; Jiang, L.; Nagai, H.; Okazaki, Y.; Murakami, H.; Sekido, Y.; Arai, E.; Kanai, Y.; Hino, O.; Takahashi, T.; Nakagama, H.; Toyokuni, S. Fenton Reaction Induced Cancer in Wild Type Rats Recapitulates Genomic Alterations Observed in Human Cancer. *PLoS One* **2012**, 7 (8), e43403. <https://doi.org/10.1371/journal.pone.0043403>.
- (9) Torti, S. V.; Torti, F. M. Iron and Cancer: More Ore to Be Mined. *Nat. Rev. Cancer* **2013**, 13 (5), 342–355. <https://doi.org/10.1038/nrc3495>.
- (10) Deng, Y.; Zhao, R. Advanced Oxidation Processes (AOPs) in Wastewater Treatment. *Curr. Pollut. Reports* **2015**, 1 (3), 167–176. <https://doi.org/10.1007/s40726-015-0015-z>.
- (11) Guerra-Castellano, A.; Díaz-Quintana, A.; Pérez-Mejías, G.; Elena-Real, C. A.; González-Arzola, K.; García-Mauriño, S. M.; De la Rosa, M. A.; Díaz-

- Moreno, I. Oxidative Stress Is Tightly Regulated by Cytochrome *&lt;Em>C*; Phosphorylation and Respirasome Factors in Mitochondria. *Proc. Natl. Acad. Sci.* **2018**, *115* (31), 7955 LP – 7960. <https://doi.org/10.1073/pnas.1806833115>.
- (12) Wong, H. R. Endogenous Cytoprotective Mechanisms. In *Natural Immunity*; Bertók, L., Chow, D. A. B. T.-N. B., Eds.; Elsevier, 2005; Vol. 5, pp 49–65. [https://doi.org/10.1016/S1567-7443\(05\)80008-0](https://doi.org/10.1016/S1567-7443(05)80008-0).
- (13) Fontecave, M. Iron-Sulfur Clusters: Ever-Expanding Roles. *Nat. Chem. Biol.* **2006**, *2* (4), 171–174. <https://doi.org/10.1038/nchembio0406-171>.
- (14) Guengerich, F. P. Cytochrome P450 and Chemical Toxicology. *Chem. Res. Toxicol.* **2008**, *21* (1), 70–83. <https://doi.org/10.1021/tx700079z>.
- (15) Munro, A. W.; McLean, K. J.; Grant, J. L.; Makris, T. M. Structure and Function of the Cytochrome P450 Peroxygenase Enzymes. *Biochem. Soc. Trans.* **2018**. <https://doi.org/10.1042/BST20170218>.
- (16) Munoz, M.; de Pedro, Z. M.; Pliego, G.; Casas, J. A.; Rodriguez, J. J. Chlorinated Byproducts from the Fenton-like Oxidation of Polychlorinated Phenols. *Ind. Eng. Chem. Res.* **2012**, *51* (40), 13092–13099. <https://doi.org/10.1021/ie3013105>.
- (17) Carvalho, R. N.; Ceriani, L.; Ippolito, A.; Lettieri, T. *Development of the First Watch List under the Environmental Quality Standards Directive. Report EUR 27142 EN*; 2015. <https://doi.org/10.2788/101376>.
- (18) Cortes, L. G.; Marinov, D.; Sanseverino, I.; Cuenca, A. N.; Niegowska, M.; Rodriguez, E. P.; Lettieri, T. *Selection of Substances for the 3 Rd Watch List under the Water Framework Directive*; 2020. <https://doi.org/10.2760/194067>.
- (19) Tse, S.; Powell, K. D.; MacLennan, S. J.; Moorman, A. R.; Paterson, C.; Bell, R. R. Skin Permeability and Pharmacokinetics of Diclofenac Epolamine Administered by Dermal Patch in Yorkshire-Landrace Pigs. *J. Pain Res.* **2012**, *5*, 401–408. <https://doi.org/10.2147/JPR.S35450>.
- (20) Davies, N. M.; Anderson, K. E. Clinical Pharmacokinetics of Diclofenac. Therapeutic Insights and Pitfalls. *Clin. Pharmacokinet.* **1997**, *33* (3), 184–213. <https://doi.org/10.2165/00003088-199733030-00003>.
- (21) Kuhl, H. Pharmacology of Estrogens and Progestogens: Influence of Different Routes of Administration. *Climacteric* **2005**, *8* (supl), 3–63. <https://doi.org/10.1080/13697130500148875>.
- (22) Ryan, K. J. Biochemistry of Aromatase: Significance to Female Reproductive Physiology. *Cancer Res.* **1982**, *42* (8 Suppl), 3342s-3344s.

- (23) Rehberger, K.; Wernicke von Siebenthal, E.; Bailey, C.; Bregy, P.; Fasel, M.; Herzog, E. L.; Neumann, S.; Schmidt-Posthaus, H.; Segner, H. Long-Term Exposure to Low 17 $\alpha$ -Ethinylestradiol (EE2) Concentrations Disrupts Both the Reproductive and the Immune System of Juvenile Rainbow Trout, *Oncorhynchus Mykiss*. *Environ. Int.* **2020**, *142*, 105836. <https://doi.org/https://doi.org/10.1016/j.envint.2020.105836>.
- (24) Schug, T. T.; Janesick, A.; Blumberg, B.; Heindel, J. J. Endocrine Disrupting Chemicals and Disease Susceptibility. *J. Steroid Biochem. Mol. Biol.* **2011**, *127* (3–5), 204–215. <https://doi.org/10.1016/j.jsbmb.2011.08.007>.
- (25) Petrakis, D.; Vassilopoulou, L.; Mamoulakis, C.; Psycharakis, C.; Anifantaki, A.; Sifakis, S.; Docea, A. O.; Tsiaoussis, J.; Makrigiannakis, A.; Tsatsakis, A. M. Endocrine Disruptors Leading to Obesity and Related Diseases. *Int. J. Environ. Res. Public Health* **2017**, *14* (10), 1282. <https://doi.org/10.3390/ijerph14101282>.
- (26) Kahn, L. G.; Philippat, C.; Nakayama, S. F.; Slama, R.; Trasande, L. Endocrine-Disrupting Chemicals: Implications for Human Health. *Lancet Diabetes Endocrinol.* **2020**, *8* (8), 703–718. [https://doi.org/https://doi.org/10.1016/S2213-8587\(20\)30129-7](https://doi.org/https://doi.org/10.1016/S2213-8587(20)30129-7).
- (27) Baquero, F.; Martínez, J.-L.; Cantón, R. Antibiotics and Antibiotic Resistance in Water Environments. *Curr. Opin. Biotechnol.* **2008**, *19* (3), 260–265. <https://doi.org/https://doi.org/10.1016/j.copbio.2008.05.006>.
- (28) Sanseverino, I.; Navarro, A.; Loos, R.; Marinov, D. *State of the Art on the Contribution of Water to Antimicrobial Resistance*; 2018. <https://doi.org/10.2760/82376>.
- (29) Koh, Y. K. K.; Chiu, T. Y.; Boobis, A.; Cartmell, E.; Scrimshaw, M. D.; Lester, J. N. Treatment and removal strategies for estrogens from wastewater. *Environ. Technol.* **2008**, *29* (3), 245–267. <https://doi.org/10.1080/09593330802099122>.
- (30) Gomes, J.; Domingues, E.; Gmurek, M.; Quinta-Ferreira, R. M.; Martins, R. C. Advanced Oxidation Processes for Recalcitrant Compounds Removal Comparison with Biofiltration by *Corbicula Fluminea*. *Energy Reports* **2020**, *6*, 666–671. <https://doi.org/https://doi.org/10.1016/j.egyr.2019.09.047>.
- (31) Kurniawan, T. A.; Lo, W.; Chan, G. Y. S. Physico-Chemical Treatments for Removal of Recalcitrant Contaminants from Landfill Leachate. *J. Hazard. Mater.* **2006**, *129* (1), 80–100. <https://doi.org/https://doi.org/10.1016/j.jhazmat.2005.08.010>.
- (32) Tijani, J. O.; Fatoba, O. O.; Madzivire, G.; Petrik, L. F. A Review of Combined Advanced Oxidation Technologies for the Removal of Organic

- Pollutants from Water. *Water, Air, Soil Pollut.* **2014**, 225 (9), 2102. <https://doi.org/10.1007/s11270-014-2102-y>.
- (33) Seltzer, J. M. Biological Contaminants. *J. Allergy Clin. Immunol.* **1994**, 94 (2), 318–326. <https://doi.org/10.1053/ai.1994.v94.a56011>.
- (34) Schirnding, Y. E. von; Onzivu, W.; Adede, A. O. *International Environmental Law and Global Public Health*; 2002.
- (35) Fenwick, A. Waterborne Infectious Diseases - Could They Be Consigned to History? *Science* (80). **2006**, 313 (5790), 1077–1081. <https://doi.org/10.1126/science.1127184>.
- (36) Hodges, K.; Gill, R. Infectious Diarrhea: Cellular and Molecular Mechanisms. *Gut Microbes* **2010**, 1 (1), 4–21. <https://doi.org/10.4161/gmic.1.1.11036>.
- (37) Mokomane, M.; Kasvosve, I.; de Melo, E.; Pernica, J. M.; Goldfarb, D. M. The Global Problem of Childhood Diarrhoeal Diseases: Emerging Strategies in Prevention and Management. *Ther. Adv. Infect. Dis.* **2018**, 5 (1), 29–43. <https://doi.org/10.1177/2049936117744429>.
- (38) DeMarini, D. M. Genotoxicity of Disinfection By-Products: Comparison to Carcinogenicity. In *Encyclopedia of Environmental Health*; Nriagu, J. O., Ed.; Elsevier: Burlington, 2011; pp 920–926. <https://doi.org/https://doi.org/10.1016/B978-0-444-52272-6.00104-5>.
- (39) Umphres, M. D.; Trussell, A. R.; Tate, C. H.; Trussell, H. R. *Trihalomethanes in Drinking Water*; 1981.
- (40) Lee, C.; Yoon, J.; Von Gunten, U. Oxidative Degradation of N-Nitrosodimethylamine by Conventional Ozonation and the Advanced Oxidation Process Ozone/Hydrogen Peroxide. *Water Res.* **2007**, 41 (3), 581–590. <https://doi.org/https://doi.org/10.1016/j.watres.2006.10.033>.
- (41) Heeb, M. B.; Criquet, J.; Zimmermann-Steffens, S. G.; Von Gunten, U. Oxidative Treatment of Bromide-Containing Waters: Formation of Bromine and Its Reactions with Inorganic and Organic Compounds - A Critical Review. *Water Res.* **2014**, 48 (1), 15–42. <https://doi.org/10.1016/j.watres.2013.08.030>.
- (42) Schreck, A.; Knorr, A.; Wehrstedt, K. D.; Wandrey, P. A.; Gmeinwieser, T.; Steinbach, J. Investigation of the Explosive Hazard of Mixtures Containing Hydrogen Peroxide and Different Alcohols. *J. Hazard. Mater.* **2004**, 108 (1–2), 1–7. <https://doi.org/10.1016/j.jhazmat.2004.01.003>.
- (43) Shah, A. D.; Liu, Z. Q.; Salhi, E.; Höfer, T.; Werschkun, B.; Von Gunten, U. Formation of Disinfection By-Products during Ballast Water Treatment with Ozone, Chlorine, and Peracetic Acid: Influence of Water Quality

- Parameters. *Environ. Sci. Water Res. Technol.* **2015**, *1* (4), 465–480. <https://doi.org/10.1039/c5ew00061k>.
- (44) Al-Otoum, F.; Al-Ghouti, M. A.; Ahmed, T. A.; Abu-Dieyeh, M.; Ali, M. Disinfection By-Products of Chlorine Dioxide (Chlorite, Chlorate, and Trihalomethanes): Occurrence in Drinking Water in Qatar. *Chemosphere* **2016**, *164*, 649–656. <https://doi.org/10.1016/j.chemosphere.2016.09.008>.
- (45) Campa, M. F.; Techtmann, S. M.; Ladd, M. P.; Yan, J.; Patterson, M.; Amaral, A. G. de M.; Carter, K. E.; Ulrich, N.; Grant, C. J.; Hettich, R. L.; Lamendella, R.; Hazen, T. C. Surface Water Microbial Community Response to the Biocide 2,2-Dibromo-3-Nitrilopropionamide, Used in Unconventional Oil and Gas Extraction. *Appl. Environ. Microbiol.* **2019**, *85* (21), 1–37. <https://doi.org/10.1128/AEM.01336-19>.
- (46) Kahrilas, G. A.; Blotevogel, J.; Stewart, P. S.; Borch, T. Biocides in Hydraulic Fracturing Fluids: A Critical Review of Their Usage, Mobility, Degradation, and Toxicity. *Environ. Sci. Technol.* **2015**, *49* (1), 16–32. <https://doi.org/10.1021/es503724k>.
- (47) Irwin, S. V.; Fisher, P.; Graham, E.; Malek, A.; Robidoux, A. Sulfites Inhibit the Growth of Four Species of Beneficial Gut Bacteria at Concentrations Regarded as Safe for Food. *PLoS One* **2017**, *12* (10), 1–14. <https://doi.org/10.1371/journal.pone.0186629>.
- (48) Gerba, C. P. Quaternary Ammonium Biocides: Efficacy in Application. *Appl. Environ. Microbiol.* **2015**, *81* (2), 464–469. <https://doi.org/10.1128/AEM.02633-14>.
- (49) Fenton, H. J. H. LXXIII.—Oxidation of Tartaric Acid in Presence of Iron. *J. Chem. Soc. Trans.* **1894**, *65* (0), 899–910. <https://doi.org/10.1039/CT8946500899>.
- (50) Goldstein, S.; Meyerstein, D.; Czapski, G. The Fenton Reagents. *Free Radic. Biol. Med.* **1993**, *15* (4), 435–445. [https://doi.org/https://doi.org/10.1016/0891-5849\(93\)90043-T](https://doi.org/https://doi.org/10.1016/0891-5849(93)90043-T).
- (51) Peluffo, M.; Pardo, F.; Santos, A.; Romero, A. Use of Different Kinds of Persulfate Activation with Iron for the Remediation of a PAH-Contaminated Soil. *Sci. Total Environ.* **2016**, *563–564*, 649–656. <https://doi.org/https://doi.org/10.1016/j.scitotenv.2015.09.034>.
- (52) Ao, X. wei; Eloranta, J.; Huang, C. H.; Santoro, D.; Sun, W. jun; Lu, Z. dong; Li, C. Peracetic Acid-Based Advanced Oxidation Processes for Decontamination and Disinfection of Water: A Review. *Water Res.* **2021**, *188*. <https://doi.org/10.1016/j.watres.2020.116479>.
- (53) Behin, J.; Akbari, A.; Mahmoudi, M.; Khajeh, M. Sodium Hypochlorite as an Alternative to Hydrogen Peroxide in Fenton Process for Industrial

- Scale. *Water Res.* **2017**, *121*, 120–128. <https://doi.org/10.1016/j.watres.2017.05.015>.
- (54) Fu, X.; Gu, X.; Lu, S.; Sharma, V. K.; Brusseau, M. L.; Xue, Y.; Danish, M.; Fu, G. Y.; Qiu, Z.; Sui, Q. Benzene Oxidation by Fe(III)-Activated Percarbonate: Matrix-Constituent Effects and Degradation Pathways. *Chem. Eng. J.* **2017**, *309*, 22–29. <https://doi.org/https://doi.org/10.1016/j.cej.2016.10.006>.
- (55) Haber, F.; Weiss, J. The Catalytic Decomposition of Hydrogen Peroxide by Iron Salts. **1932**, 332–351. <https://doi.org/10.1098/rspa.1934.0221>.
- (56) Haber, F.; Weiss, J.; Pope, W. J. The Catalytic Decomposition of Hydrogen Peroxide by Iron Salts. *Proc. R. Soc. London. Ser. A - Math. Phys. Sci.* **1934**, *147* (861), 332–351. <https://doi.org/10.1098/rspa.1934.0221>.
- (57) Bossmann, S. H.; Oliveros, E.; Göb, S.; Siegwart, S.; Dahlen, E. P.; Payawan, L.; Straub, M.; Wörner, M.; Braun, A. M. New Evidence against Hydroxyl Radicals as Reactive Intermediates in the Thermal and Photochemically Enhanced Fenton Reactions. *J. Phys. Chem. A* **1998**, *102* (28), 5542–5550. <https://doi.org/10.1021/jp980129j>.
- (58) Bossmann, S. H.; Oliveros, E.; Kantor, M.; Niebler, S.; Bonfill, A.; Shahin, N.; Wörner, M.; Braun, A. M. New Insights into the Mechanisms of the Thermal Fenton Reactions Occurring Using Different Iron(II)-Complexes. *Water Sci. Technol.* **2004**, *49* (4), 75–80.
- (59) Pignatello, J. J.; Liu, D.; Huston, P. Evidence for an Additional Oxidant in the Photoassisted Fenton Reaction. *Environ. Sci. Technol.* **1999**, *33* (11), 1832–1839. <https://doi.org/10.1021/es980969b>.
- (60) Minero, C.; Lucchiari, M.; Maurino, V.; Vione, D. A Quantitative Assessment of the Production of  $\cdot\text{OH}$  and Additional Oxidants in the Dark Fenton Reaction: Fenton Degradation of Aromatic Amines. *RSC Adv.* **2013**, *3* (48), 26443–26450. <https://doi.org/10.1039/C3RA44585B>.
- (61) Wink, D. A.; Nims, R. W.; Saavedra, J. E.; Utermahlen, W. E.; Ford, P. C. The Fenton Oxidation Mechanism: Reactivities of Biologically Relevant Substrates with Two Oxidizing Intermediates Differ from Those Predicted for the Hydroxyl Radical. *Proc. Natl. Acad. Sci.* **1994**, *91* (14), 6604–6608. <https://doi.org/10.1073/pnas.91.14.6604>.
- (62) Neyens, E.; Baeyens, J. A Review of Classic Fenton's Peroxidation as an Advanced Oxidation Technique. *J. Hazard. Mater.* **2003**, *98* (1–3), 33–50. [https://doi.org/10.1016/S0304-3894\(02\)00282-0](https://doi.org/10.1016/S0304-3894(02)00282-0).
- (63) Kanakaraju, D.; Glass, B. D.; Oelgemöller, M. Advanced Oxidation Process-Mediated Removal of Pharmaceuticals from Water: A Review. *J. Environ. Manage.* **2018**, *219*, 189–207.

- <https://doi.org/10.1016/j.jenvman.2018.04.103>.
- (64) Miklos, D. B.; Remy, C.; Jekel, M.; Linden, K. G.; Drewes, J. E.; Hübner, U. Evaluation of Advanced Oxidation Processes for Water and Wastewater Treatment – A Critical Review. *Water Res.* **2018**, *139*, 118–131. <https://doi.org/10.1016/j.watres.2018.03.042>.
- (65) Williams, G. H. chapter 7 - Hydroxylation and some other substitution reactions. In *International Series of Monographs on Organic Chemistry*; Williams, G. H. B. T.-H. A. S., Ed.; Pergamon, 1960; pp 110–125. <https://doi.org/https://doi.org/10.1016/B978-0-08-009246-1.50012-3>.
- (66) Babuponnusami, A.; Muthukumar, K. Advanced Oxidation of Phenol: A Comparison between Fenton, Electro-Fenton, Sono-Electro-Fenton and Photo-Electro-Fenton Processes. *Chem. Eng. J.* **2012**, *183*, 1–9. <https://doi.org/https://doi.org/10.1016/j.cej.2011.12.010>.
- (67) Sean X. Liu. Physicochemical Wastewater Treatment Processes. In *Food and Agricultural Wastewater Utilization and Treatment*; Wiley Online Books; 2014; pp 45–102. <https://doi.org/https://doi.org/10.1002/9781118353967.ch3>.
- (68) Woodard & Curran, I. 7 - *Methods for Treating Wastewaters from Industry*; Woodard & Curran BT - Industrial Waste Treatment Handbook (Second Edition), I., Ed.; Butterworth-Heinemann: Burlington, 2006. <https://doi.org/https://doi.org/10.1016/B978-075067963-3/50009-6>.
- (69) Jones, D. B.; Saglam, A.; Song, H.; Karanfil, T. The Impact of Bromide/Iodide Concentration and Ratio on Iodinated Trihalomethane Formation and Speciation. *Water Res.* **2012**, *46* (1), 11–20. <https://doi.org/10.1016/j.watres.2011.10.005>.
- (70) Diya'uddeen, B. H.; A.R., A. A.; Daud, W. M. A. W. On the Limitation of Fenton Oxidation Operational Parameters: A Review. *Int. J. Chem. React. Eng.* **2012**, *10* (1). <https://doi.org/https://doi.org/10.1515/1542-6580.2913>.
- (71) Oloo, W. N.; Que, L. *Hydrocarbon Oxidations Catalyzed by Bio-Inspired Nonheme Iron and Copper Catalysts*; Elsevier Ltd., 2013; Vol. 6. <https://doi.org/10.1016/B978-0-08-097774-4.00627-6>.
- (72) Que, L.; Tolman, W. B. Biologically Inspired Oxidation Catalysis. *Nature* **2008**, *455* (7211), 333–340. <https://doi.org/10.1038/nature07371>.
- (73) Groves, J. T. High-Valent Iron in Chemical and Biological Oxidations. *J. Inorg. Biochem.* **2006**, *100* (4), 434–447. <https://doi.org/10.1016/j.jinorgbio.2006.01.012>.
- (74) Bollinger, J. M.; Price, J. C.; Hoffart, L. M.; Barr, E. W.; Krebs, C. Mechanism of Taurine:  $\alpha$ -Ketoglutarate Dioxygenase (TauD) from

- Escherichia Coli. *Eur. J. Inorg. Chem.* **2005**, No. 21, 4245–4254. <https://doi.org/10.1002/ejic.200500476>.
- (75) Sarah, B.; Gregory, C. Mechanism and Catalytic Diversity of Rieske Non-Heme Iron-Dependent Oxygenases. *ACS Catal.* **2013**, 3 (10), 1–7. <https://doi.org/10.1021/cs400087p>. Mechanism.
- (76) Sachar, M.; Anderson, K. E.; Ma, X. Protoporphyrin IX: The Good, the Bad, and the Ugly. *J. Pharmacol. Exp. Ther.* **2016**, 356 (2), 267 LP – 275. <https://doi.org/10.1124/jpet.115.228130>.
- (77) Makris, T. M.; Koenig, K. von; Schlichting, I.; Sligar, S. G. The Status of High-Valent Metal Oxo Complexes in the P450 Cytochromes. *J. Inorg. Biochem.* **2006**, 100 (4), 507–518. <https://doi.org/10.1016/j.jinorgbio.2006.01.025>.
- (78) Olivo, G.; Farinelli, G.; Barbieri, A.; Lanzalunga, O.; Di Stefano, S.; Costas, M. Supramolecular Recognition Allows Remote, Site-Selective C-H Oxidation of Methylenic Sites in Linear Amines. *Angew. Chemie - Int. Ed.* **2017**, 56 (51). <https://doi.org/10.1002/anie.201709280>.
- (79) Bernhardt, R. Cytochromes P450 as Versatile Biocatalysts. *J. Biotechnol.* **2006**, 124 (1), 128–145. <https://doi.org/https://doi.org/10.1016/j.jbiotec.2006.01.026>.
- (80) Kumar, S.; Jin, M.; Weemhoff, J. L. Cytochrome P450-Mediated Phytoremediation Using Transgenic Plants: A Need for Engineered Cytochrome P450 Enzymes. *J. Pet. Environ. Biotechnol.* **2012**, 03 (05). <https://doi.org/10.4172/2157-7463.1000127>.
- (81) Kumar, S. Engineering Cytochrome P450 Biocatalysts for Biotechnology, Medicine and Bioremediation. *Expert Opin. Drug Metab. Toxicol.* **2010**, 6 (2), 115–131. <https://doi.org/10.1517/17425250903431040>.
- (82) Collins, T. J. TAML Oxidant Activators: A New Approach to the Activation of Hydrogen Peroxide for Environmentally Significant Problems. *Acc. Chem. Res.* **2002**, 35 (9), 782–790. <https://doi.org/10.1021/ar010079s>.
- (83) Chahbane, N.; Popescu, D.-L.; Mitchell, D. A.; Chanda, A.; Lenoir, D.; Ryabov, A. D.; Schramm, K.-W.; Collins, T. J. Fe(III)–TAML-Catalyzed Green Oxidative Degradation of the Azo Dye Orange II by H<sub>2</sub>O<sub>2</sub> and Organic Peroxides: Products, Toxicity, Kinetics, and Mechanisms. *Green Chem.* **2007**, 9 (1), 49–57. <https://doi.org/10.1039/B604990G>.
- (84) Sen Gupta, S.; Stadler, M.; Noser, C. A.; Ghosh, A.; Steinhoff, B.; Lenoir, D.; Horwitz, C. P.; Schramm, K. W.; Collins, T. J. Rapid Total Destruction of Chlorophenols by Activated Hydrogen Peroxide. *Science (80)*. **2002**, 296 (5566), 326–328. <https://doi.org/10.1126/science.1069297>.



- 
- (85) Ghosh, A.; Mitchell, D. A.; Chanda, A.; Ryabov, A. D.; Popescu, D. L.; Upham, E. C.; Collins, G. J.; Collins, T. J. Catalase–Peroxidase Activity of Iron(III)–TAML Activators of Hydrogen Peroxide. *J. Am. Chem. Soc.* **2008**, *130* (45), 15116–15126. <https://doi.org/10.1021/ja8043689>.
- (86) Mondal, S.; Hangun-Balkir, Y.; Alexandrova, L.; Link, D.; Howard, B.; Zandhuis, P.; Cugini, A.; Horwitz, C. P.; Collins, T. J. Oxidation of Sulfur Components in Diesel Fuel Using Fe-TAML<sup>®</sup> catalysts and Hydrogen Peroxide. *Catal. Today* **2006**, *116* (4), 554–561. <https://doi.org/10.1016/j.cattod.2006.06.025>.
- (87) Farinelli, G.; Minella, M.; Pazzi, M.; Giannakis, S.; Pulgarin, C.; Vione, D.; Tiraferri, A. Natural Iron Ligands Promote a Metal-Based Oxidation Mechanism for the Fenton Reaction in Water Environments. *J. Hazard. Mater.* **2020**, *393*. <https://doi.org/10.1016/j.jhazmat.2020.122413>.
- (88) Silva, A. M. N.; Kong, X.; Parkin, M. C.; Cammack, R.; Hider, R. C. Iron(III) Citrate Speciation in Aqueous Solution. *Dalt. Trans.* **2009**, No. 40, 8616–8625. <https://doi.org/10.1039/b910970f>.
- (89) Rush, J. D.; Maskos, Z.; Koppenol, W. H. Distinction between Hydroxyl Radical and Ferryl Species. *Methods Enzymol.* **1990**, *186* (C), 148–156. [https://doi.org/10.1016/0076-6879\(90\)86104-4](https://doi.org/10.1016/0076-6879(90)86104-4).
- (90) Rush, J. D.; Koppenol, W. H. Reactions of Iron(II) Nitrilotriacetate and Iron(II) Ethylenediamine-N,N'-Diacetate Complexes with Hydrogen Peroxide. *J. Am. Chem. Soc.* **1988**, *110* (15), 4957–4963. <https://doi.org/10.1021/ja00223a013>.
- (91) Sutton, H. C.; Vile, G. F.; Winterbourn, C. C. Radical Driven Fenton Reactions—Evidence from Paraquat Radical Studies for Production of Tetravalent Iron in the Presence and Absence of Ethylenediaminetetraacetic Acid. *Arch. Biochem. Biophys.* **1987**, *256* (2), 462–471. [https://doi.org/https://doi.org/10.1016/0003-9861\(87\)90603-5](https://doi.org/https://doi.org/10.1016/0003-9861(87)90603-5).
- (92) Mirzaei, A.; Chen, Z.; Haghighat, F.; Yerushalmi, L. Removal of Pharmaceuticals from Water by Homo/Heterogonous Fenton-Type Processes – A Review. *Chemosphere* **2017**, *174*, 665–688. <https://doi.org/https://doi.org/10.1016/j.chemosphere.2017.02.019>.
- (93) Pignatello, J. J.; Oliveros, E.; MacKay, A. Advanced Oxidation Processes for Organic Contaminant Destruction Based on the Fenton Reaction and Related Chemistry. *Crit. Rev. Environ. Sci. Technol.* **2006**, *36* (1), 1–84. <https://doi.org/10.1080/10643380500326564>.
- (94) Duesterberg, C. K.; Mylon, S. E.; Waite, T. D. PH Effects on Iron-Catalyzed Oxidation Using Fenton's Reagent. *Environ. Sci. Technol.* **2008**, *42* (22), 8522–8527. <https://doi.org/10.1021/es801720d>.

- (95) Banerjee, D.; Markley, A. L.; Yano, T.; Ghosh, A.; Berget, P. B.; Minkley, E. G.; Khetan, S. K.; Collins, T. J. "Green" Oxidation Catalysis for Rapid Deactivation of Bacterial Spores. *Angew. Chemie - Int. Ed.* **2006**, *45* (24), 3974–3977. <https://doi.org/10.1002/anie.200504511>.
- (96) Beach, E. S.; Duran, J. L.; Horwitz, C. P.; Collins, T. J. Activation of Hydrogen Peroxide by an Fe-TAML Complex in Strongly Alkaline Aqueous Solution: Homogeneous Oxidation Catalysis with Industrial Significance. *Ind. Eng. Chem. Res.* **2009**, *48* (15), 7072–7076. <https://doi.org/10.1021/ie9005723>.
- (97) Chahbane, N.; Popescu, D. L.; Mitchell, D. A.; Chanda, A.; Lenoir, D.; Ryabov, A. D.; Schramm, K. W.; Collins, T. J. Fe(III)-TAML-Catalyzed Green Oxidative Degradation of the Azo Dye Orange II by H<sub>2</sub>O<sub>2</sub> and Organic Peroxides: Products, Toxicity, Kinetics, and Mechanisms. *Green Chem.* **2007**, *9* (1), 49–57. <https://doi.org/10.1039/b604990g>.
- (98) Ghosh, A.; Mitchell, D. A.; Chanda, A.; Ryabov, A. D.; Popescu, D. L.; Upham, E. C.; Collins, G. J.; Collins, T. J.; Pennsylv, V. Catalase - Peroxidase Activity of Iron ( III ) - TAML Activators of Hydrogen Peroxide. *J. Am. Chem. Soc.* **2008**, *130* (11), 15116–15126. <https://doi.org/10.1021/ja8043689>.
- (99) Buxton, G. V.; Greenstock, C. L.; Helman, W. P.; Ross, A. B. Pure Food Bill. *J. Am. Med. Assoc.* **1905**, *XLV* (24), 1805. <https://doi.org/10.1001/jama.1905.02510240037008>.
- (100) Tang, L. L.; Denardo, M. A.; Schuler, C. J.; Mills, M. R.; Gayathri, C.; Gil, R. R.; Kanda, R.; Collins, T. J. Homogeneous Catalysis under Ultradilute Conditions: TAML/NaClO Oxidation of Persistent Metaldehyde. *J. Am. Chem. Soc.* **2017**, *139* (2), 879–887. <https://doi.org/10.1021/jacs.6b11145>.
- (101) Canosa, P.; Rodríguez, I.; Rubí, E.; Negreira, N.; Cela, R. Formation of Halogenated By-Products of Parabens in Chlorinated Water. *Anal. Chim. Acta* **2006**, *575* (1), 106–113. <https://doi.org/10.1016/j.aca.2006.05.068>.
- (102) Chowdhury, S.; Champagne, P.; McLellan, P. J. Models for Predicting Disinfection Byproduct (DBP) Formation in Drinking Waters: A Chronological Review. *Sci. Total Environ.* **2009**, *407* (14), 4189–4206. <https://doi.org/10.1016/j.scitotenv.2009.04.006>.
- (103) Komulainen, H. Experimental Cancer Studies of Chlorinated By-Products. *Toxicology* **2004**, *198* (1–3), 239–248. <https://doi.org/10.1016/j.tox.2004.01.031>.
- (104) Li, D.; Yan, Y.; Wang, H. Recent Advances in Polymer and Polymer Composite Membranes for Reverse and Forward Osmosis Processes. *Prog. Polym. Sci.* **2016**, *61*, 104–155. <https://doi.org/10.1016/j.progpolymsci.2016.03.003>.

- (105) Chekli, L.; Phuntsho, S.; Kim, J. E.; Kim, J.; Choi, J. Y.; Choi, J. S.; Kim, S.; Kim, J. H.; Hong, S.; Sohn, J.; Shon, H. K. A Comprehensive Review of Hybrid Forward Osmosis Systems: Performance, Applications and Future Prospects. *J. Memb. Sci.* **2016**, *497*, 430–449. <https://doi.org/10.1016/j.memsci.2015.09.041>.
- (106) Commission, E. SCIENTIFIC COMMITTEE ON CONSUMER PRODUCTS SCCP Opinion on Hydrogen Peroxide in Tooth Whitening Products. **2005**, No. March.
- (107) Brandt, C.; van Eldik, R. Transition Metal-Catalyzed Oxidation of Sulfur(IV) Oxides. Atmospheric-Relevant Processes and Mechanisms. *Chem. Rev.* **1995**, *95* (1), 119–190. <https://doi.org/10.1021/cr00033a006>.
- (108) Balahura, R. J.; Sorokin, A.; Bernadou, J.; Meunier, B. Origin of the Oxygen Atom in C-H Bond Oxidations Catalyzed by a Water-Soluble Metalloporphyrin. *Inorg. Chem.* **1997**, *36* (16), 3488–3492. <https://doi.org/10.1021/ic9700765>.
- (109) Wietzerbin, K.; Muller, J. G.; Jameton, R. A.; Pratviel, G.; Bernadou, J.; Meunier, B.; Burrows, C. J. Hydroxylation, Epoxidation, and DNA Cleavage Reactions Mediated by the Biomimetic Mn-TMPyP/O<sub>2</sub>/Sulfite Oxidation System *Inorg. Chem.* **1999**, *38* (18), 4123–4127. <https://doi.org/10.1021/ic990537h>.
- (110) Tanaka, T.; Fujii, M.; Mori, H.; Hirono, I. Carcinogenicity Test of Potassium Metabisulfite in Mice. *Ecotoxicol. Environ. Saf.* **1979**, *3* (4), 451–453. [https://doi.org/10.1016/0147-6513\(79\)90034-4](https://doi.org/10.1016/0147-6513(79)90034-4).
- (111) Shi, Y.; Zhan, X.; Ma, L.; Li, L.; Li, C. Evaluation of Antioxidants Using Oxidation Reaction Rate Constants. *Front. Chem. China* **2007**, *2* (2), 140–145. <https://doi.org/10.1007/s11458-007-0029-1>.
- (112) Lavoie, J.-C.; Lachance, C.; Chessex, P. Antiperoxide Activity of Sodium Metabisulfite: A Double-Edged Sword. *Biochem. Pharmacol.* **1994**, *47* (5), 871–876. [https://doi.org/https://doi.org/10.1016/0006-2952\(94\)90487-1](https://doi.org/https://doi.org/10.1016/0006-2952(94)90487-1).
- (113) Ghosh, A.; Ryabov, A. D.; Mayer, S. M.; Horner, D. C.; Prasuhn, D. E.; Sen Gupta, S.; Vuocolo, L.; Culver, C.; Hendrich, M. P.; Rickard, C. E. F.; Norman, R. E.; Horwitz, C. P.; Collins, T. J. Understanding the Mechanism of H<sup>+</sup>-Induced Demetalation as a Design Strategy for Robust Iron(III) Peroxide-Activating Catalysts. *J. Am. Chem. Soc.* **2003**, *125* (41), 12378–12379. <https://doi.org/10.1021/ja0367344>.
- (114) Polshin, V.; Popescu, D. L.; Fischer, A.; Chanda, A.; Horner, D. C.; Beach, E. S.; Henry, J.; Qian, Y. L.; Horwitz, C. P.; Lente, G.; Fabian, I.; Münck, E.; Bominaar, E. L.; Ryabov, A. D.; Collins, T. J. Attaining Control by Design over the Hydrolytic Stability of Fe-TAML Oxidation Catalysts. *J. Am. Chem. Soc.* **2008**, *130* (13), 4497–4506.

<https://doi.org/10.1021/ja7106383>.

- (115) Beach, E. S.; Malecky, R. T.; Gil, R. R.; Horwitz, C. P.; Collins, T. J. Fe-TAML/Hydrogen Peroxide Degradation of Concentrated Solutions of the Commercial Azo Dye Tartrazine. *Catal. Sci. Technol.* **2011**, *1* (3), 437–443. <https://doi.org/10.1039/c0cy00070a>.
- (116) Minella, M.; De Bellis, N.; Gallo, A.; Giagnorio, M.; Minero, C.; Bertinetti, S.; Sethi, R.; Tiraferri, A.; Vione, D. Coupling of Nanofiltration and Thermal Fenton Reaction for the Abatement of Carbamazepine in Wastewater. *ACS Omega* **2018**, *3* (8), 9407–9418. <https://doi.org/10.1021/acsomega.8b01055>.
- (117) Haynes, W. M. *CRC Handbook of Chemistry and Physics*; CRC Press, 2016.
- (118) Brust, M.; Fink, J.; Bethell, D.; Schiffrin, D. J.; Kiely, C. Synthesis and Reactions of Functionalised Gold Nanoparticles. *J. Chem. Soc. Chem. Commun.* **1995**, No. 16, 1655–1656. <https://doi.org/10.1039/C39950001655>.
- (119) Luo, M.; Zhang, X.-H.; Darensbourg, D. J. An Examination of the Steric and Electronic Effects in the Copolymerization of Carbonyl Sulfide and Styrene Oxide. *Macromolecules* **2015**, *48* (17), 6057–6062. <https://doi.org/10.1021/acs.macromol.5b01427>.
- (120) Filipe Tiago de Oliveira, Arani Chanda, Deboshri Banerjee, Xiaopeng Shan, Sujit Mondal, Lawrence Que Jr., Emile L. Bominaar, Eckard Münck, T. J. C. Chemical and Spectroscopic Evidence for an Fe(V)-Oxo Complex. **2007**, *315* (February), 835–838.
- (121) Nishimoto, K.; Fujishiro, R. Electronic Structure of Phenol. *Bull. Chem. Soc. Jpn.* **1958**, *31* (9), 1036–1040. <https://doi.org/10.1246/bcsj.31.1036>.
- (122) Popova, A. D.; Velcheva, E. A.; Stamboliyska, B. A. DFT and Experimental Study on the IR Spectra and Structure of Acesulfame Sweetener. *J. Mol. Struct.* **2012**, *1009*, 23–29. <https://doi.org/10.1016/j.molstruc.2011.07.039>.
- (123) Mark S. Chen; White, M. C. Observed H Atoms to Act as an Energy Transfer Medium to the Bulk, Specifically for Diamond Surfaces in Sliding Contact (37). *Science* (80). **2007**, *318* (November), 783–787. <https://doi.org/10.1126/science.1148597>.
- (124) Mahdi Ahmed, M.; Barbaty, S.; Doumenq, P.; Chiron, S. Sulfate Radical Anion Oxidation of Diclofenac and Sulfamethoxazole for Water Decontamination. *Chem. Eng. J.* **2012**, *197*, 440–447. <https://doi.org/10.1016/j.cej.2012.05.040>.

- (125) Avetta, P.; Pensato, A.; Minella, M.; Malandrino, M.; Maurino, V.; Minero, C.; Hanna, K.; Vione, D. Activation of Persulfate by Irradiated Magnetite: Implications for the Degradation of Phenol under Heterogeneous Photo-Fenton-like Conditions. *Environ. Sci. Technol.* **2015**, *49* (2), 1043–1050. <https://doi.org/10.1021/es503741d>.
- (126) Méndez-Díaz, J.; Sánchez-Polo, M.; Rivera-Utrilla, J.; Canonica, S.; von Gunten, U. Advanced Oxidation of the Surfactant SDBS by Means of Hydroxyl and Sulphate Radicals. *Chem. Eng. J.* **2010**, *163* (3), 300–306. <https://doi.org/https://doi.org/10.1016/j.cej.2010.08.002>.
- (127) Buxton, G. V.; Greenstock, C. L.; Helman, W. P.; Ross, A. B. Critical Review of Rate Constants for Reactions of Hydrated Electrons, Hydrogen Atoms and Hydroxyl Radicals ( $\cdot\text{OH}/\text{O}^-$  in Aqueous Solution. *J. Phys. Chem. Ref. Data* **1988**, *17* (2), 513–886. <https://doi.org/10.1063/1.555805>.
- (128) Neta, P.; Huie, R. E.; Ross, A. B. Rate Constants for Reactions of Inorganic Radicals in Aqueous Solution. *J. Phys. Chem. Ref. Data* **1988**, *17* (3), 1027–1284. <https://doi.org/10.1063/1.555808>.
- (129) Boukari, S. O. B.; Pellizzari, F.; Karpel Vel Leitner, N. Influence of Persulfate Ions on the Removal of Phenol in Aqueous Solution Using Electron Beam Irradiation. *J. Hazard. Mater.* **2011**, *185* (2–3), 844–851. <https://doi.org/10.1016/j.jhazmat.2010.09.097>.
- (130) Pierini, G. D.; Llamas, N. E.; Fragoso, W. D.; Lemos, S. G.; Di Nezio, M. S.; Centurión, M. E. Simultaneous Determination of Acesulfame-K and Aspartame Using Linear Sweep Voltammetry and Multivariate Calibration. *Microchem. J.* **2013**, *106*, 347–350. <https://doi.org/https://doi.org/10.1016/j.microc.2012.09.006>.
- (131) Suryanarayanan, V.; Zhang, Y.; Yoshihara, S.; Shirakashi, T. Voltammetric Assay of Naproxen in Pharmaceutical Formulations Using Boron-Doped Diamond Electrode. *Electroanalysis* **2005**, *17* (11), 925–932. <https://doi.org/https://doi.org/10.1002/elan.200403205>.
- (132) Lima, A. B.; Torres, L. M. F. C.; Guimarães, C. F. R. C.; Verly, R. M.; Silva, L. M. da; Carvalho Jãtextordmasculinenior, ã. D.; Santos, W. T. P. dos. Simultaneous Determination of Paracetamol and Ibuprofen in Pharmaceutical Samples by Differential Pulse Voltammetry Using a Boron-Doped Diamond Electrode. *J. Braz. Chem. Soc.* **2014**, *25*, 478–483.
- (133) Švorc, Ľ.; Rievaj, M.; Bustin, D. Green Electrochemical Sensor for Environmental Monitoring of Pesticides: Determination of Atrazine in River Waters Using a Boron-Doped Diamond Electrode. *Sensors Actuators B Chem.* **2013**, *181*, 294–300. <https://doi.org/https://doi.org/10.1016/j.snb.2013.02.036>.
- (134) Safavi, A.; Maleki, N.; Tajabadi, F. Highly Stable Electrochemical

- Oxidation of Phenolic Compounds at Carbon Ionic Liquid Electrode. *Analyst* **2007**, *132* (1), 54–58. <https://doi.org/10.1039/B612672C>.
- (135) Sunyer, A.; González-Navarro, A.; Serra-Roig, M. P.; Serrano, N.; Díaz-Cruz, M. S.; Díaz-Cruz, J. M. First Application of Carbon-Based Screen-Printed Electrodes for the Voltammetric Determination of the Organic UV Filters Oxybenzone and Octocrylene. *Talanta* **2019**, *196*, 381–388. <https://doi.org/https://doi.org/10.1016/j.talanta.2018.12.092>.
- (136) Fotouhi, L.; Shahbaazi, H. R.; Fatehi, A.; Heravi, M. M. Voltammetric Determination of Triclosan in Waste Water and Personal Care Products. *Int. J. Electrochem. Sci.* **2010**, *5* (9), 1390–1398.
- (137) Wardman, P. Reduction Potentials of One-Electron Couples Involving Free Radicals in Aqueous Solution. *J. Phys. Chem. Ref. Data* **1989**, *18* (4), 1637–1755. <https://doi.org/10.1063/1.555843>.
- (138) Rinaudo, M. Chitin and Chitosan: Properties and Applications. *Prog. Polym. Sci.* **2006**, *31* (7), 603–632. <https://doi.org/https://doi.org/10.1016/j.progpolymsci.2006.06.001>.
- (139) Ravi Kumar, M. N. V. A Review of Chitin and Chitosan Applications. *React. Funct. Polym.* **2000**, *46* (1), 1–27. [https://doi.org/https://doi.org/10.1016/S1381-5148\(00\)00038-9](https://doi.org/https://doi.org/10.1016/S1381-5148(00)00038-9).
- (140) Bellich, B.; Agostino, I. D.; Semeraro, S.; Gamini, A.; Cesàro, A. “ *The Good , the Bad and the Ugly* ” of Chitosans; 2016. <https://doi.org/10.3390/md14050099>.
- (141) Vårum, K. M.; Myhr, M. M.; Hjerde, R. J. N.; Smidsrød, O. In Vitro Degradation Rates of Partially N-Acetylated Chitosans in Human Serum. *Carbohydr. Res.* **1997**, *299* (1), 99–101. [https://doi.org/https://doi.org/10.1016/S0008-6215\(96\)00332-1](https://doi.org/https://doi.org/10.1016/S0008-6215(96)00332-1).
- (142) Rhoades, J.; Roller, S. Antimicrobial Actions of Degraded and Native Chitosan against Spoilage Organisms in Laboratory Media and Foods. *Appl. Environ. Microbiol.* **2000**, *66* (1), 80 LP – 86. <https://doi.org/10.1128/AEM.66.1.80-86.2000>.
- (143) Raafat, D.; Sahl, H.-G. Chitosan and Its Antimicrobial Potential – a Critical Literature Survey. *Microb. Biotechnol.* **2009**, *2* (2), 186–201. <https://doi.org/10.1111/j.1751-7915.2008.00080.x>.
- (144) Qin, Y. The Chelating Properties of Chitosan Fibers. *J. Appl. Polym. Sci.* **1993**, *49* (4), 727–731. <https://doi.org/10.1002/app.1993.070490418>.
- (145) Guibal, E.; Vincent, T.; Navarro, R. Metal Ion Biosorption on Chitosan for the Synthesis of Advanced Materials. *J. Mater. Sci.* **2014**, *49* (16), 5505–5518. <https://doi.org/10.1007/s10853-014-8301-5>.

- (146) Vincent, T.; Peirano, F.; Guibal, E. Chitosan Supported Palladium Catalyst. VI. Nitroaniline Degradation. *J. Appl. Polym. Sci.* **2004**, *94* (4), 1634–1642. <https://doi.org/10.1002/app.21051>.
- (147) Qu, J.; Hu, Q.; Shen, K.; Zhang, K.; Li, Y.; Li, H.; Zhang, Q.; Wang, J.; Quan, W. The Preparation and Characterization of Chitosan Rods Modified with  $\text{Fe}^{3+}$  by a Chelation Mechanism. *Carbohydr. Res.* **2011**, *346* (6), 822–827. <https://doi.org/https://doi.org/10.1016/j.carres.2011.02.006>.
- (148) Gritsch, L.; Lovell, C.; Goldmann, W. H.; Boccaccini, A. R. Fabrication and Characterization of Copper(II)-Chitosan Complexes as Antibiotic-Free Antibacterial Biomaterial. *Carbohydr. Polym.* **2018**, *179*, 370–378. <https://doi.org/https://doi.org/10.1016/j.carbpol.2017.09.095>.
- (149) Liu, T.; Yang, X.; Wang, Z.-L.; Yan, X. Enhanced Chitosan Beads-Supported Fe(0)-Nanoparticles for Removal of Heavy Metals from Electroplating Wastewater in Permeable Reactive Barriers. *Water Res.* **2013**, *47* (17), 6691–6700. <https://doi.org/https://doi.org/10.1016/j.watres.2013.09.006>.
- (150) Liu, X.; Hu, Q.; Fang, Z.; Zhang, X.; Zhang, B. Magnetic Chitosan Nanocomposites: A Useful Recyclable Tool for Heavy Metal Ion Removal. *Langmuir* **2009**, *25* (1), 3–8. <https://doi.org/10.1021/la802754t>.
- (151) Weng, X.; Lin, S.; Zhong, Y.; Chen, Z. Chitosan Stabilized Bimetallic Fe/Ni Nanoparticles Used to Remove Mixed Contaminants-Amoxicillin and Cd (II) from Aqueous Solutions. *Chem. Eng. J.* **2013**, *229*, 27–34. <https://doi.org/https://doi.org/10.1016/j.cej.2013.05.096>.
- (152) Yu, Z.; Zhang, X.; Huang, Y. Magnetic Chitosan–Iron(III) Hydrogel as a Fast and Reusable Adsorbent for Chromium(VI) Removal. *Ind. Eng. Chem. Res.* **2013**, *52* (34), 11956–11966. <https://doi.org/10.1021/ie400781n>.
- (153) Zhang, L.; Zeng, Y.; Cheng, Z. Removal of Heavy Metal Ions Using Chitosan and Modified Chitosan: A Review. *J. Mol. Liq.* **2016**, *214*, 175–191. <https://doi.org/https://doi.org/10.1016/j.molliq.2015.12.013>.
- (154) Li, A.; Lin, R.; Lin, C.; He, B.; Zheng, T.; Lu, L.; Cao, Y. An Environment-Friendly and Multi-Functional Absorbent from Chitosan for Organic Pollutants and Heavy Metal Ion. *Carbohydr. Polym.* **2016**, *148*, 272–280. <https://doi.org/https://doi.org/10.1016/j.carbpol.2016.04.070>.
- (155) Shukla, P. R.; Wang, S.; Sun, H.; Ang, H. M.; Tadé, M. Activated Carbon Supported Cobalt Catalysts for Advanced Oxidation of Organic Contaminants in Aqueous Solution. *Appl. Catal. B Environ.* **2010**, *100* (3), 529–534. <https://doi.org/https://doi.org/10.1016/j.apcatb.2010.09.006>.
- (156) Wang, J.; Yoshida, A.; Wang, P.; Yu, T.; Wang, Z.; Hao, X.; Abudula, A.; Guan, G. Catalytic Oxidation of Volatile Organic Compound over Cerium

- Modified Cobalt-Based Mixed Oxide Catalysts Synthesized by Electrodeposition Method. *Appl. Catal. B Environ.* **2020**, *271*, 118941. <https://doi.org/https://doi.org/10.1016/j.apcatb.2020.118941>.
- (157) Rashid, S.; Shen, C.; Chen, X.; Li, S.; Chen, Y.; Wen, Y.; Liu, J. Enhanced Catalytic Ability of Chitosan–Cu–Fe Bimetal Complex for the Removal of Dyes in Aqueous Solution. *RSC Adv.* **2015**, *5* (110), 90731–90741. <https://doi.org/10.1039/C5RA14711E>.
- (158) Gao, M.; Zhang, D.; Li, W.; Chang, J.; Lin, Q.; Xu, D.; Ma, H. Degradation of Methylene Blue in a Heterogeneous Fenton Reaction Catalyzed by Chitosan Crosslinked Ferrous Complex. *J. Taiwan Inst. Chem. Eng.* **2016**, *67*, 355–361. <https://doi.org/https://doi.org/10.1016/j.jtice.2016.08.010>.
- (159) Xie, Y.; Yi, Y.; Qin, Y.; Wang, L.; Liu, G.; Wu, Y.; Diao, Z.; Zhou, T.; Xu, M. Perchlorate Degradation in Aqueous Solution Using Chitosan-Stabilized Zero-Valent Iron Nanoparticles. *Sep. Purif. Technol.* **2016**, *171*, 164–173. <https://doi.org/https://doi.org/10.1016/j.seppur.2016.07.023>.
- (160) Lee, Y.; Lee, W. Degradation of Trichloroethylene by Fe(II) Chelated with Cross-Linked Chitosan in a Modified Fenton Reaction. *J. Hazard. Mater.* **2010**, *178* (1), 187–193. <https://doi.org/https://doi.org/10.1016/j.jhazmat.2010.01.062>.
- (161) Hou, P.; Shi, C.; Wu, L.; Hou, X. Chitosan/Hydroxyapatite/Fe<sub>3</sub>O<sub>4</sub> Magnetic Composite for Metal-Complex Dye AY220 Removal: Recyclable Metal-Promoted Fenton-like Degradation. *Microchem. J.* **2016**, *128*, 218–225. <https://doi.org/https://doi.org/10.1016/j.microc.2016.04.022>.
- (162) Tiraferri, A.; Maroni, P.; Caro Rodríguez, D.; Borkovec, M. Mechanism of Chitosan Adsorption on Silica from Aqueous Solutions. *Langmuir* **2014**, *30* (17), 4980–4988. <https://doi.org/10.1021/la500680g>.
- (163) Seyed Dorraji, M. S.; Mirmohseni, A.; Carraro, M.; Gross, S.; Simone, S.; Tasselli, F.; Figoli, A. Fenton-like Catalytic Activity of Wet-Spun Chitosan Hollow Fibers Loaded with Fe<sub>3</sub>O<sub>4</sub> Nanoparticles: Batch and Continuous Flow Investigations. *J. Mol. Catal. A Chem.* **2015**, *398*, 353–357. <https://doi.org/https://doi.org/10.1016/j.molcata.2015.01.003>.
- (164) Frey, P. A.; Reed, G. H. The Ubiquity of Iron. *ACS Chem. Biol.* **2012**, *7* (9), 1477–1481. <https://doi.org/10.1021/cb300323q>.
- (165) Hernández, R. B.; Franco, A. P.; Yola, O. R.; López-Delgado, A.; Felcman, J.; Recio, M. A. L.; Mercê, A. L. R. Coordination Study of Chitosan and Fe<sup>3+</sup>. *J. Mol. Struct.* **2008**, *877* (1), 89–99. <https://doi.org/https://doi.org/10.1016/j.molstruc.2007.07.024>.
- (166) Gamblin, B. E.; Stevens, J. G.; Wilson, K. L. Structural Investigations of Chitin and Chitosan Complexed with Iron or Tin. *Hyperfine Interact.* **1998**,



- 112 (1), 117–122. <https://doi.org/10.1023/A:1011001013953>.
- (167) Sreenivasan, K. Thermal Stability Studies of Some Chitosanmetal Ion Complexes Using Differential Scanning Calorimetry. *Polym. Degrad. Stab.* **1996**, 52 (1), 85–87. [https://doi.org/10.1016/0141-3910\(95\)00220-0](https://doi.org/10.1016/0141-3910(95)00220-0).
- (168) Sipos, P.; Berkesi, O.; Tombácz, E.; St. Pierre, T. G.; Webb, J. Formation of Spherical Iron(III) Oxyhydroxide Nanoparticles Sterically Stabilized by Chitosan in Aqueous Solutions. *J. Inorg. Biochem.* **2003**, 95 (1), 55–63. [https://doi.org/10.1016/S0162-0134\(03\)00068-0](https://doi.org/10.1016/S0162-0134(03)00068-0).
- (169) Bhatia, S. C.; Ravi, N. A Mössbauer Study of the Interaction of Chitosan and D-Glucosamine with Iron and Its Relevance to Other Metalloenzymes. *Biomacromolecules* **2003**, 4 (3), 723–727. <https://doi.org/10.1021/bm020131n>.
- (170) Zeng, X.; Ruckenstein, E. Control of Pore Sizes in Macroporous Chitosan and Chitin Membranes. *Ind. Eng. Chem. Res.* **1996**, 35 (11), 4169–4175. <https://doi.org/10.1021/ie960270j>.
- (171) Cui, L.; Gao, S.; Song, X.; Huang, L.; Dong, H. Preparation and Characterization of Chitosan. **2018**, 28433–28439. <https://doi.org/10.1039/c8ra05526b>.
- (172) Kästner, J. Umbrella Sampling. *WIREs Comput. Mol. Sci.* **2011**, 1 (6), 932–942. <https://doi.org/10.1002/wcms.66>.
- (173) Wang, J.; Wolf, R. M.; Caldwell, J. W.; Kollman, P. A.; Case, D. A. Development and Testing of a General Amber Force Field. *J. Comput. Chem.* **2004**, 25 (9), 1157–1174. <https://doi.org/10.1002/jcc.20035>.
- (174) Wang, J.; Wang, W.; Kollman, P. A.; Case, D. A. Automatic Atom Type and Bond Type Perception in Molecular Mechanical Calculations. *J. Mol. Graph. Model.* **2006**, 25 (2), 247–260. <https://doi.org/10.1016/j.jmgm.2005.12.005>.
- (175) Phillips, J. C.; Braun, R.; Wang, W.; Gumbart, J.; Tajkhorshid, E.; Villa, E.; Chipot, C.; Skeel, R. D.; Kalé, L.; Schulten, K. Scalable Molecular Dynamics with NAMD. *J. Comput. Chem.* **2005**, 26 (16), 1781–1802. <https://doi.org/10.1002/jcc.20289>.
- (176) Cossio-Pérez, R.; Pierdominici-Sottile, G.; Sobrado, P.; Palma, J. Molecular Dynamics Simulations of Substrate Release from Trypanosoma Cruzi UDP-Galactopyranose Mutase. *J. Chem. Inf. Model.* **2019**, 59 (2), 809–817. <https://doi.org/10.1021/acs.jcim.8b00675>.
- (177) Tsereteli, L.; Grafmüller, A. *An Accurate Coarse-Grained Model for Chitosan Polysaccharides in Aqueous Solution*; 2017; Vol. 12.

<https://doi.org/10.1371/journal.pone.0180938>.

- (178) Staroverov, V. N.; Scuseria, G. E.; Tao, J.; Perdew, J. P. Comparative Assessment of a New Nonempirical Density Functional: Molecules and Hydrogen-Bonded Complexes. *J. Chem. Phys.* **2003**, *119* (23), 12129–12137. <https://doi.org/10.1063/1.1626543>.
- (179) Tao, J.; Perdew, J. P.; Staroverov, V. N.; Scuseria, G. E. Climbing the Density Functional Ladder: Nonempirical Meta-Generalized Gradient Approximation Designed for Molecules and Solids. *Phys. Rev. Lett.* **2003**, *91* (14), 3–6. <https://doi.org/10.1103/PhysRevLett.91.146401>.
- (180) Weigend, F.; Ahlrichs, R. Balanced Basis Sets of Split Valence, Triple Zeta Valence and Quadruple Zeta Valence Quality for H to Rn: Design and Assessment of Accuracy. *Phys. Chem. Chem. Phys.* **2005**, *7* (18), 3297–3305. <https://doi.org/10.1039/b508541a>.
- (181) Schäfer, A.; Klamt, A.; Sattel, D.; Lohrenz, J. C. W.; Eckert, F. COSMO Implementation in TURBOMOLE: Extension of an Efficient Quantum Chemical Code towards Liquid Systems. *Phys. Chem. Chem. Phys.* **2000**, *2* (10), 2187–2193. <https://doi.org/10.1039/b000184h>.
- (182) Ahlrichs, R.; Bär, M.; Häser, M.; Horn, H.; Kölmel, C. Electronic Structure Calculations on Workstation Computers: The Program System Turbomole. *Chem. Phys. Lett.* **1989**, *162* (3), 165–169. [https://doi.org/10.1016/0009-2614\(89\)85118-8](https://doi.org/10.1016/0009-2614(89)85118-8).
- (183) Häser, M.; Ahlrichs, R. Improvements on the Direct SCF Method. *J. Comput. Chem.* **1989**, *10* (1), 104–111. <https://doi.org/10.1002/jcc.540100111>.
- (184) Hoops, S.; Gauges, R.; Lee, C.; Pahle, J.; Simus, N.; Singhal, M.; Xu, L.; Mendes, P.; Kummer, U. COPASI - A COMplex PATHway Simulator. *Bioinformatics* **2006**, *22* (24), 3067–3074. <https://doi.org/10.1093/bioinformatics/btl485>.
- (185) De Laat, J.; Gallard, H. Catalytic Decomposition of Hydrogen Peroxide by Fe(III) in Homogeneous Aqueous Solution: Mechanism and Kinetic Modeling. *Environ. Sci. Technol.* **1999**, *33* (16), 2726–2732. <https://doi.org/10.1021/es981171v>.
- (186) Kiwi, J.; Lopez, A.; Nadtochenko, V. Mechanism and Kinetics of the OH<sup>•</sup> Radical Intervention during Fenton Oxidation in the Presence of a Significant Amount of Radical Scavenger (Cl<sup>-</sup>). *Environ. Sci. Technol.* **2000**, *34* (11), 2162–2168. <https://doi.org/10.1021/es991406i>.
- (187) Farinelli, G.; Minella, M.; Pazzi, M.; Giannakis, S.; Pulgarin, C.; Vione, D.; Tiraferri, A. Natural Iron Ligands Promote a Metal-Based Oxidation Mechanism for the Fenton Reaction in Water Environments. *J. Hazard.*

- Mater.* **2020**, *393*, 122413.  
<https://doi.org/https://doi.org/10.1016/j.jhazmat.2020.122413>.
- (188) Lu, M.; Chen, J. Effect of inorganic ions on the oxidation of dichlorvos insecticide with fenton ' s reagent. **1997**, *35* (10), 2285–2293.
- (189) Pignatello, J. J. Dark and Photoassisted Iron(III)-Catalyzed Degradation of Chlorophenoxy Herbicides by Hydrogen Peroxide. *Environ. Sci. Technol.* **1992**, *26* (5), 944–951. <https://doi.org/10.1021/es00029a012>.
- (190) Farinelli, G.; Minella, M.; Sordello, F.; Vione, D.; Tiraferri, A. Metabisulfite as an Unconventional Reagent for Green Oxidation of Emerging Contaminants Using an Iron-Based Catalyst. *ACS Omega* **2019**, *4* (24), 20732–20741. <https://doi.org/10.1021/acsomega.9b03088>.
- (191) Cunha, R. A.; Soares, T. A.; Rusu, V. H.; Pontes, F. J. S.; Franca, E. F.; Lins, R. D. The Molecular Structure and Conformational Dynamics of Chitosan Polymers: An Integrated Perspective from Experiments and Computational Simulations; 2020. <https://doi.org/10.5772/51803>.
- (192) Braier, N. C.; Jishi, R. A. Density Functional Studies of Cu<sup>2+</sup> and Ni<sup>2+</sup> Binding to Chitosan. *J. Mol. Struct. THEOCHEM* **2000**, *499* (1–3), 51–55. [https://doi.org/10.1016/S0166-1280\(99\)00288-2](https://doi.org/10.1016/S0166-1280(99)00288-2).
- (193) Ghosh, A.; Tangen, E.; Ryeng, H.; Taylor, P. R. Electronic Structure of High-Spin Iron(IV) Complexes. *Eur. J. Inorg. Chem.* **2004**, *2004* (23), 4555–4560. <https://doi.org/10.1002/ejic.200400362>.
- (194) Mader, S. L.; Bräuer, A.; Groll, M.; Kaila, V. R. I. Catalytic Mechanism and Molecular Engineering of Quinolone Biosynthesis in Dioxygenase AsqJ. *Nat. Commun.* **2018**, *9* (1), 1168. <https://doi.org/10.1038/s41467-018-03442-2>.
- (195) Kazaryan, A.; Baerends, E. J. Ligand Field Effects and the High Spin–High Reactivity Correlation in the H Abstraction by Non-Heme Iron(IV)–Oxo Complexes: A DFT Frontier Orbital Perspective. *ACS Catal.* **2015**, *5* (3), 1475–1488. <https://doi.org/10.1021/cs501721y>.
- (196) Hsu, S.-C.; Don, T.-M.; Chiu, W.-Y. Free Radical Degradation of Chitosan with Potassium Persulfate. *Polym. Degrad. Stab.* **2002**, *75* (1), 73–83. [https://doi.org/https://doi.org/10.1016/S0141-3910\(01\)00205-1](https://doi.org/https://doi.org/10.1016/S0141-3910(01)00205-1).
- (197) Erkselius, S.; Karlsson, O. J. Free Radical Degradation of Hydroxyethyl Cellulose. *Carbohydr. Polym.* **2005**, *62* (4), 344–356. <https://doi.org/https://doi.org/10.1016/j.carbpol.2005.08.013>.
- (198) Nagahama, H.; Maeda, H.; Kashiki, T.; Jayakumar, R.; Furuike, T.; Tamura, H. Preparation and Characterization of Novel Chitosan/Gelatin Membranes Using Chitosan Hydrogel. *Carbohydr. Polym.* **2009**, *76* (2),

- 255–260. <https://doi.org/https://doi.org/10.1016/j.carbpol.2008.10.015>.
- (199) Hohenberger, J.; Ray, K.; Meyer, K. The Biology and Chemistry of High-Valent Iron-Oxo and Iron-Nitrido Complexes. *Nat. Commun.* **2012**, *3*. <https://doi.org/10.1038/ncomms1718>.
- (200) Clarizia, L.; Russo, D.; Somma, I. Di; Marotta, R.; Andreozzi, R. Homogeneous Photo-Fenton Processes at near Neutral pH: A Review. *Appl. Catal. B Environ.* **2017**, *209*, 358–371. <https://doi.org/https://doi.org/10.1016/j.apcatb.2017.03.011>.
- (201) Messele, S. A.; Bengoa, C.; Stüber, F. E.; Giralt, J.; Fortuny, A.; Fabregat, A.; Font, J. Enhanced Degradation of Phenol by a Fenton-Like System (Fe/EDTA/H<sub>2</sub>O<sub>2</sub>) at Circumneutral PH. *Catalysts* **2019**, *9* (5). <https://doi.org/10.3390/catal9050474>.
- (202) Giannakis, S.; Polo López, M. I.; Spuhler, D.; Sánchez Pérez, J. A.; Fernández Ibáñez, P.; Pulgarin, C. Solar Disinfection Is an Augmentable, in Situ-Generated Photo-Fenton Reaction—Part 1: A Review of the Mechanisms and the Fundamental Aspects of the Process. *Appl. Catal. B Environ.* **2016**, *199*, 199–223. <https://doi.org/https://doi.org/10.1016/j.apcatb.2016.06.009>.
- (203) Zhang, Y.; Zhou, M. A Critical Review of the Application of Chelating Agents to Enable Fenton and Fenton-like Reactions at High PH Values. *J. Hazard. Mater.* **2019**, *362*, 436–450. <https://doi.org/https://doi.org/10.1016/j.jhazmat.2018.09.035>.
- (204) Yamazaki, I.; Piette, L. H. ESR Spin-Trapping Studies on the Reaction of Fe<sup>2+</sup> ions with H<sub>2</sub>O<sub>2</sub>-Reactive Species in Oxygen Toxicity in Biology. *J. Biol. Chem.* **1990**, *265* (23), 13589–13594.
- (205) Voelker, B. M.; Sulzberger, B. Effects of Fulvic Acid on Fe(II) Oxidation by Hydrogen Peroxide. *Environ. Sci. Technol.* **1996**, *30* (4), 1106–1114. <https://doi.org/10.1021/es9502132>.
- (206) Park, J. S. B.; Wood, P. M.; Davies, M. J.; Gilbert, B. C.; Whitwood, A. C. A Kinetic and ESR Investigation of Iron(II) Oxalate Oxidation by Hydrogen Peroxide and Dioxygen as a Source of Hydroxyl Radicals. *Free Radic. Res.* **1997**, *27* (5), 447–458. <https://doi.org/10.3109/10715769709065785>.
- (207) Rush, J. D.; Koppenol, W. H. Oxidizing Intermediates in the Reaction of Ferrous EDTA with Hydrogen Peroxide. Reactions with Organic Molecules and Ferrocyclochrome C. *J. Biol. Chem.* **1986**, *261* (15), 6730–6733.
- (208) Iwahashi, H.; Ishii, T.; Sugata, R.; Kido, R. The Effects of Caffeic Acid and Its Related Catechols on Hydroxyl Radical Formation by 3-

- Hydroxyanthranilic Acid, Ferric Chloride, and Hydrogen Peroxide. *Arch. Biochem. Biophys.* **1990**, *276* (1), 242–247. [https://doi.org/https://doi.org/10.1016/0003-9861\(90\)90033-U](https://doi.org/https://doi.org/10.1016/0003-9861(90)90033-U).
- (209) Klopstra, M.; Roelfes, G.; Hage, R.; Kellogg, R. M.; Feringa, B. L. Non-Heme Iron Complexes for Stereoselective Oxidation: Tuning of the Selectivity in Dihydroxylation Using Different Solvents. *Eur. J. Inorg. Chem.* **2004**, No. 4, 846–856. <https://doi.org/10.1002/ejic.200300667>.
- (210) England, J.; Davies, C. R.; Banaru, M.; White, A. J. P.; Britovseka, G. J. P. Catalyst Stability Determines the Catalytic Activity of Non-Heme Iron Catalysts in the Oxidation of Alkanes. *Adv. Synth. Catal.* **2008**, *350* (6), 883–897. <https://doi.org/10.1002/adsc.200700462>.
- (211) Russell, G. A. Deuterium-Isotope Effects in the Autoxidation of Aalkyl Hydrocarbons. Mechanism of the Interaction of Peroxy Radicals. *J. Am. Chem. Soc.* **1957**, *79* (14), 3871–3877. <https://doi.org/10.1021/ja01571a068>.
- (212) Ricceri, F.; Giagnorio, M.; Farinelli, G.; Blandini, G.; Minella, M.; Vione, D.; Tiraferri, A. Desalination of Produced Water by Membrane Distillation: Effect of the Feed Components and of a Pre-Treatment by Fenton Oxidation. *Sci. Rep.* **2019**, *9* (1). <https://doi.org/10.1038/s41598-019-51167-z>.
- (213) Rahhal, S.; Richter, H. W. Reduction of Hydrogen Peroxide by the Ferrous Iron Chelate of Diethylenetriamine-N,N,N',N'',N''-Pentaacetate. *J. Am. Chem. Soc.* **1988**, *110* (10), 3126–3133. <https://doi.org/10.1021/ja00218a022>.
- (214) Harris, D. C. *Quantitative Chemical Analysis, Seventh Edition*; 2006. <https://doi.org/10.1016/j.micron.2011.01.004>.
- (215) Bataineh, H.; Pestovsky, O.; Bakac, A. PH-Induced Mechanistic Changeover from Hydroxyl Radicals to Iron(IV) in the Fenton Reaction. *Chem. Sci.* **2012**, *3* (5), 1594–1599. <https://doi.org/10.1039/c2sc20099f>.
- (216) Black & Veatch. Chlorine: History, Manufacture, Properties, Hazards, and Uses. In *White's Handbook of Chlorination and Alternative Disinfectants*; John Wiley & Sons, Ltd, 2009; pp 1–67. <https://doi.org/https://doi.org/10.1002/9780470561331.ch1>.
- (217) Holah, J. T.; Taylor, J. H.; Dawson, D. J.; Hall, K. E. Biocide Use in the Food Industry and the Disinfectant Resistance of Persistent Strains of *Listeria Monocytogenes* and *Escherichia Coli*. *J. Appl. Microbiol.* **2002**, *92* (s1), 111S–120S. <https://doi.org/10.1046/j.1365-2672.92.5s1.18.x>.
- (218) Rutala, W. A.; Weber, D. J. Disinfection and Sterilization in Health Care Facilities: What Clinicians Need to Know. *Clin. Infect. Dis.* **2004**, *39* (5),

- 702–709. <https://doi.org/10.1086/423182>.
- (219) Windler, L.; Height, M.; Nowack, B. Comparative Evaluation of Antimicrobials for Textile Applications. *Environ. Int.* **2013**, *53*, 62–73. <https://doi.org/10.1016/j.envint.2012.12.010>.
- (220) Griebbe, T.; Flemming, H.-C. Biocide-Free Antifouling Strategy to Protect RO Membranes from Biofouling. *Desalination* **1998**, *118* (1), 153–IN9. [https://doi.org/https://doi.org/10.1016/S0011-9164\(98\)00113-1](https://doi.org/https://doi.org/10.1016/S0011-9164(98)00113-1).
- (221) Maillard, J.-Y. Antimicrobial Biocides in the Healthcare Environment: Efficacy, Usage, Policies, and Perceived Problems. *Ther. Clin. Risk Manag.* **2005**, *1* (4), 307–320.
- (222) Kim, D.; Jung, S.; Sohn, J.; Kim, H.; Lee, S. Biocide Application for Controlling Biofouling of SWRO Membranes — an Overview. *Desalination* **2009**, *238* (1), 43–52. <https://doi.org/https://doi.org/10.1016/j.desal.2008.01.034>.
- (223) Fujioka, T.; Ngo, M. T. T.; Boivin, S.; Kawahara, K.; Takada, A.; Nakamura, Y.; Yoshikawa, H. Controlling Biofouling and Disinfection By-Product Formation during Reverse Osmosis Treatment for Seawater Desalination. *Desalination* **2020**, *488*, 114507. <https://doi.org/https://doi.org/10.1016/j.desal.2020.114507>.
- (224) Richardson, S. D.; Plewa, M. J.; Wagner, E. D.; Schoeny, R.; DeMarini, D. M. Occurrence, Genotoxicity, and Carcinogenicity of Regulated and Emerging Disinfection by-Products in Drinking Water: A Review and Roadmap for Research. *Mutat. Res. - Rev. Mutat. Res.* **2007**, *636* (1–3), 178–242. <https://doi.org/10.1016/j.mrrev.2007.09.001>.
- (225) Fukuzaki, S. Mechanisms of Actions of Sodium Hypochlorite in Cleaning and Disinfection Processes. *Biocontrol Sci.* **2006**, *11* (4), 147–157. <https://doi.org/10.4265/bio.11.147>.
- (226) Gómez-López, V. M.; Marín, A.; Medina-Martínez, M. S.; Gil, M. I.; Allende, A. Generation of Trihalomethanes with Chlorine-Based Sanitizers and Impact on Microbial, Nutritional and Sensory Quality of Baby Spinach. *Postharvest Biol. Technol.* **2013**, *85*, 210–217. <https://doi.org/10.1016/j.postharvbio.2013.05.012>.
- (227) Lee, W. N.; Huang, C. H. Formation of Disinfection Byproducts in Wash Water and Lettuce by Washing with Sodium Hypochlorite and Peracetic Acid Sanitizers. *Food Chem. X* **2019**, *1* (October 2018), 100003. <https://doi.org/10.1016/j.fochx.2018.100003>.
- (228) Domínguez Henao, L.; Turolla, A.; Antonelli, M. Disinfection By-Products Formation and Ecotoxicological Effects of Effluents Treated with Peracetic Acid: A Review. *Chemosphere* **2018**, *213*, 25–40.

- <https://doi.org/10.1016/j.chemosphere.2018.09.005>.
- (229) Stevens, A. A. Reaction Products of Chlorine Dioxide. *Environ. Health Perspect.* **1982**, Vol. 46 (c), 101–110. <https://doi.org/10.1289/ehp.8246101>.
- (230) Xue, R.; Shi, H.; Ma, Y.; Yang, J.; Hua, B.; Inniss, E. C.; Adams, C. D.; Eichholz, T. Evaluation of Thirteen Haloacetic Acids and Ten Trihalomethanes Formation by Peracetic Acid and Chlorine Drinking Water Disinfection. *Chemosphere* **2017**, 189, 349–356. <https://doi.org/10.1016/j.chemosphere.2017.09.059>.
- (231) Yang, X.; Guo, W.; Zhang, X.; Chen, F.; Ye, T.; Liu, W. Formation of Disinfection By-Products after Pre-Oxidation with Chlorine Dioxide or Ferrate. *Water Res.* **2013**, 47 (15), 5856–5864. <https://doi.org/https://doi.org/10.1016/j.watres.2013.07.010>.
- (232) Beekley, P. K.; Hoffman, G. R. Effects of Sulfur Dioxide Fumigation on Photosynthesis, Respiration, and Chlorophyll Content of Selected Lichens. *Bryologist* **1981**, 84 (3), 379. <https://doi.org/10.2307/3242857>.
- (233) Shimazaki, K. I.; Sugahara, K. Specific Inhibition of Photosystem II Activity in Chloroplasts by Fumigation of Spinach Leaves with SO<sub>2</sub>. *Plant Cell Physiol.* **1979**, 20 (5), 947–955. <https://doi.org/10.1093/oxfordjournals.pcp.a075889>.
- (234) Wodzinski, R. S.; Labeda, D. P.; Alexander, M. Effects of Low Concentrations of Bisulfite-Sulfite and Nitrite on Microorganisms. *Appl. Environ. Microbiol.* **1978**, 35 (4), 718–723. <https://doi.org/10.1128/aem.35.4.718-723.1978>.
- (235) Yang, S.; Wang, J.; Cong, W.; Cai, Z.; Ouyang, F. Effects of Bisulfite and Sulfite on the Microalga *Botryococcus Braunii*. *Enzyme Microb. Technol.* **2004**, 35 (1), 46–50. <https://doi.org/https://doi.org/10.1016/j.enzmictec.2004.03.014>.
- (236) Farinelli, G.; Minella, M.; Sordello, F.; Vione, D.; Tiraferri, A. Metabisulfite as an Unconventional Reagent for Green Oxidation of Emerging Contaminants Using an Iron-Based Catalyst. *ACS Omega* **2019**, 4 (24). <https://doi.org/10.1021/acsomega.9b03088>.
- (237) Chernysh, Y.; Balintova, M.; Plyatsuk, L.; Holub, M.; Demcak, S. The Influence of Phosphogypsum Addition on Phosphorus Release in Biochemical Treatment of Sewage Sludge. *Int. J. Environ. Res. Public Health* **2018**, 15 (6), 1–14. <https://doi.org/10.3390/ijerph15061269>.
- (238) Gross, W. Ecophysiology of Algae Living in Highly Acidic Environments. *Hydrobiologia* **2000**, 433, 31–37. <https://doi.org/10.1023/A:1004054317446>.

- (239) Hirooka, S.; Hirose, Y.; Kanesaki, Y.; Higuchi, S.; Fujiwara, T.; Onuma, R.; Era, A.; Ohbayashi, R.; Uzuka, A.; Nozaki, H.; Yoshikawa, H.; Miyagishima, S. Acidophilic Green Algal Genome Provides Insights into Adaptation to an Acidic Environment. *Proc. Natl. Acad. Sci.* **2017**, *114* (39), E8304–E8313. <https://doi.org/10.1073/pnas.1707072114>.
- (240) Gut, H.; Pennacchietti, E.; John, R. A.; Bossa, F.; Capitani, G.; De Biase, D.; Grütter, M. G. Escherichia Coli Acid Resistance: PH-Sensing, Activation by Chloride and Autoinhibition in GadB. *EMBO J.* **2006**, *25* (11), 2643–2651. <https://doi.org/10.1038/sj.emboj.7601107>.
- (241) Jordan, K. N.; Oxford, L.; O’Byrne, C. P. Survival of Low-PH Stress by Escherichia Coli O157:H7: Correlation between Alterations in the Cell Envelope and Increased Acid Tolerance. *Appl. Environ. Microbiol.* **1999**, *65* (7), 3048–3055. <https://doi.org/10.1128/aem.65.7.3048-3055.1999>.
- (242) de Jonge, R.; Ritmeester, W. S.; van Leusden, F. M. Adaptive Responses of Salmonella Enterica Serovar Typhimurium DT104 and Other S. Typhimurium Strains and Escherichia Coli O157 to Low PH Environments. *J. Appl. Microbiol.* **2003**, *94* (4), 625–632. <https://doi.org/https://doi.org/10.1046/j.1365-2672.2003.01875.x>.
- (243) Giannakis, S.; Merino Gamo, A. I.; Darakas, E.; Escalas-Cañellas, A.; Pulgarin, C. Impact of Different Light Intermittence Regimes on Bacteria during Simulated Solar Treatment of Secondary Effluent: Implications of the Inserted Dark Periods. *Sol. Energy* **2013**, *98*, 572–581. <https://doi.org/https://doi.org/10.1016/j.solener.2013.10.022>.
- (244) Taubert, K.; Kraus, S.; Schulze, B. Isothiazol-3(2H)-ones, Part I: Synthesis, Reactions and Biological Activity. *Sulfur Reports* **2002**, *23* (1), 79–121. <https://doi.org/10.1080/01961770208047968>.
- (245) Kitis, M. Disinfection of Wastewater with Peracetic Acid: A Review. *Environ. Int.* **2004**, *30* (1), 47–55. [https://doi.org/https://doi.org/10.1016/S0160-4120\(03\)00147-8](https://doi.org/https://doi.org/10.1016/S0160-4120(03)00147-8).
- (246) Maillard, J.-Y. Bacterial Target Sites for Biocide Action. *J. Appl. Microbiol.* **2002**, *92* (s1), 16S-27S. <https://doi.org/10.1046/j.1365-2672.92.5s1.3.x>.
- (247) Ofori, I.; Maddila, S.; Lin, J.; Jonnalagadda, S. B. Chlorine Dioxide Oxidation of Escherichia Coli in Water—A Study of the Disinfection Kinetics and Mechanism. *J. Environ. Sci. Heal. - Part A Toxic/Hazardous Subst. Environ. Eng.* **2017**, *52* (7), 598–606. <https://doi.org/10.1080/10934529.2017.1293993>.
- (248) Tutumi, M.; Imamura, K.; Hatano, s.; Watanabe, T. Antimicrobial Action of Peracetic Acid. *Food Hyg. Saf. Sci. (Shokuhin Eiseigaku Zasshi)* **1973**, *14* (5), 443–447. <https://doi.org/10.3358/shokueishi.14.443>.



- (249) Xia, D.; Li, Y.; Huang, G.; Yin, R.; An, T.; Li, G.; Zhao, H.; Lu, A.; Wong, P. K. Activation of Persulfates by Natural Magnetic Pyrrhotite for Water Disinfection: Efficiency, Mechanisms, and Stability. *Water Res.* **2017**, *112*, 236–247. <https://doi.org/https://doi.org/10.1016/j.watres.2017.01.052>.
- (250) Ghanbari, F.; Giannakis, S.; Lin, K.-Y. A.; Wu, J.; Madihi-Bidgoli, S. Acetaminophen Degradation by a Synergistic Peracetic Acid/UVC-LED/Fe(II) Advanced Oxidation Process: Kinetic Assessment, Process Feasibility and Mechanistic Considerations. *Chemosphere* **2021**, *263*, 128119. <https://doi.org/https://doi.org/10.1016/j.chemosphere.2020.128119>.
- (251) Feng, L.; Peillex-Delphe, C.; Lü, C.; Wang, D.; Giannakis, S.; Pulgarin, C. Employing Bacterial Mutations for the Elucidation of Photo-Fenton Disinfection: Focus on the Intracellular and Extracellular Inactivation Mechanisms Induced by UVA and H<sub>2</sub>O<sub>2</sub>. *Water Res.* **2020**, *182*, 116049. <https://doi.org/https://doi.org/10.1016/j.watres.2020.116049>.
- (252) Wang, W.; Wang, H.; Li, G.; An, T.; Zhao, H.; Wong, P. K. Catalyst-Free Activation of Persulfate by Visible Light for Water Disinfection: Efficiency and Mechanisms. *Water Res.* **2019**, *157*, 106–118. <https://doi.org/https://doi.org/10.1016/j.watres.2019.03.071>.
- (253) Ruales-Lonfat, C.; Barona, J. F.; Sienkiewicz, A.; Bensimon, M.; Vélez-Colmenares, J.; Benítez, N.; Pulgarín, C. Iron Oxides Semiconductors Are Efficient for Solar Water Disinfection: A Comparison with Photo-Fenton Processes at Neutral PH. *Appl. Catal. B Environ.* **2015**, *166–167*, 497–508. <https://doi.org/https://doi.org/10.1016/j.apcatb.2014.12.007>.
- (254) Williams, T. M. The Mechanism of Action of Isothiazolone Biocides. *NACE - Int. Corros. Conf. Ser.* **2006**, *9* (1), 060901–0609017.
- (255) Venieri, D.; Karapa, A.; Panagiotopoulou, M.; Gounaki, I. Application of Activated Persulfate for the Inactivation of Fecal Bacterial Indicators in Water. *J. Environ. Manage.* **2020**, *261*, 110223. <https://doi.org/https://doi.org/10.1016/j.jenvman.2020.110223>.
- (256) Conner, D. E.; Kotrola, J. S. Growth and Survival of Escherichia Coli O157:H7 under Acidic Conditions. *Appl. Environ. Microbiol.* **1995**, *61* (1), 382–385. <https://doi.org/10.1128/AEM.61.1.382-385.1995>.
- (257) Dell’Erba, A.; Falsanisi, D.; Liberti, L.; Notarnicola, M.; Santoro, D. Disinfection By-Products Formation during Wastewater Disinfection with Peracetic Acid. *Desalination* **2007**, *215* (1–3), 177–186. <https://doi.org/10.1016/j.desal.2006.08.021>.
- (258) Shah, A. D.; Liu, Z. Q.; Salhi, E.; Höfer, T.; Von Gunten, U. Peracetic Acid Oxidation of Saline Waters in the Absence and Presence of H<sub>2</sub>O<sub>2</sub>: Secondary Oxidant and Disinfection Byproduct Formation. *Environ. Sci.*

- Technol.* **2015**, 49 (3), 1698–1705. <https://doi.org/10.1021/es503920n>.
- (259) Korolkov, I. V; Mashentseva, A. A.; Güven, O.; Niyazova, D. T.; Barsbay, M.; Zdorovets, M. V. The Effect of Oxidizing Agents/Systems on the Properties of Track-Etched PET Membranes. *Polym. Degrad. Stab.* **2014**, 107, 150–157. <https://doi.org/https://doi.org/10.1016/j.polymdegradstab.2014.05.008>.
- (260) Kang, G.-D.; Gao, C.-J.; Chen, W.-D.; Jie, X.-M.; Cao, Y.-M.; Yuan, Q. Study on Hypochlorite Degradation of Aromatic Polyamide Reverse Osmosis Membrane. *J. Memb. Sci.* **2007**, 300 (1), 165–171. <https://doi.org/https://doi.org/10.1016/j.memsci.2007.05.025>.
- (261) Castanedo-Tardana, M. P.; Zug, K. A. Methylisothiazolinone. *Dermatitis* **2013**, 24 (1), 2–6. <https://doi.org/10.1097/DER.0b013e31827edc73>.
- (262) Groot, A. C. de; Weyland, J. W. Kathon CG: A Review. *J. Am. Acad. Dermatol.* **1988**, 18 (2, Part 1), 350–358. [https://doi.org/https://doi.org/10.1016/S0190-9622\(88\)70051-1](https://doi.org/https://doi.org/10.1016/S0190-9622(88)70051-1).
- (263) Hannuksela, M. Rapid Increase in Contact Allergy to Kathon® CG in Finland. *Contact Dermatitis* **1986**, 15 (4), 211–214. <https://doi.org/10.1111/j.1600-0536.1986.tb01338.x>.
- (264) Burnett, C. L.; Bergfeld, W. F.; Belsito, D. V; Klaassen, C. D.; Marks, J. G. J.; Shank, R. C.; Slaga, T. J.; Snyder, P. W.; Alan Andersen, F. Final Report of the Safety Assessment of Methylisothiazolinone. *Int. J. Toxicol.* **2010**, 29 (4 Suppl), 187S–213S. <https://doi.org/10.1177/1091581810374651>.
- (265) Schnuch, A.; Geier, J.; Uter, W.; Frosch, P. J. Patch Testing with Preservatives, Antimicrobials and Industrial Biocides. Results from a Multicentre Study. *Br. J. Dermatol.* **1998**, 138 (3), 467–476. <https://doi.org/10.1046/j.1365-2133.1998.02126.x>.
- (266) Kim, J.; Huang, C.-H. Reactivity of Peracetic Acid with Organic Compounds: A Critical Review. *ACS ES&T Water* **2020**. <https://doi.org/10.1021/acsestwater.0c00029>.
- (267) Hassaballah, A. H.; Bhatt, T.; Nyitrai, J.; Dai, N.; Sassoubre, L. Inactivation of E. Coli Enterococcus Spp. Somatic Coliphage and Cryptosporidium Parvum in Wastewater by Peracetic Acid (PAA) Sodium Hypochlorite and Combined PAA-Ultraviolet Disinfection. *Environ. Sci. Water Res. Technol.* **2020**, 6 (1), 197–209. <https://doi.org/10.1039/C9EW00837C>.
- (268) Hassaballah, A. H.; Nyitrai, J.; Hart, C. H.; Dai, N.; Sassoubre, L. M. A Pilot-Scale Study of Peracetic Acid and Ultraviolet Light for Wastewater Disinfection. *Environ. Sci. Water Res. Technol.* **2019**, 5 (8), 1453–1463.

- <https://doi.org/10.1039/C9EW00341J>.
- (269) Luukkonen, T.; Prokkola, H.; Pehkonen, S. O. Peracetic Acid for Conditioning of Municipal Wastewater Sludge: Hygienization, Odor Control, and Fertilizing Properties. *Waste Manag.* **2020**, *102*, 371–379. <https://doi.org/https://doi.org/10.1016/j.wasman.2019.11.004>.
- (270) Turolla, A.; Sabatino, R.; Fontaneto, D.; Eckert, E. M.; Colinas, N.; Corno, G.; Citterio, B.; Biavasco, F.; Antonelli, M.; Mauro, A.; Mangiaterra, G.; Di Cesare, A. Defence Strategies and Antibiotic Resistance Gene Abundance in Enterococci under Stress by Exposure to Low Doses of Peracetic Acid. *Chemosphere* **2017**, *185*, 480–488. <https://doi.org/10.1016/j.chemosphere.2017.07.032>.
- (271) Antonelli, M.; Turolla, A.; Mezzanotte, V.; Nurizzo, C. Peracetic Acid for Secondary Effluent Disinfection: A Comprehensive Performance Assessment. *Water Sci. Technol. a J. Int. Assoc. Water Pollut. Res.* **2013**, *68* (12), 2638–2644. <https://doi.org/10.2166/wst.2013.542>.
- (272) Corporation, B. & V. Chlorine: History, Manufacture, Properties, Hazards, and Uses. In *White's Handbook of Chlorination and Alternative Disinfectants*; John Wiley & Sons, Ltd, 2009; pp 1–67. <https://doi.org/https://doi.org/10.1002/9780470561331.ch1>.
- (273) Popescu, E. M.; Pantea, O.; Gologan, D.; Doukeh, R. Hydrogen Peroxide and Peracetic Acid Oxidizing Potential in the Treatment of Water. *Rev. Chim.* **2019**, *70* (6), 2036–2039. <https://doi.org/10.37358/rc.19.6.7270>.
- (274) Dul'neva, L. V.; Moskvina, A. V. Kinetics of Formation of Peroxyacetic Acid. *Russ. J. Gen. Chem.* **2005**, *75* (7), 1125–1130. <https://doi.org/10.1007/s11176-005-0378-8>.
- (275) Janković, M.; Sinadinović-Fišer, S. Prediction of the Chemical Equilibrium Constant for Peracetic Acid Formation by Hydrogen Peroxide. *J. Am. Oil Chem. Soc.* **2005**, *82* (4), 301–303. <https://doi.org/10.1007/s11746-005-1070-9>.
- (276) Lu, C.; Chu, C. Effects of Acetic Acid on the Regrowth of Heterotrophic Bacteria in the Drinking Water Distribution System. *World J. Microbiol. Biotechnol.* **2005**, *21* (6), 989–998. <https://doi.org/10.1007/s11274-004-7554-6>.
- (277) Leggett, M. J.; Schwarz, J. S.; Burke, P. A.; McDonnell, G.; Denyer, S. P.; Maillard, J.-Y. Mechanism of Sporicidal Activity for the Synergistic Combination of Peracetic Acid and Hydrogen Peroxide. *Appl. Environ. Microbiol.* **2016**, *82* (4), 1035–1039. <https://doi.org/10.1128/AEM.03010-15>.
- (278) Monarca, S.; Richardson, S. D.; Feretti, D.; Grottolo, M.; Thruston, A. D.

- J.; Zani, C.; Navazio, G.; Ragazzo, P.; Zerbini, I.; Alberti, A. Mutagenicity and Disinfection By-Products in Surface Drinking Water Disinfected with Peracetic Acid. *Environ. Toxicol. Chem.* **2002**, *21* (2), 309–318.
- (279) Baldry, M. G. C.; French, M. S. Disinfection of Sewage Effluent with Peracetic Acid. *Water Sci. Technol.* **1989**, *21* (3), 203–206. <https://doi.org/10.2166/wst.1989.0100>.
- (280) Monarca, S.; Feretti, D.; Zerbini, I.; Zani, C.; Alberti, A.; Richardson, S. D.; Thruston A.D., J.; Ragazzo, P.; Guzzella, L. Studies on Mutagenicity and Disinfection By-Products in River Drinking Water Disinfected with Peracetic Acid or Sodium Hypochlorite. *Water Supply* **2002**, *2* (3), 199–204. <https://doi.org/10.2166/ws.2002.0103>.
- (281) Monarca, S.; Zani, C.; Richardson, S.; Thruston, A. D.; Moretti, M.; Feretti, D.; Villarini, M. A New Approach to Evaluating the Toxicity and Genotoxicity of Disinfected Drinking Water. *Water Res.* **2004**, *38* 17, 3809–3819.
- (282) Booth, R. A.; Lester, J. N. The Potential Formation of Halogenated By-Products during Peracetic Acid Treatment of Final Sewage Effluent. *Water Res.* **1995**, *29* (7), 1793–1801. [https://doi.org/10.1016/0043-1354\(94\)00263-7](https://doi.org/10.1016/0043-1354(94)00263-7).
- (283) Domínguez-Henao, L.; Turolla, A.; Monticelli, D.; Antonelli, M. Assessment of a Colorimetric Method for the Measurement of Low Concentrations of Peracetic Acid and Hydrogen Peroxide in Water. *Talanta* **2018**, *183*, 209–215. <https://doi.org/10.1016/j.talanta.2018.02.078>.
- (284) Galbán, J.; Sanz, V.; de Marcos, S. Selective Peracetic Acid Determination in the Presence of Hydrogen Peroxide Using a Label Free Enzymatic Method Based on Catalase. *Anal. Bioanal. Chem.* **2010**, *398* (5), 2117–2124. <https://doi.org/10.1007/s00216-010-4145-2>.
- (285) Wagner, M.; Brumelis, D.; Gehr, R. Disinfection of Wastewater by Hydrogen Peroxide or Peracetic Acid: Development of Procedures for Measurement of Residual Disinfectant and Application to a Physicochemically Treated Municipal Effluent. *Water Environ. Res.* **2002**, *74* (1), 33–50. <https://doi.org/https://doi.org/10.2175/106143002X139730>.
- (286) Patil, R. S.; Juvekar, V. A.; Naik, V. M. Oxidation of Chloride Ion on Platinum Electrode: Dynamics of Electrode Passivation and Its Effect on Oxidation Kinetics. *Ind. Eng. Chem. Res.* **2011**, *50* (23), 12946–12959. <https://doi.org/10.1021/ie200663a>.
- (287) GHOSH, Pushpito, Kumar; Central Salt & TM), European Marine Chemicals Research Institute, Gijubhai Badheka Marg, Bhavnagar, Gujarat 364021 (IN). UPADHYAY, Sumesh, Chandra; Central Salt & Marine Chemicals search Institute, Gijubhai Badheka Marg, Bhavnagar, G. 36402

- 1 (IN). Production of high purity salt with reduced levels of impurities, 2013.
- (288) Crathorne, B.; Fawell, J.; Irving, T. E.; Authority, N. R. *Sewage Disinfection: By-Product Formation, Ecotoxicology and Microbiological Efficacy April 1989 - March 1991*; R & D note; National Rivers Authority, 1992.
- (289) Choudary, B. M.; Someshwar, T.; Reddy, C. V.; Kantam, M. L.; Ratnam, K. J.; Sivaji, L. V. The First Example of Bromination of Aromatic Compounds with Unprecedented Atom Economy Using Molecular Bromine **2003**, *251*, 397–409. [https://doi.org/10.1016/S0926-860X\(03\)00379-X](https://doi.org/10.1016/S0926-860X(03)00379-X).
- (290) Endemann, H. Berichte Der Deutschen Chemischen Gesellschaft. *J. Am. Chem. Soc.* **1880**, *2* (8), 366–371. <https://doi.org/10.1021/ja02139a003>.
- (291) Volhard, J. 4) Ueber Darstellung  $\alpha$ -Bromirter Säuren. *Justus Liebig's Ann. der Chemie* **1887**, *242* (1–2), 141–163. <https://doi.org/10.1002/jlac.18872420107>.
- (292) Eberline, A. R. Enol Intermediates Derived From Carboxylic Acids , Esters And Amides, 1995.
- (293) Rossberg, M.; Lendle, W.; Pfeleiderer, G.; Tögel, A.; Dreher, E.-L.; Langer, E.; Rassaerts, H.; Kleinschmidt, P.; Strack, H.; Cook, R.; Beck, U.; Lipper, K.-A.; Torkelson, T. R.; Löser, E.; Beutel, K. K.; Mann, T. Chlorinated Hydrocarbons. *Ullmann's Encyclopedia of Industrial Chemistry*. July 15, 2006. [https://doi.org/https://doi.org/10.1002/14356007.a06\\_233.pub2](https://doi.org/https://doi.org/10.1002/14356007.a06_233.pub2).
- (294) Farinelli, G.; Di Luca, A.; Kaila, V. R. I.; MacLachlan, M. J.; Tiraferri, A. Fe-Chitosan Complexes for Oxidative Degradation of Emerging Contaminants in Water: Structure, Activity, and Reaction Mechanism. *J. Hazard. Mater.* **2020**, 124662. <https://doi.org/https://doi.org/10.1016/j.jhazmat.2020.124662>.